AN ABSTRACT OF THE THESIS OF

Meredith C. Payne for the degree of Master of Science in Oceanography presented on March 12, 2012

Title: Development and Use of Satellite-Derived Sea-Surface Temperature Data for the Nearshore North Pacific and Arctic Oceans: Temperature Pattern Analysis and Implications for Climate Change at Ecoregional Scale

Abstract approved:

____

Philip W. Mote

The quantification and description of sea surface temperature (SST) is critically important because it can influence the distribution, migration, and invasion of marine species; furthermore, SSTs are expected to be affected by climate change. Recent research indicates that there has been a warming trend in ocean temperatures over the last 50 years. Hence, we sought to identify and demonstrate how a particularly germane SST dataset can be used within the scope of global climate change research. For this project we assembled a 29-year nearshore time series of mean monthly SSTs along the North Pacific coastline, as well as mean monthly SSTs for ice-free regions of the Arctic, using remotely-sensed satellite data collected with the Advanced Very High Resolution Radiometer (AVHRR) instrument. By providing detailed information concerning both dataset generation and data limitations, we aimed to make these data comprehensible to an expanded audience concentrating on life sciences rather than the traditionally physical science-based community. Furthermore, by making these data freely and publically available in multiple formats, including GIS (geographic information systems) layers, we expand their visibility and the extent of their use. We then used the dataset to describe SST patterns of nearshore (< 20 km offshore) regions of 16 North Pacific ecoregions, and of ice-free

regions of 20 Arctic ecoregions, as delineated by the Marine Ecoregions of the World (MEOW) hierarchical schema. Our work creates a better understanding of present temperature regimes in these critically sensitive areas, from which we can draw several basic conclusions. 1) AVHRR SST measurements alone are sufficient to identify temperature patterns pertinent to determining health of ecosystems; 2) Within the nearshore North Pacific, ecoregions along the California Current System are most vulnerable to habitat-altering SST changes; 3) sea ice distribution is a major factor affecting SSTs in Arctic ecoregions, causing concern for the welfare of Arctic species.

Development and Use of Satellite-Derived Sea-Surface Temperature Data for the Nearshore North Pacific and Arctic Oceans: Temperature Pattern Analysis and Implications for Climate Change at Ecoregional Scale

by
Meredith C. Payne

A THESIS

submitted to

Oregon State University

in partial fulfillment of
the requirements for the
degree of

Master of Science

Presented March 12, 2012
Commencement June 2012

Master of Science thesis of Meredith C. Payne presented on March 12, 2012.

APPROVED:

____

Major Professor, representing Oceanography

____

Dean of the College of Earth, Ocean, and Atmospheric Sciences

____

Dean of the Graduate School

I understand that my thesis will become part of the permanent collection of Oregon State University libraries. My signature below authorizes release of my thesis to any reader upon request.

____

Meredith C. Payne, Author

CONTRIBUTION OF AUTHORS

Meredith C. Payne is a geologist/oceanographer interested in the physical geography and geology of the North Pacific. She is actively engaged in using remote sensing and geographic information systems science to investigate the potential effects of climate change on nearshore and estuarine environments.

Deborah A. Reusser is a geographer at the USGS Western Fisheries Research Center, Newport Duty Station, interested in ecoinformatics and biogeography. She is actively engaged in research to quantify the biogeographical patterns of native and non-indigenous species and how distribution patterns may be altered by a changing climate.

Henry Lee II is a marine biologist at the Pacific Coastal Ecology Branch of the EPA Western Ecology Division (Newport, OR), specializing in soft-bottom benthic organisms. He is interested in the biogeography of native and non-indigenous marine and estuarine species and is actively engaged in research to identify species at risk due to climate change and sea level rise.

Cheryl A. Brown is an oceanographer at the Pacific Coastal Ecology Branch of the EPA Western Ecology Division (Newport, OR). Her interests and work focus on developing coupled physical-biological models of coastal and estuarine ecosystems, and using numerical simulation models to interpret complex biogeochemical data sets.

The authors represent the fields of oceanography, geography, marine biology and ecology. Their common interests include the prediction and modeling of climate change impacts on nearshore and estuarine regions of the Pacific, and the consequential implications for biogeography. They are actively engaged in interagency, multidisciplinary research projects that study climate patterns in critical marine environments. The team members derived the study's concepts and

analysis plan together. All authors contributed to analysis and writing. M. C. P. processed the data and M. C. P., H. L., and C. A. B. led the writing.

TABLE OF CONTENTS

Page

TABLE OF CONTENTS (Continued)

LIST OF FIGURES

LIST OF TABLES

Development and Use of Satellite-Derived Sea-Surface Temperature Data for the Nearshore North Pacific and Arctic Oceans: Temperature Pattern Analysis and Implications for Climate Change at Ecoregional Scale

Chapter 1 – General Introduction

This thesis comprises three published papers. The collection of articles herein represents a compilation of work investigating the use of geospatial and geostatistical analyses of sea-surface temperature (SST) data to categorize marine ecoregions of the North Pacific and Arctic Oceans. These works were generated as deliverables for a joint project between the United States Geologic Survey (USGS) and the United States Environmental Protection Agency (US EPA). The purpose of this body of work is to increase the comprehensibility and accessibility of satellite remote sensing data to a life-science audience composed of biogeographers, marine biologists and ecologists and other investigators working on marine habitat mapping and/or climate studies.

Recent climate studies report a warming trend in Pacific Ocean temperatures over the last 50 years [*IPCC*, 2007]. However, much less is known about temperature change in the near-coastal environment, which is particularly sensitive to climatic change [*Rivadeneira and Fernandez*, 2005; *Sorte et al.*, 2010; *Stram and Evans*, 2009]. In nearshore regions *in situ* sea surface temperature (SST) measurements are typically made via buoy; however, these are irregular in both space and time. This generates a need for a satellite-derived SST product capable of covering as much coastline as possible while keeping resolution and file size reasonable.

Recent climate studies report a warming trend in Pacific Ocean temperatures over the last 50 years [*IPCC*, 2007]. However, much less is known about temperature change in the near-coastal environment, which is particularly sensitive to climatic change [*Rivadeneira and Fernandez*, 2005; *Sorte et al.*, 2010; *Stram and Evans*, 2009]. In nearshore regions *in situ* sea surface temperature (SST) measurements are typically made via buoy; however, these are irregular in both space and time. This generates a need for a satellite-derived SST product capable of covering as much coastline as possible while keeping resolution and file size reasonable.

Remote sensing and GIS technologies are gaining acceptance as tools used in the synthesis of data for climate change research. They facilitate the linking of *in situ* observations with models of small-scale Earth systems processes. Satellite remote-sensing observations have the advantage of extensive spatial coverage and high repeatability that is not possible with field observations. In particular, considerable progress has been made in understanding ocean dynamics through the use of remote sensing of sea surface temperature (hereafter SST) [*Casey and Cornillon*, 1999; 2001; *Casey and Adamec*, 2002; *Castelao et al.*, 2005; *Castelao et al.*, 2006; *Chelton et al.*, 2007; *Espinosa-Carreon et al.*, 2004; *Keister and Strub*, 2008; *Trenberth et al.*, 1992; *Venegas et al.*, 2008; *Walker et al.*, 2003]. However, there have been relatively few studies of nearshore or Arctic regions using SST using satellite instruments. Potential contamination by land signal and coastal weather events (e.g. clouds, fog, sea ice) often hampers the effort to compile a comprehensive (in space and time) coastal SST dataset. Nevertheless, compilation of a satellite-derived nearshore SST record is of use to a variety of marine-oriented fields.

Examples of the relatively few regional studies of nearshore SST using satellite instruments include *Pearce et al.* [2006]; *Blanchette et al.* [2008]; and *Broitman et al.* [2008]. For example, *Blanchette et al.* [2008] examined the relationship between temperature and species assemblages in rocky shores from southeast Alaska to Baja California. In a similar study, *Broitman et al.* [2008] conducted a detailed 4-year biogeographic investigation (1997-2001) of a much smaller region along the coasts of Oregon and California using satellite SST data. Both inquiries experienced an issue with missing pixels, forcing them to spatially average the SST data at their coastal sites. Despite these difficulties, *Pearce et al.* [2006] found that monthly mean values of remotely-sensed nearshore SSTs were viable for examining seasonal patterns in the nearshore region, and *Vazquez-Cuervo et al.* [2010] demonstrated significant improvements in resolution (from 9 km to 4 km) of coastal SSTs in the version of Pathfinder SST data used in this study. These studies exemplify the use of SST records for a variety of marine-related research.

Here we seek to enhance the significant contribution of satellite remote sensing to oceanographic studies by addressing the need for a SST product capable of covering as much area as possible while keeping resolution and file size reasonable. We undertook to fill the SST data gap by generating tri-decadal, moderate-resolution (4 km grid cell size) SST datasets that cover the coastline of the North Pacific Ocean and ice-free areas of the Arctic Ocean with a monthly temporal resolution. We provide a spatio-temporally continuous SST dataset of global extent that will enable broad-scale studies of physical and biological ocean characteristics over decadal time scales and that can help address macroecological questions relating to biogeographical patterns, invasions, and climate change.

We focus on SST data collected by the suite of Advanced Very-High Resolution Radiometer (AVHRR) instruments that have flown onboard various National Oceanic and Atmospheric Administration (NOAA) Polar Orbiting Environmental Satellites (POES) since 1981. We acknowledge that AVHRR is not the sole satellite instrument capable of collecting SST data. However, other instruments including the Moderate Resolution Imaging Spectroradiometer (MODIS; currently flying on both the Terra and Aqua Earth observation satellites (EOS)), as well as microwave instruments (e.g. Special Sensor Microwave/Imager (SSM/I) or Advanced Microwave Scanning Radiometer for EOS (AMSR-E)) have neither the record length nor the spatial coverage attributable to AVHRR. Furthermore, while other NOAA instruments flying upon geostationary orbiters (GOES series) generate data of comparable temporal resolution to AVHRR, their orbits dictate a necessarily lower spatial resolution. Therefore, we selected the AVHRR-derived Pathfinder monthly-mean SST dataset [*Kilpatrick et al.,* 2001] versions 5.0 (years 1985 – 2009) and 5.1 (years 1981 – 1985; PFSST V50 and V51, respectively) for its global coverage at moderate resolution (each grid cell measures approximately 4 km x 4 km), long data record relative to other satellite missions, and substantial level of processing, including extensive calibration and atmospheric correction. The AVHRR is a multi-generational, multi-channel sensor that has flown on board a series of National Oceanic and Atmospheric Administration (NOAA) polar-orbiting satellites, and has been providing reliable SST data since 1981 (e.g. [*Kilpatrick et al.,* 2001]).

The PFSST V50 data were produced specifically for use in the analysis of global change and have improved the resolution compared to PFSST V41 in coastal regions [*Vazquez-Cuervo et al.*, 2010]. The data are evaluated on pixel-by-pixel performance with respect to a number of tests that estimate validity and consistency of brightness temperature readings, sun angle effects, and cloudiness, which are combined to establish an overall quality rating.

We tailored these SST data for researchers working on North Pacific and Arctic Ocean regions by organizing them by ecoregion in accordance with the Marine Ecoregions of the World (MEOW) biogeographical schema devised by The Nature Conservancy [*Spalding et al.,* 2007]. (More detailed information explaining the ecoregional classification is contained in Chapter 2 of this document). In doing this, we achieve the objective to generate a consistent set of North Pacific and Arctic SSTs of a known quality, and to make these data freely and publically available in a readily useable format. The data include raster and shapefile geographical information systems (GIS) data, as well as data in Access database and text formats. Furthermore, we make available the Python scripts used to generate them. As such, we provide an appendix containing sufficient background on the generation of the data and their quality for use by ecologists and biogeographers addressing questions about the effects of temperature on the distribution of near-shore organisms and to serve as a readily-available baseline for climate studies.

We then fulfill a second objective to demonstrate the utility of these datasets by using them to identify patterns in the seasonal SST cycle for each ecoregion in the North Pacific and Arctic Oceans. These studies exemplify the use of SST records to a variety of marine-oriented fields. A spatio-temporally continuous SST dataset at ecoregional scale can help address macroecological questions relating to biogeographical patterns, invasions, and climate change. At this scale temperature is a major factor affecting distributions of native and nonindigenous (NIS) organisms [*Briggs*, 1974; *Adey and Steneck*, 2001; *Longhurst*, 2007], whose habitats, populations, and distributions are expected to be highly influenced by climate change [*Broitman et al.*, 2008a, *Wethey and Woodin*, 2008; *Broitman et al.*, 2009].

This thesis is organized as follows:

The thesis is composed of three papers that appear in peer-reviewed publications; all are available online. Each paper is prefaced by a Chapter Heading Page indicting where and by whom they were published for easy reference by the reader.

Chapter 2, *Payne et al.* [2012a], describes seasonal cycle characteristics and patterns within the nearshore zones of North Pacific ecoregions.

Chapter 3, *Payne et al.* [2012b], has very similar themes as Chapter 2, but the SST analyses encompass the Arctic Ocean ecoregions in their entirety (i.e. they are not limited to coastal, nearshore regions).

Chapter 4 presents general conclusions for this body of work. It is followed by a general bibliography containing all references cited in this document. They are listed in alphabetical order by last name of first authors and conform to the reference style of the American Geophysical Union (AGU).

Finally, Appendix A, *Payne et al.* [2011], was the first paper generated for this project. It appears as an appendix due to the in-depth degree to which the data assembly and processing steps are described.. We encourage any reader with the desire to fully understand the origins and accuracy of the data to refer to Appendix A and to the references listed therein.

ECOREGIONAL ANALYSIS OF NEARSHORE SEA-SURFACE TEMPERATURE IN THE NORTH PACIFIC

Meredith C. Payne[1, 2], Cheryl A. Brown[3], Deborah A. Reusser[1, 2], Henry Lee II[3]

[1]Western Fisheries Research Center, United States Geological Survey, Newport, Oregon, United States of America, [2]Oregon State University, Corvallis, Oregon, United States of America, [3]Pacific Coastal Ecology Branch, Western Ecology Division, United States Environmental Protection Agency, Newport, Oregon, United States of America

PLoS ONE

U.S. Headquarters
Public Library of Science
1160 Battery Street,
Koshland Building East, Suite 100
San Francisco, CA 94111
United States

January 2012 | Volume 7 | Issue 1 | e30105

Chapter 2 – Ecoregional analysis of nearshore sea-surface temperature in the North Pacific

Abstract

The quantification and description of sea surface temperature (SST) is critically important because it can influence the distribution, migration, and invasion of marine species; furthermore, SSTs are expected to be affected by climate change. To better understand present temperature regimes, we assembled a 29-year nearshore time series of mean monthly SSTs along the North Pacific coastline using remotely-sensed satellite data collected with the Advanced Very High Resolution Radiometer (AVHRR) instrument. We then used the dataset to describe nearshore (< 20 km offshore) SST patterns of 16 North Pacific ecoregions delineated by the Marine Ecoregions of the World (MEOW) hierarchical schema. Annual mean temperature varied from 3.8 °C along the Kamchatka ecoregion to 24.8 °C in the Cortezian ecoregion. There are smaller annual ranges and less variability in SST in the Northeast Pacific relative to the Northwest Pacific. Within the 16 ecoregions, 31-94% of the variance in SST is explained by the annual cycle, with the annual cycle explaining the least variation in the Northern California ecoregion and the most variation in the Yellow Sea ecoregion. Clustering on mean monthly SSTs of each ecoregion showed a clear break between the ecoregions within the Warm and Cold Temperate provinces of the MEOW schema, though several of the ecoregions contained within the provinces did not show a significant difference in mean seasonal temperature patterns. Comparison of these temperature patterns shared some similarities and differences with previous biogeographic classifications by *Hall* [1964] and the Large Marine Ecosystems (LMEs). Finally, we provide a web link to the processed data for use by other researchers.

Introduction

Considerable progress has been made in understanding ocean dynamics through the analysis of remotely-sensed sea surface temperature (hereafter SST) data [*Casey and Adamec*, 2002; *Keister and*

Strub, 2008; *Pirhalla et al.*, 2009; *Venegas et al.*, 2008]. However, potential contamination by land signal and coastal weather often hampers efforts to compile a comprehensive nearshore SST dataset. This issue was encountered in the study by *Blanchette et al.* [2008], which examined the relationship between temperature and species assemblages in rocky shores from southeast Alaska to Baja California, and in a study by *Broitman et al.* [2008] of a smaller region along the coasts of Oregon and California. Both inquiries experienced an issue with missing pixels, forcing them to spatially average the SST data at their coastal sites. Despite these difficulties, *Pearce et al.* [2006] found that monthly mean values of remotely-sensed nearshore SSTs were viable for examining seasonal patterns in the nearshore region.

These studies exemplify the use of nearshore SST records for a variety of marine-related research. A spatio-temporally continuous coastal SST dataset at a broad spatial scale can help address macroecological questions relating to biogeographical patterns, invasions, and climate change. At a biogeographic scale, temperature is a major factor affecting distributions of native and nonindigenous species (NIS) [*Adey and Steneck*, 2001; *Briggs*, 1974; *Golikov et al.*, 1990; *Longhurst*, 2007]. One specific example of this type of application is predicting potential areas susceptible to invasion of NIS using environmental matching based on temperature [*Gollash*, 2006; *Herborg et al.*, 2007]. Furthermore, these types of climate studies are critical because nearshore environments and the distributions of organisms within them are expected to be highly influenced by climate change [*Broitman et al.*, 2008; *Broitman et al.*, 2009; *Wethey and Woodin*, 2008].

In nearshore regions, *in situ* SST measurements are typically made by moored buoys; however, while there is a paucity of SST data, the mooring sites and sampling intervals are irregular in both space and time. Hence, there is a need for a satellite-derived SST product capable of covering extensive areas of the coastline. Satellite remote-sensing observations have the advantage of extensive spatial coverage and high repeatability in relatively inaccessible regions that is not often possible with field observations. The trade-off, however, is that satellite data have lower spatial resolution compared with field measurements and therefore often cannot resolve more localized processes important in coastal areas. Furthermore, high-resolution image mosaics of an expansive area often consist of a massive amount of data, making them impractical for many users.

To address this data gap, a SST product capable of covering as much coastline as possible while keeping resolution and file size reasonable is needed. Therefore, we generated a consistent SST product of a known quality for the nearshore region of the North Pacific Basin based on SST measurements from the Advanced Very High Resolution Radiometer (AVHRR) Pathfinder data. The resulting tri-decadal, moderate-resolution dataset was used to evaluate nearshore SST, providing a regional-scale view of seasonal temperature patterns for the entire North Pacific coast. We provide sufficient background on the generation of the data and their quality for use by ecologists and biogeographers and to serve as a readily-available baseline for climate studies.

Materials and Methods

Study Area

In the effort to characterize nearshore ecosystems at a regional scale, we analyzed SST measurements by marine "ecoregions" as defined by The Nature Conservancy in their MEOW biogeographic schema [*Spalding et al.*, 2007]. The MEOW schema is a global hierarchical classification system of coastal zones that divides the world's coastal areas into 12 distinct marine "realms." The realms are further broken down into 62 marine "provinces" which are further divided into 232 "ecoregions." In generating this schema, the objective was to develop a "hierarchical system based on taxonomic configurations, influenced by evolutionary history, patterns of dispersal, and isolation" [*Spalding et al.*, 2007]. We focused the present analysis on the ecoregions within the Temperate North Pacific realm, which is comprised of four Provinces containing 17 individual ecoregions (Figure 2-1). Additionally, we used the breakout of the Northeast Pacific Region and Northwest Pacific Region as defined by *Reusser and Lee* [2011] to distinguish between ecoregions on the two sides of the North

Pacific. We limited our analysis to expansive coastal regions and therefore did not include the Puget Trough/Georgia Basin ecoregion in this analysis.

SST Data Description

We selected the AVHRR-derived Pathfinder monthly-mean SST dataset [*Kilpatrick et al.*, 2001] versions 5.0 (years 1985 – 2009) and 5.1 (years 1981 – 1985; PFSST V50 and V51, respectively) for its global coverage at moderate resolution (each grid cell measures approximately 4 km x 4 km), long data record relative to other satellite missions, and substantial level of processing, including extensive calibration and atmospheric correction. We obtained the PFSST V50 "hierarchical data format scientific dataset" (HDF-SDS) data from the NASA JPL Physical Oceanography Distributed Active Archive Center (PO.DAAC, ftp://podaac.jpl.nasa.gov/OceanTemperature/avhrr/L3/pathfinder_v5/) and the PFSST V51 data for 1981-1985 from NODC (ftp://data.nodc.noaa.gov/pub/data.nodc/pathfinder).

The PFSST V50 data were produced specifically for use in the analysis of global change and have improved resolution (from 9 km to 4 km) compared to PFSST V41 in coastal regions [*Jorge Vazquez-Cuervo et al.*, 2010]. The PFSST data include a quality flag in which each SST grid cell is designated a value ranging from 0 (worst quality) to 7 (best quality). These quality flags convey the level of confidence attributed to the SST value calculated for each grid cell location. Level of confidence is evaluated on pixel-by-pixel performance based on a number of tests that estimate validity and consistency of brightness temperature readings, sun angle effects, and cloudiness, which are combined to establish an overall quality rating. While daytime data have a more pronounced diurnal warming effect, it has been shown that they are not necessarily inferior to nighttime data [*Casey*, 2002]. Therefore, we used the PFSST daytime series because daytime data were more abundant in the nearshore regions of interest, especially in areas that experience frequent evening ground fog, such as along the coasts of Washington and Oregon, USA.

SST Data Processing Stream

Subsequent to downloading the Pathfinder data, the Marine Geospatial Ecology Tools v. 0.8 (MGET) extension was used to convert the PFSST data from its native HDF-SDS format to Environmental Systems Research Institute (ESRI) ArcGIS rasters [*Roberts et al.*, 2010]. The PFSST V41 dataset (the PFSST dataset preceding V50, which was retired in 2005) included a standard product called "best SST," or "BSST," which included only grid cells with quality flags greater than 3 [*Kilpatrick et al.*, 2001]. For this study, we used the same quality threshold as BSST. The next step was to eliminate unlikely SST values (< -2.0 °C) that occasionally appear in the subarctic or Arctic. The remaining data were scaled using the equation provided in the AVHRR metadata in order to obtain SST values in degrees Celsius.

As the focus of this research is on nearshore environments, we limited the study area to within 20 km of the coastline (Figure 2-1). Often, the grid cell closest to the coast was eliminated from the analysis due to a low quality rating related to land-contamination. We selected grid cells by counting four grid cells seaward of the coastline defined by the Global Self-consistent, Hierarchical, High-resolution Shoreline (GSHHS) dataset [*Wessel and Smith*, 1996]. ArcGIS was used to isolate the grid cells in each monthly-mean SST raster. These steps were systematically repeated to generate a point shapefile of nearshore SST values—one for each month of each year for the interval of September 1981 to December 2009. The resulting dataset consisted of more than 2 million points representing individual spatial locations for each month stored in 340 ESRI shapefiles, which were aggregated into three smaller datasets based on month, MEOW provinces and ecoregions. These steps were automated using open source R statistical software [*R Development Core Team*, 2009] scripts. Synthesized data and scripts used in this analysis are available from *Payne et al.* [2011], (http://pubs.usgs.gov/of/2010/1251/index.html).

SST analysis using MEOW as a geographic framework

We used the following protocol to describe the nearshore SST patterns within an ecoregion. We pooled all 29 years of the derived SST values of mean monthly SST grid cells within an ecoregion and calculated the monthly-mean SSTs for each ecoregion, as well as a suite of other metrics derived from the monthly means as summarized in Figures 2-2 and 2-3. To evaluate spatial similarities in seasonal temperature patterns, we performed group hierarchical clustering on the ecoregions using these monthly SST metrics (n=12 months x 16 ecoregions). A permutation test (SIMPROF) was used to identify branches that were not significantly different ($p < 0.05$). As a complement to the cluster analysis, the seasonal pattern of monthly-mean SSTs from each of the ecoregions was analyzed using nonparametric multi-dimensional scaling (nMDS). Euclidian distance was used to quantify the dissimilarity in seasonal temperature patterns among the ecoregions in the clustering and nMDS analyses. These analyses were conducted using the PRIMER software package v. 6.1.6 [*Clarke and Gorley*, 2006].

Results

Missing Data

Several of the ecoregions had considerable missing data during some months. Ecoregions in the subarctic (e.g. Sea of Okhotsk), as well as other typically cloudy/foggy regions (e.g. Yellow Sea ecoregion and Oregon, Washington, Vancouver Coast and Shelf ecoregion, hereafter referred to as the "Oregonian") can have upwards of 70% missing data for any one month (Figure 2-4). However, since the data included more than a half-million potential SST values per month, even 10% of the data yielded tens of thousands of values—enough to perform a robust analysis of ecoregional patterns. Although a concentration of acceptable SST values at one particular location within an ecoregion could potentially introduce a spatial bias, the data were examined visually, and it was determined that that was not the case.

Long-term Mean SST and Annual Cycle

Figure 2-2 provides an illustration and description of the metrics used in our analysis, while Table 2-S provides summary statistics for most of those metrics. The mean annual SST (29-year mean) among the Temperate North Pacific ecoregions varies from about 4°C in Okhotsk and Kamchatka ecoregions to a maximum of about 25 °C in the Cortezian ecoregion (Table 2-S). There is a significant decreasing trend of mean annual SST with mean latitude (Pearson Product Moment Correlation, r = -0.94, p<0.001). The variance in SST is greater for Northwest Pacific ecoregions than in the Northeast Pacific (Table 2-S). The ecoregions with the greatest variance are the Yellow Sea and Sea of Japan, while those with the least variance are the Aleutian, Northern California, and Oregonian ecoregions. The mean annual cycles in SST in the North Pacific ecoregions are shown in Figure 2-3. The percent of variance in SST explained by the annual cycle varies from 31% for the Northern California ecoregion to 94% in the Yellow Sea ecoregion (Table 2-S). In the Northeast Pacific, the three ecoregions extending from Vancouver to Southern California had the lowest percent variance (ranging from 31 to 63%) explained by the annual cycle. For the remainder of the ecoregions in the Northeast Pacific, the amount of variance explained by the annual cycle ranged from 74% to 83%. In the Northwest Pacific, the East China Sea and Sea of Japan ecoregions had the lowest percent variance explained by the annual cycle (58% and 71%, respectively). For the remainder of the ecoregions in the Northwest Pacific, most (80-94%) of the variance in SST was associated with the annual cycle.

Within an ecoregion, the range of the annual cycle is defined by the difference between the minimum 29-year monthly-mean and the maximum 29-year monthly-mean SST (Table 2-S). Generally, the minimum monthly-mean SST in the Temperate North Pacific occurs in February and March, with the exception of the Magdalena and Northern California ecoregions which have minimum SSTs in April. The annual cycle temperature ranges are greater in the Northwest Pacific (mean range of 8 ecoregions = 15 °C) as compared to the Northeast Pacific (mean range of 8 ecoregions = 7 °C). The greatest annual cycle temperature range occurs in the Yellow Sea ecoregion, which has a range > 23 °C, while the Northern California ecoregion has the smallest range of about 3 °C. In the Northeast Pacific, there is a smaller range in the annual cycle at mid-latitudes. A complementary analysis evaluated the number of months within each ecoregion falling within five temperature ranges (Table 2-1). For example, the Northern

California ecoregion falls within only two of the five classes. By contrast, the Yellow Sea has months within all five classes.

The second type of temporal fluctuation experienced within each ecoregion is referred to as within-month SST variations, which is defined as the span of 5th and 95th quantiles and shown as the dotted envelopes in Figure 2-3. Of all the ecoregions the Sea of Japan ecoregion exhibits the highest within-month SST variation (12-15 °C), across all months. In the Northwest Pacific, the Northeast Honshu and East China Sea ecoregions experience maximum within-month variation during the winter, with the East China Sea ecoregion exhibiting within-month SST variations of about 15 °C. In contrast, the northern ecoregions in the Northwest Pacific (Kamchatka, Sea of Okhotsk, and Oyashio) have maximum within-month SST variation during the summer. The Central Kuroshio and Yellow Sea ecoregions have the lowest within-month SST variation in the Northwest Pacific. The magnitude of within-month SST variations is much less in the Northeast Pacific than in the Northwest Pacific. In addition, the seasonal patterns in within-month SST variations are less pronounced in the Northeast Pacific (with the exception of the Cortezian) as compared to the Northwest Pacific. In the Northeast Pacific, the Cortezian ecoregion exhibits large within-month variation (10 °C) during the winter and minimal variation during the summer.

Clustering Analysis

To evaluate similarity in temperature regimes, we performed an Euclidean-distance measure hierarchical clustering analysis based on ecoregion temperature means, medians, 5^{th} and 95^{th} quantiles, and ranges. In each case, the ecoregional SSTs group into two major branches (Figure 2-5) irrespective of what SST metric was used. These two major branches correspond to the Warm and Cold Temperate provinces on either side of the Pacific, splitting the MEOW ecoregions accordingly (Table 2-S). Within the warm temperate cluster, the Central Kuroshio Current and East China Sea ecoregions show no significant difference ($p < 0.05$), while the Southern California ecoregion is the least similar of the five warm temperate ecoregions. Additionally, the Cortezian differs from Southern California and the rest of the warm temperate group. Finally, the Magdalena Transition is segregated from the Central Kuroshio Current-East China Sea grouping.

The cold temperate cluster splits roughly at 35 °N into two secondary branches, which correspond to the northern and southern ecoregions within the Cold Temperate provinces. Within the southern sub-branch, the ecoregions partition to either side of the ocean basin. The Northern California and Oregonian ecoregions are not significantly different, nor are the Northeast Honshu and Sea of Japan ecoregions, while the Yellow Sea differs from both of these sub-branches. Within the northern sub-cluster, a further division separates the West and East Pacific locales, similar to the southern sub-cluster described above. To the east, the North American Pacific Fijordland and Gulf of Alaska ecoregions are not significantly different, though they do differ from the Aleutian Islands ecoregion. In the Western Pacific, the Kamchatka and the Sea of Okhotsk group together, separating from the Oyashio Current. An analysis using nMDS showed a very similar pattern to the clustering (not presented).

Figure 2-6 illustrates a different way to relate the thermal regimes by combining both the extent of similarity based on clustering of monthly-mean SST and temperature ranges (minimum and maximum monthly-mean SST). It is a unique way to visualize both geographic and temperature ranges simultaneously. Each ecoregion is plotted by the minimum and maximum monthly temperature observed over the 29-year record, with the solid line segments linking the ecoregions ordered by latitude on each side of the Pacific. The further offset an ecoregion is from the 45-degree line, the greater the range in the annual cycle. Highly variable ecoregions noted in Table 2-S and Figure 2-3, such as the Cortezian and the Yellow Sea, deviate substantially from the line, while less variable ecoregions lay closer to the line. At the same time, similarity among ecoregions in overall seasonal patterns is captured by concentric ellipses representing different Euclidean distances that were derived from clustering on mean seasonal temperatures (Figure 2-5). In this case, Euclidean distances of 8.7 and 17 were chosen as they represent the maximum dissimilarity for any non-significant split (Gulf of Alaska and Pacific Fijordland) and the value that separates Southern California from the rest of the Warm Temperate ecoregions (Figure 2-5).

Discussion

Data uncertainties, challenges, and availability

Determining SST values in nearshore environments over a regional scale presented a significant challenge. Seasonal patterns in sea fog result in high levels of missing data, such as during the summer in the Yellow Sea [*Zhang et al.*, 2009] and Okhotsk ecoregions [*Tokinaga and Xie*, 2009]. Upwelling regions, such as the Oregonian and Northern California ecoregions, also have missing data related to fog and cloud cover associated with strong thermal gradients between the land and coastal ocean [*Johnstone and Dawson*, 2010; *J. Vazquez-Cuervo et al.*, 2004; *Jorge Vazquez-Cuervo et al.*, 2010]. Presence of sea ice also accounts for missing data, as the Sea of Okhotsk and Kamchatka Sea are partially covered with ice during winter months [*Reynolds et al.*, 2002].

Moreover, failure of the AVHRR atmospheric correction to accurately deal with aerosol contamination due to Saharan dust storms and volcanic eruptions (e.g. Pinitubo in 1991) also led to long periods (months) of missing data [*Diaz et al.*, 2001; *J. Vazquez-Cuervo et al.*, 2004]. In addition, our decision to limit the SST data based on quality criteria and, to a much lesser extent, elimination of SST values < -2 °C resulted in missing data. Due to varying data quality, there are differences in the extent of missing data between ecoregions and between months. For example, there is a high level of missing data in the Subarctic Northwest Pacific ecoregions during the winter (Figure 2-4). The worst case was Okhotsk in February with more than 90% of the data not meeting the quality standard. Conversely, 95% of the data values fell within acceptable quality limits in the Magdalena Transition ecoregion for the same month. In fact, mid-latitude ecoregions of the Northeast Pacific generally had good coverage year round (> 80%). The abundance of data aggregated at the ecoregional scale overcomes the problem with missing data. Additionally, our SST analysis agrees with previous studies, such as large annual range in Yellow Sea [*Chu et al.*, 2005] and small annual range in Northern California [*Wyrtki*, 1965], suggesting that data are adequate for a seasonal and ecoregional analysis.

Oceanographic Drivers

Sea surface temperature variations result from the interaction of heat exchange at the sea surface, circulation patterns, and mixing processes [*Wyrtki*, 1965]. The primary circulation of the North Pacific is driven by the anticyclonic North Pacific Gyre (Figure 2-1), which consists of the swiftly-moving, poleward flowing, Kuroshio Current System (KCS) and the relatively slow-moving, equatorward flowing, California Current (CCS) connected by the East-West aligned North Pacific Current (NPC) and North Equatorial Current (NEC). The KCS and CCS are the main north-south boundary currents that largely regulate Pacific Ocean temperatures by transporting warm equatorial waters poleward by the KCS and vice versa by the CCS. The KCS is a deep, narrow, high-volume, swiftly-moving [*Qiu*, 2001] western boundary current that extends from the East China Sea north to its confluence with the subarctic, south-flowing Oyashio Current (OC, [*Qiu*, 2001]). Conversely, the CCS is a shallow (~200 m), broad (~1000 km), slow-moving [*Checkley Jr and Barth*, 2009] current that flows equatorward from the Gulf of Alaska, along the coasts of British Columbia to California [*Chelton*, 1984]. At the point of Baja California, it turns westward, becoming the North Equatorial Current (NEC).

Nearshore SSTs within the CCS are also influenced by alongshore wind stress that result in high upwelling variability, especially in spring and summer [*Barth et al.*, 2005; *Barth et al.*, 2007]. This upwelling results in the relatively constant year-round SSTs (Figure 2-3, Table 2-S) from Vancouver Island (Canada) to Southern California (USA). The warmer and more variable regions of SST in Baja California and the Cortezian result from sparse cloud cover at low latitudes and rapid solar heating [*Huyer*, 1983]. In the west, the KCS features a more complicated ocean current system. Temperatures are governed by the confluence of the clockwise-flowing North Pacific Gyre and the anti-clockwise flowing Western

Subarctic Gyre. The merging of warm, salty waters of the KCS from the south with relatively cooler, fresher waters of the OC and EKC from the north (Figure 2-1) generates a seasonally-complex SST pattern in the Northwest Pacific [*Qiu*, 2001]. The OC-KCS convergence occurs off the east coast of Hokkaido, Japan, forming the Eastward-flowing Kuroshio Extension (KE, Figure 2-1), which infiltrates the inland seas of Japan and Okhotsk, creating a complicated and seasonally wide-ranging temperature pattern along their shores.

Ecoregional Analysis

In this paper, we evaluated temperature patterns within coastal ecoregions in the North Pacific as defined in the MEOW biogeographic schema ([*Spalding et al.*, 2007], Figure 2-1), which offers several pragmatic advantages. First, aggregating the data by ecoregion mitigates the problems associated with missing data, particularly in the high latitude ecoregions. Second, several types of analyses were impossible or at least impractical with over 500,000 individual data points, such as clustering to reveal similarities and dissimilarities in temperature regimes along the coast. The third is that analysis at this scale reduces the effects of small-scale noise in the data. Ecoregional analysis also allows relating regional temperature patterns to large-scale distributional patterns of individual species and types of assemblages (e.g., coral reefs, kelp forests). While not the focus of this paper, overlaying species' biogeographic distributions on ecoregion temperature regimes allows the generation of a general thermal classification for a species (e.g., see [*Hall*, 1964]). Our decision to use the MEOW framework was based on the fact that MEOW is a biogeographic system for coastal marine areas based on taxonomic configurations and patterns of dispersal. Furthermore, MEOW allows for a more detailed ecoregional analysis than previous broader-scale schemes (e.g. [*Golikov et al.*, 1990; *Pauley et al.*, 2008]), and is being utilized by ecologists evaluating regional patterns (e.g. [*Piepenburg et al.*, 2011]), the Ocean Biogeographic Information System (OBIS, http://iobis.org/home), and organizations (e.g., the "Non-indigenous Aquatic Species" Working group of the North Pacific Marine Science Organization).

There are, of course, questions that cannot be addressed by summarizing SST by ecoregion, such as comparing the latitudinal rate of temperature change in the Northwest and Northeast Pacific or identifying the temperatures associated with the thermal breaks at the borders of an ecoregion (e.g., [*Blanchette et al.*, 2008]). However, as mentioned, the processed data are provided [*Payne et al.*, 2011] for such analyses.

The major aim of this effort was to evaluate regional temperature patterns in the North Pacific. In general, the mean annual SSTs (29-year mean) in this study are consistent with previous published studies from respective regions [*Wyrtki*, 1965; *Yashayaev and Zveryaev*, 2001]. One broad pattern found in this analysis is that the Northwest Pacific ecoregions at all latitudes experience a greater range in the annual cycle than do the Northeast Pacific ecoregions (Figure 2-3 and Table 2-S), which is consistent with previous studies [*Wyrtki*, 1965; *Yashayaev and Zveryaev*, 2001]. For example, the range of annual cycle was from about 3 °C to 9 °C in the Cold Temperate Northeast Pacific province ecoregions, compared to a range of 12 °C to almost 24°C in the Cold Temperate Northwest Pacific province ecoregions. While less pronounced, a similar pattern was also observed in the Warm Temperate ecoregions, which show an annual range of about 6 to 12 °C in the Northeast Pacific versus a range of about 11 to 14 °C in the Northwest Pacific. The Yellow Sea experiences the largest range in annual cycle, which is attributed to the influence of the Asian monsoon [*Chu et al.*, 2005]. Conversely, the nearshore waters of the Oregonian ecoregion show the smallest seasonal amplitude in the annual cycle range, similar to the findings of *Wyrtki* [1965] and *Yashayaev and Zveryaev* [2001].

Previous studies of SSTs in the central portion of the North Pacific basin have found that approximately 95% of the variance in SST is associated with the mean annual cycle and the percent variance associated with the mean annual cycle decreases near the coasts particularly in the Northeast Pacific [*Yashayaev and Zveryaev*, 2001]. In our analysis, the variance in SST associated with the annual cycle varied from 31% to 94%, and the annual cycle explained less of the variance in the northeastern ecoregions than for those in the northwestern ecoregions. It is not surprising that the amount of variance associated with the annual cycle were less than those in the central portion of the Pacific basin, since nearshore SSTs are influenced by coastal upwelling, riverine and land effects, and other nearshore processes.

Moreover, northwestern ecoregions generally experience greater within-month temperature variations than do northeastern ecoregions at approximately the same latitude (Figure 2-3). The within-month temperature variations are a result of both temporal and spatial variability in SSTs within an ecoregion. The steeper meridional temperature gradients within ecoregions in the Northwest Pacific as compared to the Northeast Pacific are likely responsible for a portion of this variation [*Wyrtki*, 1965]. This is particularly likely in the Sea of Japan where within-month temperature variations can be as great as 15 °C. In addition, the Japan/East Sea region is known for dramatic weather-system shifts that occur over the time-scale of a few days [*Dorman et al.*, 2006], which would increase within-month variation.

Comparison of Ecoregional Temperature Patterns to Biogeographic Schema

Temperature is a driver of biotic distributions on regional and global scales [*Briggs*, 1995; *Golikov et al.*, 1990; *Mislan et al.*, 2009; *Sorte et al.*, 2010], thus we would expect some correspondence between the temperature patterns generated from the SST data and the patterns of the biologically-based MEOW provinces and ecoregions. Clustering on monthly-mean SSTs results in a primary division that corresponds unambiguously to the MEOW province categorizations of "Warm Temperate" versus "Cold Temperate" (Figure 2-5). Thus, biotic composition as inferred from the MEOW province boundaries may be related to nearshore SST. Furthermore, within each of the provinces, a number of ecoregions show distinct thermal regimes, supporting a biogeographical break. One example is the Southern California ecoregion that is markedly different from its neighboring Baja regions (Cortezian and Magdalena ecoregions). The dissimilarity is likely due to the circulation regime off the California coast; while upwelling is a critical factor in temperature mediation to the north, it is not as prevalent in the

Magdalena and Cortezian ecoregions [*Checkley Jr and Barth*, 2009; *Hickey*, 1979]. Correspondingly, the range of mean temperatures in the Southern California Bight ecoregion is 3 °C to almost 9 °C smaller than the other ecoregions within the warm temperate cluster (Table 1-S). However, there was no significant difference in mean seasonal regimes with five pairs of neighboring ecoregions. One possibility is that some other component of the thermal regime other than the overall mean seasonal pattern drives the biogeographic patterns. For example, the occurrence of four months with a mean temperature < 5°C in the Gulf of Alaska (Table 2-1) may be a key biological factor separating the biota in the Gulf from the North American Pacific Fijordland to the south. Alternatively, some factor(s) other than temperature may be important in generating distinct biotas between ecoregions, such as regional differences in primary productivity or effects of circulation patterns on larval dispersal. The last possibility is that the similarities in temperature patterns may indicate that the biotas in the neighboring ecoregions are not as distinct as suggested by the ecoregional demarcation. It is beyond the scope of this paper to evaluate these alternatives, but we suggest that further analyses of the biotic similarity in these ecoregions across a range of different taxa would be fruitful.

It is also informative to compare SST patterns with the biogeographic schema defined by *Hall* [1964] and by NOAA's Large Marine Ecosystems (LMEs) [*Pauley et al.*, 2008; *Sherman et al.*, 2007]. The ecoregion clustering in Figure 2-7 is represented by combining MEOW ecoregions between which our clustering analysis found no significant differences (see Figure 2-5) into single entities that we term "SST clusters." For example, the Oregonian and Northern California ecoregions group together to form a single SST cluster. It is clear that some of Hall's marine climate classifications in the Northeast Pacific match reasonably well with the clustering based on temperature. In the Northeast Pacific, Hall's "Outer Tropical" climate envelopes the Magdalena Transition; similarly, his "Warm Temperate" climate encompasses the Southern California Bight of the Warm Temperate Northeast Pacific province. Hall's "Mild Temperate" climate roughly corresponds to the SST cluster comprised of the combined Northern

California and Oregonian ecoregions. However, Hall's "Cold" and "Cool Temperate" divisions do not agree as well with the subarctic SST clusters. Hall's "Cold" climate encompasses the Gulf of Alaska, Kamchatka, and Sea of Okhotsk ecoregions. Our results do not indicate that the Gulf of Alaska should fall within the "Cold" climate, as it has warmer minimum monthly temperatures than the Kamchatka and Sea of Okhotsk and its thermal regime does not differ from the North American Pacific Fjordland.

The correspondence of Hall's classifications in the Northwest Pacific is more complex. The Kamchatka and Sea of Okhotsk SST cluster falls completely within Hall's "Cold" marine climate, while the Oyashio ecoregion falls within Hall's "Cool Temperate" ecoregions, and has a thermal regime which differs from adjacent ecoregions. These breakouts appear generally consistent with our observed SST patterns. However, our cluster analysis found no difference between Hall's "Inner Tropical" and "Outer Tropical" climates in that Kuroshio and East China Sea ecoregions were not distinct in thermal patterns. Similarly, the Northeastern Honshu and Sea of Japan SST cluster that runs between the Pacific Ocean-facing sides of Honshu and Hokkaido Islands spans Hall's "Warm Temperate" and "Mild Temperate" marine climate zones.

As shown in Figure 2-7, our SST clusters do not agree as well with LMEs, in particular in the Northeast Pacific. This difference is most apparent where the "California Current" LME combines the three distinct thermal SST clusters of the Northern California - Oregonian, the Southern California Bight, and the Magdalena Transition. As such, the "California Current" LME traverses the border between the Warm Temperate Northeast Pacific and Cold Temperate Northeast Pacific provinces. As seen in Table 2-S, there is a two-fold difference in SST range between southernmost (Magdalena) and northernmost (Oregonian) ecoregions contained within this single LME. Furthermore, significant differences between LMEs and the cluster-defined SST clusters of this analysis exist in the Northwest Pacific, where LME boundaries find similarities in different locations than indicated in our analysis. The SST cluster scheme lumps the East China Sea and Central Kuroshio Current ecoregions, which are separate according to the

LME classification, while LMEs combine the Kuroshio and Honshu that we found had distinct thermal regimes. Some potential reasons for these discrepancies are that LME divisions are based on physiographic and trophic interactions [*Sherman et al.*, 2007] and encompass the entire shelf area compared to our nearshore analysis.

Our clustering efforts are based on nearshore SST within MEOW ecoregions, which are derived from a synthesis of previous biogeographic efforts [*Spalding et al.*, 2007]. In several cases, clustering of mean temperatures failed to pick up the differences on an ecoregional scale, that is, some neighboring ecoregions showed no significant difference when clustered based on mean SST. Comparison of the thermal patterns with the Hall and LME schemas also demonstrated several differences. As mentioned above there are several potential causes for differences between the temperature patterns and the biogeographic boundaries. These areas of major discrepancies deserve further study to evaluate the biotic reality of the boundaries and, assuming an ecologically realistic boundary, the cause(s) for biotic separation with neighboring regions with similar thermal regimes. In particular, all three biogeographic schemas have notable differences in the interface between the sub-arctic and arctic. This raises questions on how this interface should be defined, since this boundary is expected to shift poleward due to climate change [*IPCC*, 2007].

Potential Relationships to Climate Change

Nearshore SSTs will change in the future in response to climate change [*Mislan et al.*, 2009]. The North Pacific is especially vulnerable to environmental change, as it is reported to be warming 2-3 times faster than the South Pacific [*Rivadeneira and Fernandez*, 2005]. The present analysis and the processed data available in Payne et al. [*Payne et al.*, 2011] provide nearshore temperature data against which to evaluate future measurements of SSTs in nearshore environments and a baseline on which to project potential climate change scenarios. Additionally, using the present regional temperature patterns, it is possible to speculate which ecoregions might be most susceptible to temperature increases, assuming that, in general, organisms living in areas with smaller temperature variations would be more susceptible to temperature increases (see *Huey et al.* [2009]). Thus, the nearshore flora and fauna of Northeast Pacific ecoregions may be more susceptible to temperature increases than organisms in Northwest Pacific ecoregions, assuming an equivalent temperature increase. In particular, organisms in the Northern California ecoregion may be highly susceptible given the ecoregion's low annual temperature range, while organisms in the Aleutian ecoregion may be highly susceptible based on the ecoregion's low within month variation (Table 2-S, Figure 2-3). This speculation needs to be evaluated both by comparing the actual temperature ranges of organisms from field surveys and by evaluating temperature tolerances with experimental studies. Nonetheless, we suggest that analyses of existing temperature regimes can provide insights into what organisms and regions will be at the greatest risk from this aspect of climate change.

Acknowledgments

This publication was subjected to review by the National Health and Environmental Effects Research Laboratory's Western Ecology Division of the EPA, and the USGS Western Fisheries Research Center, and is approved for publication. However, approval does not signify that the contents reflect the views of the U.S. EPA. The use of trade, firm, or corporation names in this publication are for the information and convenience of the reader; such use does not constitute official endorsement or approval by the U. S. Department of Interior, the U. S. Geological Survey, or the U. S. Environmental Protection Agency of any product or service to the exclusion of others that may be suitable. We wish to thank D. Douglas and J. Vazquez-Cuervo for their insightful reviews that helped strengthen this manuscript, and Melanie Frazier, who provided assistance with using R for data analysis. We also thank the anonymous reviewers whose comments substantially improved our manuscript.

References

Adey, W. H., and R. S. Steneck (2001), Thermogeography over time creates biogeographic regions: a temperature/space/time-integrated model and an abundance-weighted test for benthic marine algae, *Journal of Phycology*, *37*(5), 677-698.

Barth, J. A., S. D. Pierce, and T. J. Cowles (2005), Mesoscale structure and its seasonal evolution in the northern California Current System, *Deep-Sea Research Part Ii-Topical Studies in Oceanography*, *52*(1-2), 5-28.

Barth, J. A., B. A. Menge, J. Lubchenco, F. Chan, J. M. Bane, A. R. Kirincich, M. A. McManus, K. J. Nielsen, S. D. Pierce, and L. Washburn (2007), Delayed upwelling alters nearshore coastal ocean ecosystems in the northern California current, *Proceedings of the National Academy of Sciences of the United States of America*, *104*(10), 3719-3724.

Blanchette, C. A., C. M. Miner, P. T. Raimondi, D. Lohse, K. E. K. Heady, and B. R. Broitman (2008), Biogeographical patterns of rocky intertidal communities along the Pacific coast of North America, *Journal of Biogeography*, *35*(9), 1593-1607.

Briggs, J. C. (1974), *Marine zoogeography [by] John C. Briggs*, x, 475 p. pp., McGraw-Hill, New York.

Briggs, J. C. (1995), *Global Biogeography*, 1 ed., 452 pp., Elsevier Science B. V., Amsterdam, The Netherlands.

Briggs, J. C. (2007), Marine longitudinal biodiversity: causes and conservation, *Diversity and Distributions*, *13*(5), 544-555.

Broitman, B. R., N. Mieszkowska, B. Helmuth, and C. A. Blanchette (2008), Climate and Recruitment of Rocky Shore Intertidal Invertebrates in the Eastern North Atlantic, *Ecology*, *89*(11), S81-S90.

Broitman, B. R., P. L. Szathmary, K. A. S. Mislan, C. A. Blanchette, and B. Helmuth (2009), Predator-prey interactions under climate change: the importance of habitat vs body temperature, *Oikos*, *118*(2), 219-224.

Casey, K. S. (2002), Daytime vs nighttime AVHRR sea surface temperature data: A report regarding Wellington et al. (2001), *Bulletin of Marine Science*, *70*(1), 169-175.

Casey, K. S., and D. Adamec (2002), Sea surface temperature and sea surface height variability in the North Pacific Ocean from 1993 to 1999, *Journal of Geophysical Research-Oceans*, *107*(C8), 12.

Checkley Jr, D. M., and J. A. Barth (2009), Patterns and processes in the California Current System, *Progress In Oceanography*, *83*(1-4), 49-64.

Chelton, D. B. (1984), Seasonal Variability of Alongshore Geostrophic Velocity Off Central California, *J. Geophys. Res.*, *89*(C3), 3473-3486.

Chu, P., C. Yuchun, and A. Kuninaka (2005), Seasonal variability of the Yellow Sea/East China Sea surface fluxes and thermohaline structure, *Advances in Atmospheric Sciences*, *22*(1), 1-20.

Clarke, K. R., and R. N. Gorley (2006), *PRIMER v6: User Manual/Tutorial*, 190 pp., PRIMER-E Ltd., Plymouth.

Diaz, J. P., M. Arbelo, F. J. Exposito, G. Podesta, J. M. Prospero, and R. Evans (2001), Relationship between errors in AVHRR-derived sea surface temperature and the TOMS Aerosol Index, *Geophysical Research Letters*, *28*(10), 1989-1992.

Dorman, C. E., C. A. Friehe, D. Khelif, A. Scotti, J. Edson, R. C. Beardsley, R. Limeburner, and S. S. Chen (2006), Winter Atmospheric Conditions over the Japan/East Sea: The Structure and Impact of Severe Cold-Air Outbreaks, *Oceanography*, *19*(3), 96-109.

Golikov, A. N., M. A. Dolgolenko, N. V. Maximovich, and O. A. Scarlato (1990), Theoretical approaches to marine biogeography, *Marine Ecology Progress Series*, *63*, 289-301.

Gollash, S. (2006), Assessment of the introduction potential of aquatic alien species in new environments, in *Assessment and Control of Biological Invasion Risks*, edited by F. Koike, M. N. Clout, M. Kawamichi, M. De Poorter and K. Iwatsuki, pp. 88-91, Shoukadoh Book Sellers, IUCN, Kyoto, Japan; Gland, Switzerland.

Hall, C. A., Jr. (1964), Shallow-Water Marine Climates and Molluscan Provinces, *Ecology*, *45*(2), 226-234.

Herborg, L.-M., C. L. Jerde, D. M. Lodge, G. M. Ruiz, and H. J. MacIsaac (2007), Predicting Invasion Risk Using Measures of Introduction Effort and Environmental Niche Models, *Ecological Applications*, *17*(3), 663-674.

Hickey, B. M. (1979), The California current system - hypotheses and facts, *Oceanography*, *8*, 191-279.

Huey, R. B., C. A. Deutsch, J. J. Tewksbury, L. J. Vitt, P. E. Hertz, H. J. Álvarez Pérez, and T. Garland (2009), Why tropical forest lizards are vulnerable to climate warming, *Proceedings of the Royal Society B: Biological Sciences*, *276*(1664), 1939-1948.

Huyer, A. (1983), Coastal upwelling in the California current system, *Progress in Oceanography*, *12*(3), 259-284.

IPCC (2007), Climate change 2007: Impacts, adaptation and vulnerability. Contribution of Working Group II to the Fourth Assessment Report of the Intergovernmental Panel on Climage Change*Rep.*, 1-976 pp, Cambridge.

Johnstone, J. A., and T. E. Dawson (2010), Climatic context and ecological implications of summer fog decline in the coast redwood region, *Proceedings of the National Academy of Sciences*, *107*(10), 4533-4538.

Keister, J. E., and P. T. Strub (2008), Spatial and interannual variability in mesoscale circulation in the northern California Current System, *Journal of Geophysical Research-Oceans*, *113*(C4).

Kilpatrick, K. A., G. P. Podesta, and R. Evans (2001), Overview of the NOAA/NASA advanced very high resolution radiometer Pathfinder algorithm for sea surface temperature and associated matchup database, *Journal of Geophysical Research-Oceans*, *106*(C5), 9179-9197.

Longhurst, A. R. (2007), *Ecological geography of the sea --2nd ed.*, 542 pp., Elsevier Academic Press, Amsterdam ; Boston, MA

Mislan, K. A. S., D. S. Wethey, and B. Helmuth (2009), When to worry about the weather: Role of tidal cycle in determining patterns of risk in intertidal ecosystems, *Global Change Biology*, *15*, 3056-3065.

Pauley, D., et al. (2008), Fisheries in large marine ecosystems: descriptions and diagnoses, in *The UNEP Large Marine Ecosystem Report: A perspective on changing conditions in LMEs of the world's regional seas*, edited by K. S. a. G. Hempel, pp. 23-40, UNEP, Nairobi, Kenya.

Payne, M. C., D. A. Reusser, H. Lee II, and C. A. Brown (2011), Moderate-resolution sea surface temperature data for the nearshore North Pacific: U.S. Geological Survey Open-File Report 2010-1251*Rep.*, 16 pp.

Pearce, A., F. Faskel, and G. Hyndes (2006), Nearshore sea temperature variability off Rottnest Island (Western Australia) derived from satellite data, *International Journal of Remote Sensing*, *27*(12), 2503 - 2518.

Piepenburg, D., et al. (2011), Towards a pan-Arctic inventory of the species diversity of the macro- and megabenthic fauna of the Arctic shelf seas, *Marine Biodiversity*, *41*, 51-70.

Pirhalla, D. E., V. Ransibrahmanakul, R. Clark, A. Desch, T. Wynne, and M. Edwards (2009), An Oceanographic Characterization of the Olympic Coast National Marine Sanctuary and Pacific Northwest: Interpretive Summary of Ocean Climate and Regional Processes Through Satellite Remote Sensing. NOAA Technical Memorandum NOS NCCOS 90, edited, p. 53, Prepared by NCCOS's Coastal Oceanographic Assessments, Status and Trends Division in cooperation with the National Marine Sanctuary Program, Silver Spring, MD.

Qiu, B. (2001), Kuroshio and Oyashio Currents, in *Encyclopedia of Ocean Sciences*, edited by J. Steele, S. Thorpe and K. Turekian, pp. 1413-1425, Academic Press.

R Development Core Team (2009), R: A language and environment for statistical computing., edited, R Foundation for Statistical Computing, Vienna, Austria.

Reusser, D. A., and H. Lee (2011), Evolution of natural history information in the 21st century – developing an integrated framework for biological and geographical data, *J. Biogeogr.*, *38*(7), 1225-1239.

Reynolds, R. W., N. A. Rayner, T. M. Smith, D. C. Stokes, and W. Q. Wang (2002), An improved in situ and satellite SST analysis for climate, *J. Clim.*, *15*(13), 1609-1625.

Rivadeneira, M. M., and M. Fernandez (2005), Shifts in southern endpoints of distribution in rocky intertidal species along the south-eastern Pacific coast, *Journal of Biogeography*, *32*(2), 203-209.

Roberts, J. J., B. D. Best, D. C. Dunn, E. A. Treml, and P. N. Halpin (2010), Marine Geospatial Ecology Tools: An integrated framework for ecological geoprocessing with ArcGIS, Python, R, MATLAB, and C++, *Environmental Modelling & Software*, *25*(10), 1197-1207.

Sherman, K., M.-C. Aquarone, and S. Adams (2007), Global Applications of the Large Marine Ecosystem Concept 2007-2010, edited by U. S. D. o. Commerce, p. 71, National Marine Fisheries Service, Northeast Fisheries Science Center, Woods Hole, MA.

Sorte, C. J. B., S. L. Williams, and J. T. Carlton (2010), Marine range shifts and species introductions: comparative spread rates and community impacts, *Global Ecology and Biogeography*, *19*(3), 303-316.

Spalding, M. D., et al. (2007), Marine ecoregions of the world: a bioregionalization of coastal and shelf areas.(marine biogeography)(Report), *BioScience*, *57*(7), 573(511).

Tokinaga, H., and S.-P. Xie (2009), Ocean tidal cooling effect on summer sea fog over the Okhotsk Sea, *Journal of Geophysical Research*, *114*(D14102), doi:10.1029/2008JD011477.

Vazquez-Cuervo, J., E. M. Armstrong, and A. Harris (2004), The effect of aerosols and clouds on the retrieval of infrared sea surface temperatures, *J. Clim.*, *17*(20), 3921-3933.

Vazquez-Cuervo, J., E. M. Armstrong, K. S. Casey, R. Evans, and K. Kilpatrick (2010), Comparison between the Pathfinder Versions 5.0 and 4.1 Sea Surface Temperature Datasets: A Case Study for High Resolution, *Journal of Climate*, *23*(5), 1047-1059.

Venegas, R. M., P. T. Strub, E. Beier, R. Letelier, A. C. Thomas, T. Cowles, C. James, L. Soto-Mardones, and C. Cabrera (2008), Satellite-derived variability in chlorophyll, wind stress, sea surface height, and temperature in the northern California Current System, *J. Geophys. Res.*, *113*.

Wessel, P., and W. H. F. Smith (1996), A global, self-consistent, hierarchical, high-resolution shoreline database, *J. Geophys. Res.*, *101*(B4), 8741-8743.

Wethey, D. S., and S. A. Woodin (2008), Ecological hindcasting of biogeographic responses to climate change in the European intertidal zone, *Hydrobiologia*, *606*, 139-151.

Wyrtki, K. (1965), The Annual and Semiannual Variation of Sea Surface Temperature in the North Pacific Ocean, *Limnology and Oceanography*, *X*(3), 307-313.

Yashayaev, I. M., and Zveryaev, II (2001), Climate of the seasonal cycle in the North Pacific and the North Atlantic Oceans, *International Journal of Climatology*, *21*(4), 401-417.

Zhang, S.-P., S.-P. Xie, Q.-Y. Liu, Y.-Q. Yang, X.-G. Wang, and Z.-P. Ren (2009), Seasonal Variations of Yellow Sea Fog: Observations and Mechanisms, *Journal of Climate*, *22*(24), 6758-6772.

Table 2-1. Number of months in various temperature intervals for ecoregions of the Temperate North Pacific.*

		Number of Months				
Province	**Ecoregion**	**≤ 5 °C**	**> 5 °C < 12 °C**	**≥ 12 °C < 20 °C**	**≥ 20 °C < 25 °C**	**≥ 25 °C**
CTNEP	Aleutian Islands	6	6	0	0	0
	Gulf of Alaska	4	7	1	0	0
	N. American Pac. Fijordland	0	9	3	0	0
	OR, WA, Vancouver	0	7	5	0	0
	Northern CA	0	1	11	0	0
WTNEP	S. CA Bight	0	0	10	2	0
	Cortezian	0	0	3	3	6
	Magdalena Transition	0	0	4	5	3
CTNWP	Sea of Okhotsk	7	4	1	0	0
	Kamchatka Coast	7	5	0	0	0
	Oyashio Current	6	4	2	0	0
	Northeastern Honshu	0	5	5	2	0
	Sea of Japan	0	6	4	2	0
	Yellow Sea	3	2	4	2	1
WTNWP	Central Kuroshio Current	0	0	5	4	3
	East China Sea	0	0	6	3	3

*The temperature intervals shown here, based upon monthly-mean SST values, have been previously identified as being critical for marine biota [*Briggs*, 1995; 2007].

Table 2-S Summary statistics of sea surface temperatures (SSTs), including mean, minimum and maximum monthly mean, range of annual cycle, and variances in the Temperate North Pacific ecoregions. The mean latitude and longitude for each ecoregion is shown in parentheses. CTNEP = Cold Temperate Northeast Pacific; WTNEP = Warm Temperate Northeast Pacific; CTNWP = Cold Temperate Northwest Pacific; WTNWP = Warm Temperate Northwest Pacific.

		Number of Months				
Province	**Ecoregion**	**≤5°C**	**>5°C <12°C**	**≥12°C <20°C**	**≥20°C <25°C**	**≥25°C**
CTNEP	Aleutian Islands	6	6	0	0	0
	Gulf of Alaska	4	7	1	0	0
	N. American Pac. Fijordland	0	9	3	0	0
	OR, WA, Vancouver	0	7	5	0	0
	Northern CA	0	1	11	0	0
WTNEP	S. CA Bight	0	0	10	2	0
	Cortezian	0	0	3	3	6
	Magdalena Transition	0	0	4	5	3
CTNWP	Sea of Okhotsk	7	4	1	0	0
	Kamchatka Coast	7	5	0	0	0
	Oyashio Current	6	4	2	0	0
	Northeastern Honshu	0	5	5	2	0
	Sea of Japan	0	6	4	2	0
	Yellow Sea	3	2	4	2	1
WTNWP	Central Kuroshio Current	0	0	5	4	3
	East China Sea	0	0	6	3	3

*The temperature intervals shown here, based upon monthly-mean SST values, have been previously identified as being critical for marine biota [45,53].
doi:10.1371/journal.pone.0030105.t001

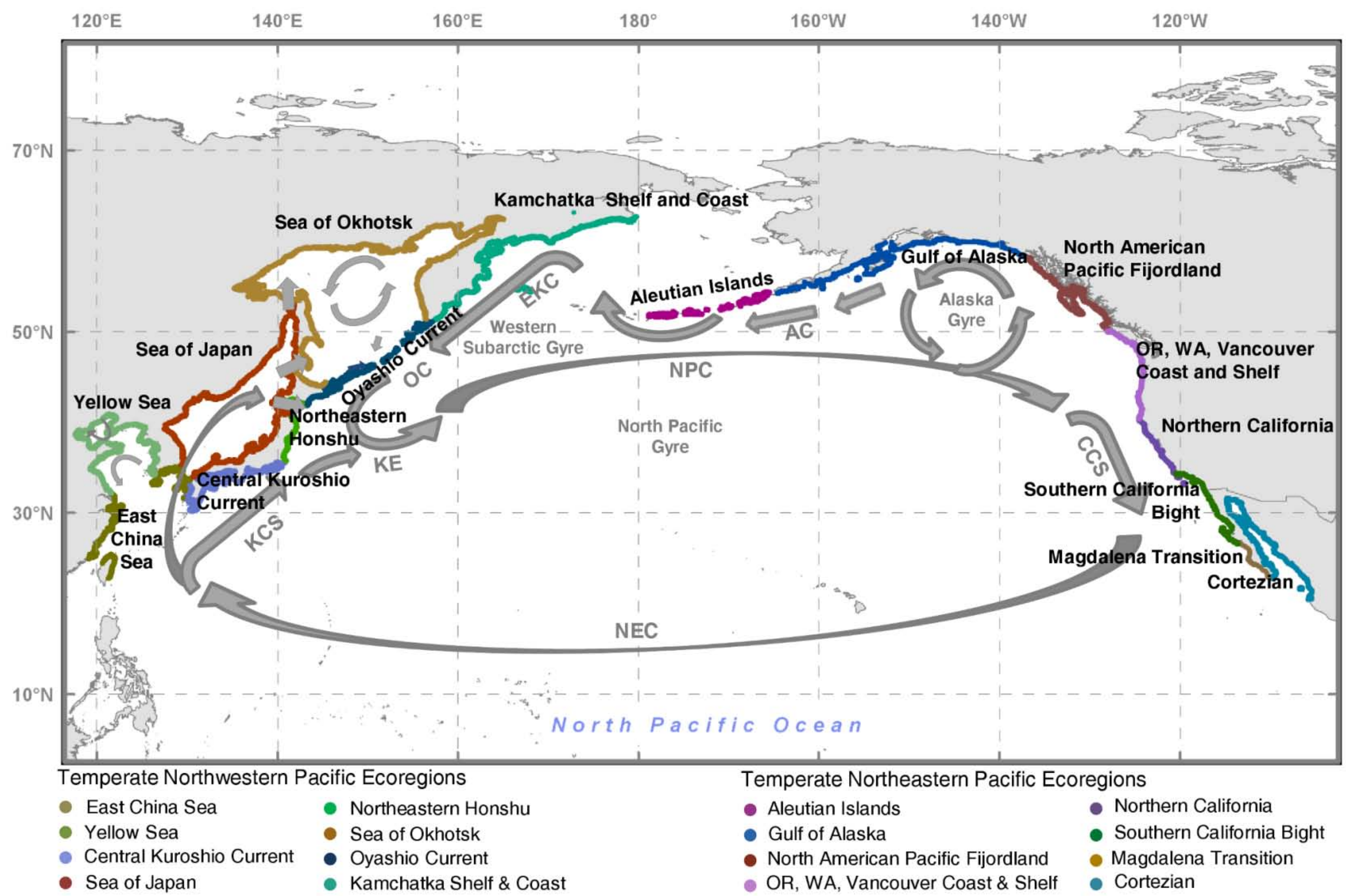

Figure 2-1. Temperate North Pacific realm, and the 16 MEOW ecoregions included in this paper. Major surface circulation pathways are labeled on the map and indicated with blue arrows, including the North Pacific Current (NPC), California Current System (CCS), North Equatorial Current (NEC), Kuroshio Current System (KCS), Kuroshio Extension (KE), Oyashio Current (OC), East Kamchatka Current (EKC).

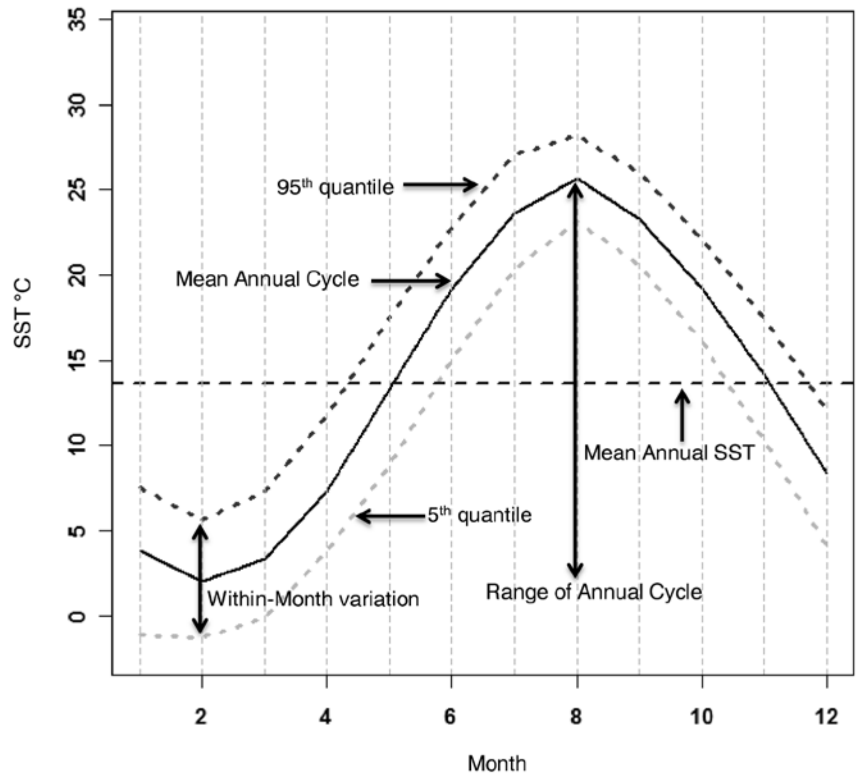

SST Analysis Metric	Metric Description	Metric Dimensions
Derived SST values	SST values derived from PFSST product. Each value represents a monthly mean for each grid cell	1 value per grid cell of acceptable quality, 1 raster per month over 29 years (340 rasters)
Monthly-mean SST per ecoregion	The 29-year average of all of the derived SST values (above product) within an ecoregion for each of the 12 months.	16 ecoregions x 12 months
Mean annual cycle	12 monthly means for each ecoregion	16 annual cycles (Figure 3B)
Range of annual cycle	Difference between warmest (maximum) monthly mean and coolest (minimum) monthly mean per ecoregion	16 ranges
Mean annual SST (29-year mean)	Mean of the monthly mean SST per ecoregion over the 29-year period	1 value x 16 ecoregions
Variance in SST	Variance of all derived SST values within an ecoregion over the 29-year period	1 value x 16 ecoregions
Within-month SST variations (5th and 95th quantiles)	The 5th and 95th quantile values for each month of all derived SST values within each ecoregion.	2 values x 12 months x 16 ecoregions

Figure 2-2. Annual cycle metrics analyzed in this study. Generalized illustration and tabular description of metrics used to evaluate the annual SST cycle in the North Pacific ecoregions. Individual, ecoregion-specific annual cycles are depicted in Figure 3.

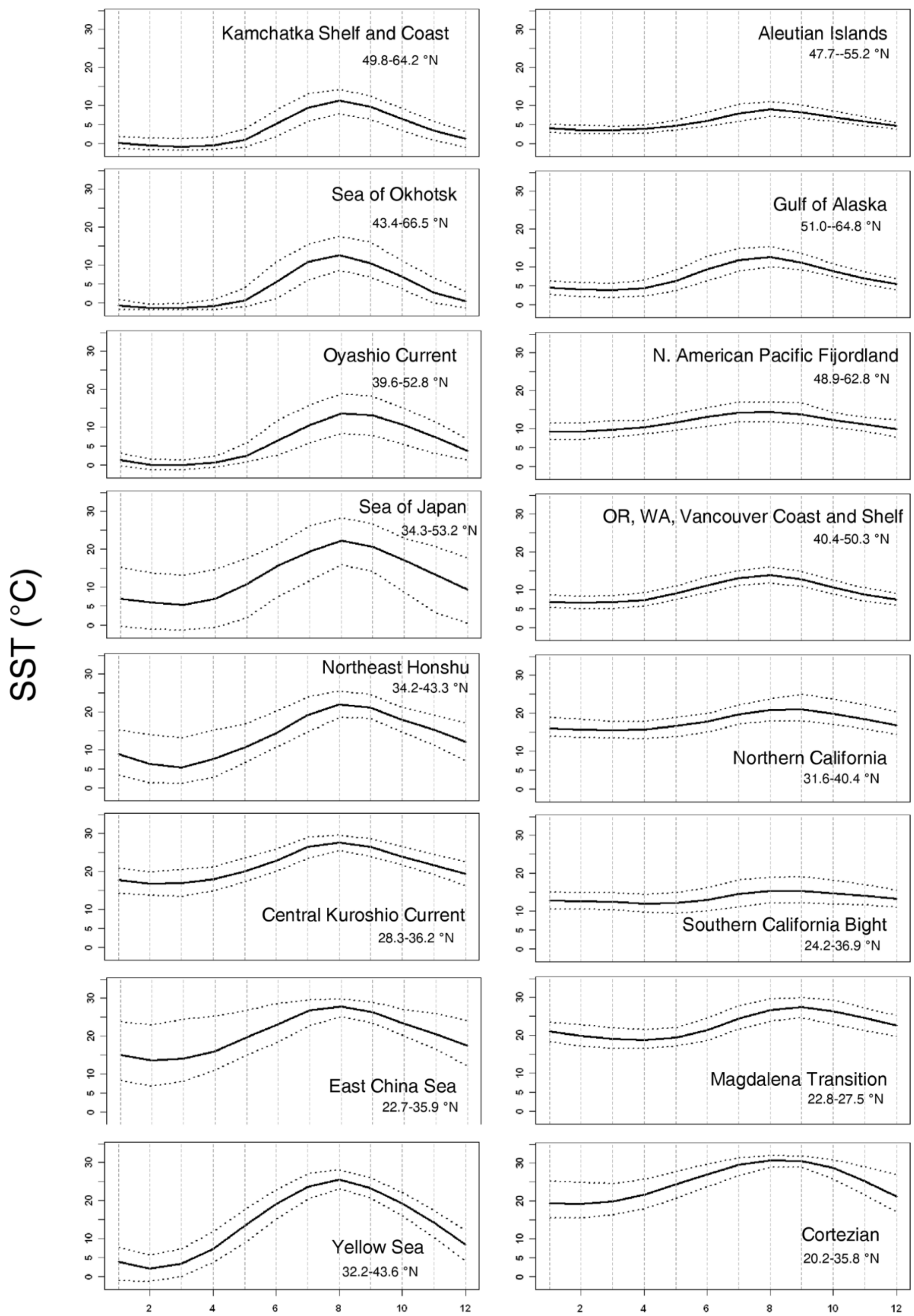

Figure 2-3. Monthly-mean SST in each of the Temperate North Pacific ecoregions based on a 29-year dataset. The horizontal axis represents months (e.g. 1 = January, 12 = December). The solid lines show the monthly-mean SST values. The dotted lines show the upper 95th and lower 5th quantiles of SST, which is a measure of within-month variation.

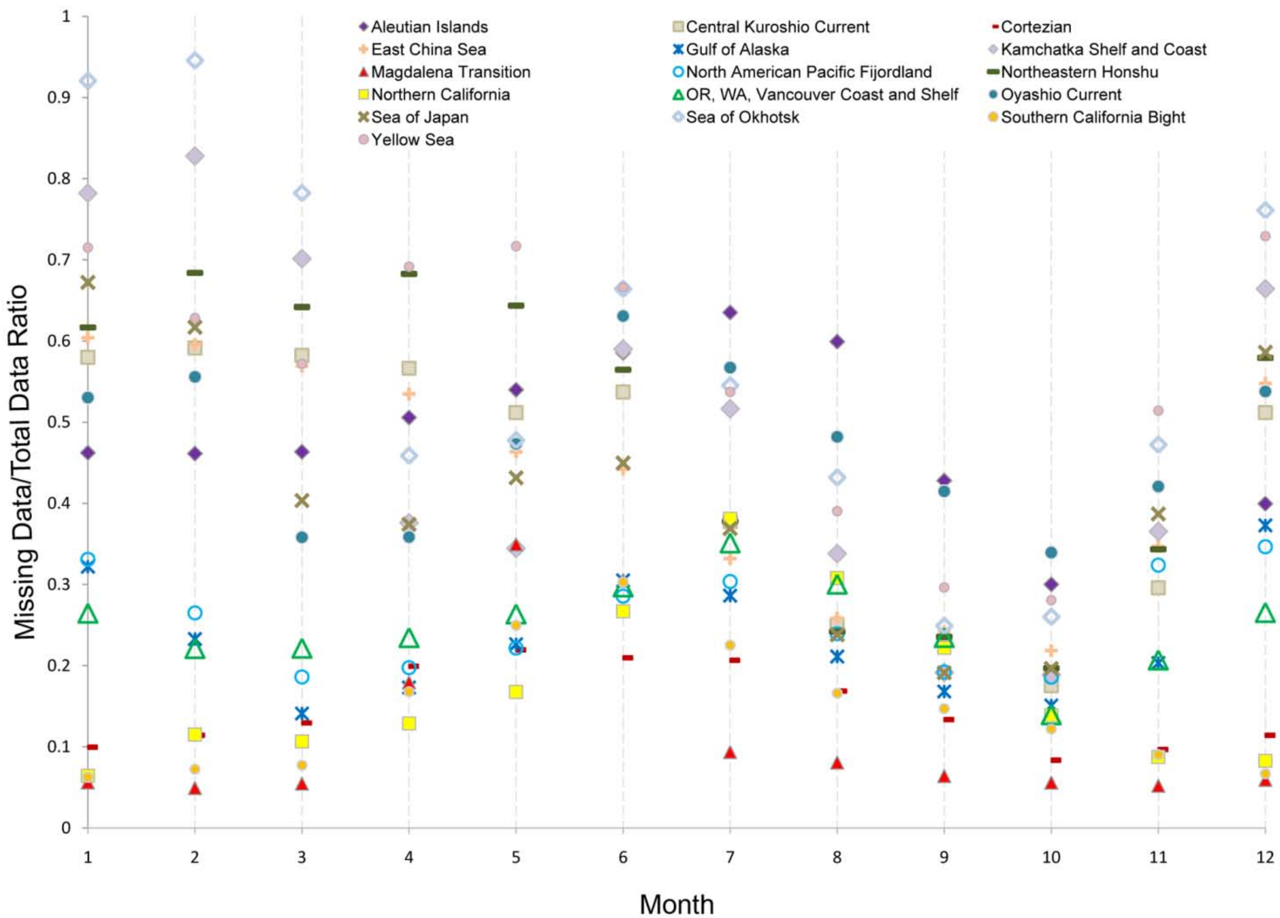

Figure 2-4. Fraction of missing data points for each month aggregated over the 29-year SST time series. Each individual month (e.g. all 29 Januarys) has over half-a-million possible SST point values. Although subarctic ecoregions tend to have a greater percent of missing data compared to lower-latitude ecoregions, at least 40,000 SST values meeting the quality criteria were present in the Temperate North Pacific study area for each of the months evaluated.

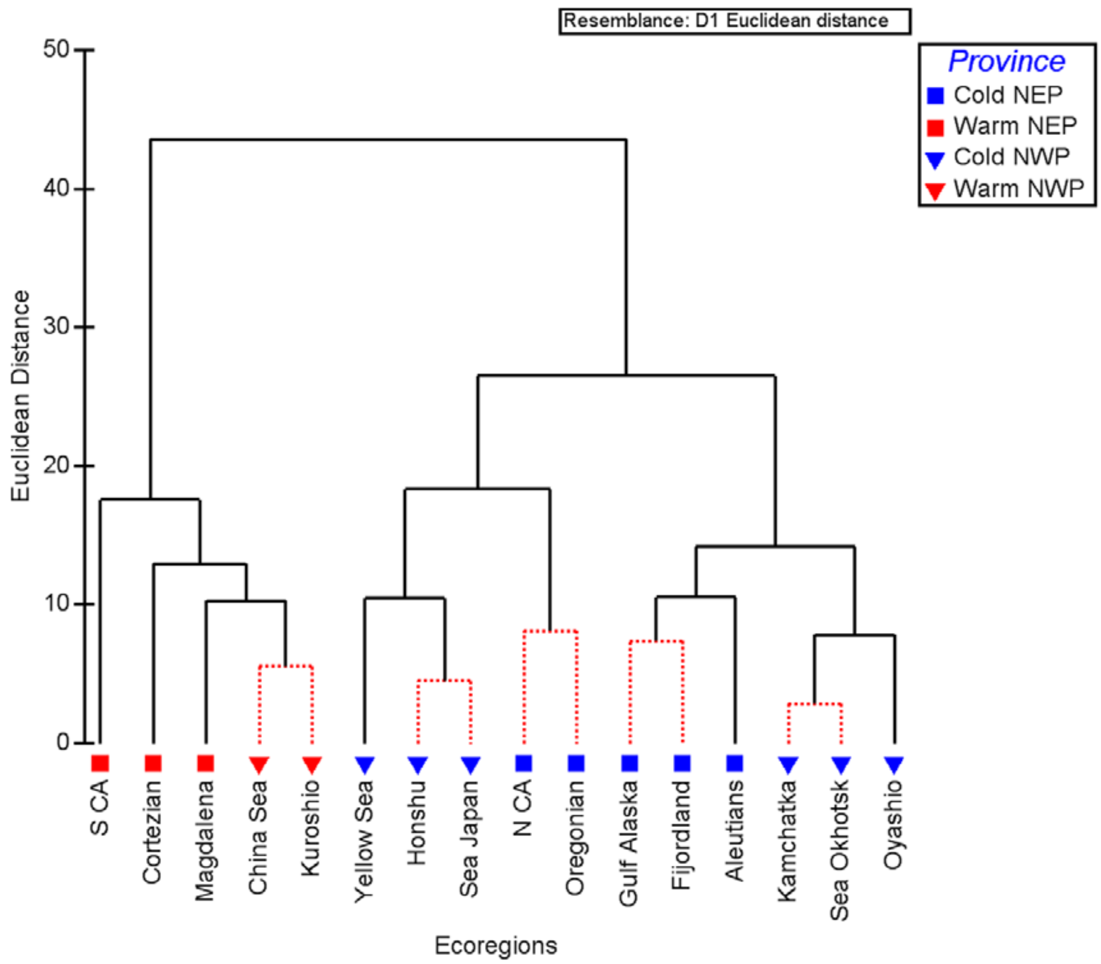

Figure 2-5 Hierarchical clustering dendrogram of 16 Temperate North Pacific ecoregions based on monthly-mean SST values. Clustering was performed with PRIMER [*Clarke and Gorley*, 2006] using 3000 iterations in SIMPROF. Distances are Euclidean. Red, dotted branches indicate no significant difference between linked ecoregions. NEP = Northeast Pacific; NWP = Northwest Pacific.

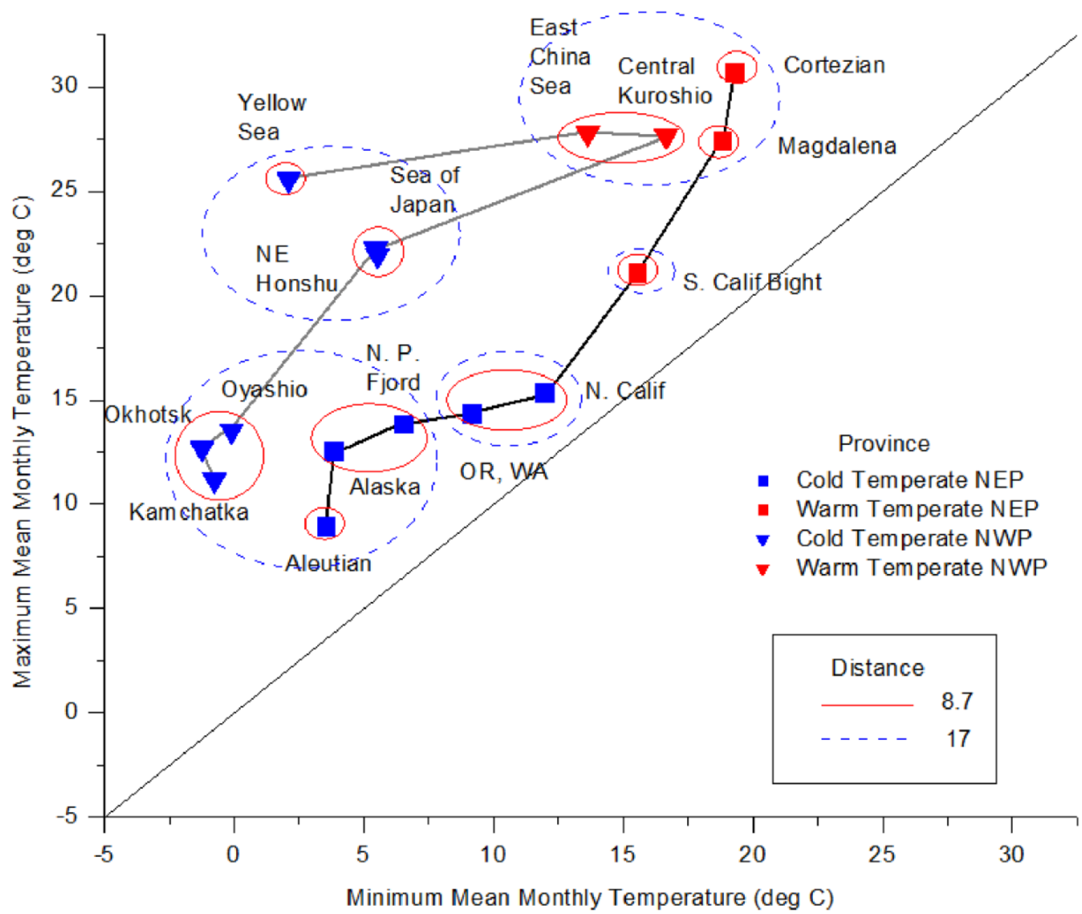

Figure 2-6 Ecoregions plotted by maximum monthly versus minimum monthly-mean SST over the 29-year record. The y = x line indicates where minimum and maximum temperatures within an ecoregion are identical. Hence, proximity to the line indicates minimal variability in seasonal monthly SST. The Euclidean distances of 8.7 and 17 were obtained through clustering analysis. Solid lines connect ecoregions in order of latitude along the NEP and NWP.

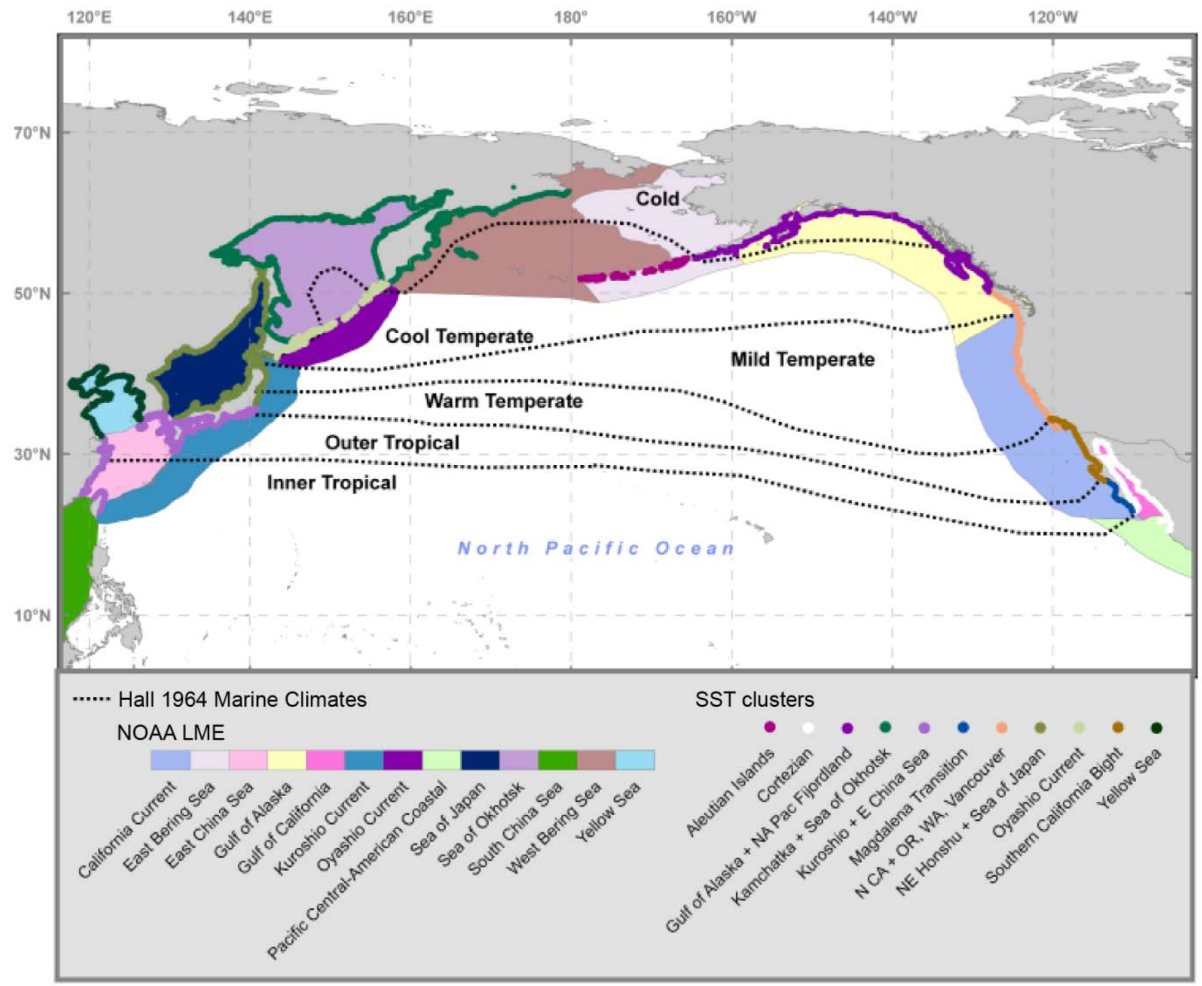

Figure 2-7 Boundary comparison among the thermal patterns based on our SST cluster analysis, marine climates of Hall [1964], SST clusters based on cluster analysis, and NOAA's Large Marine Ecosystems of the World (LMEs). The LMEs are denoted by the outer colored areas. Hall's marine climates are indicated by the dotted black lines, while the SST clusters derived by clustering MEOW ecoregions by SST are delineated by the inner colored outlines.

MODERATE-RESOLUTION SEA SURFACE TEMPERATURE DATA AND SEASONAL PATTERN ANALYSIS FOR THE ARCTIC OCEAN

Meredith C. Payne[1, 2], Deborah A. Reusser[1, 2], Henry Lee II[3]

[1]Western Fisheries Research Center, United States Geological Survey, Newport, Oregon, United States of America, [2]Oregon State University, Corvallis, Oregon, United States of America, [3]Pacific Coastal Ecology Branch, Western Ecology Division, United States Environmental Protection Agency, Newport, Oregon, United States of America

U.S. Geological Survey, Reston, Virginia

USGS National Center
12201 Sunrise Valley Drive
Reston, VA 20192
USA

February 2012 | http://pubs.usgs.gov/of/2011/1246/

Chapter 3 – Moderate-Resolution Sea Surface Temperature Data and Seasonal Pattern Analysis for the Arctic Ocean Ecoregions

Abstract

Sea surface temperature (SST) is an important environmental characteristic in determining the suitability and sustainability of habitats for marine organisms. In particular, the fate of the Arctic Ocean, which provides critical habitat to commercially important fish, is in question. This poses an intriguing problem for future research of Arctic environments—one that will require examination of long-term SST records. This publication describes and provides access to an easy-to-use Arctic SST dataset for ecologists, biogeographers, oceanographers, and other scientists conducting research on habitats and/or processes in the Arctic Ocean. The data cover the Arctic ecoregions as defined by the "Marine Ecoregions of the World" (MEOW) biogeographic schema developed by The Nature Conservancy as well as the region to the north from approximately 46 °N to about 88 °N (constrained by the season and data coverage). The data span a 29-year period from September 1981 to December 2009. These SST data were derived from Advanced Very High Resolution Radiometer (AVHRR) instrument measurements that had been compiled into monthly means at 4-kilometer grid cell spatial resolution. The processed data files are available in ArcGIS geospatial datasets (raster and point shapefiles) and also are provided in text (.csv) format. All data except the raster files include attributes identifying latitude/longitude coordinates, and realm, province, and ecoregion as defined by the MEOW classification schema. A seasonal analysis of these Arctic ecoregions reveals a wide range of SSTs experienced throughout the Arctic, both over the course of an annual cycle and within each month of that cycle. Sea ice distribution plays a major role in SST regulation in all Arctic ecoregions.

Introduction

Recent research indicates there has been a warming trend in ocean temperatures over the last 50 years [*IPCC*, 2007]. Notably, a poleward-advancing trend of warming temperatures in the Arctic has been recorded over the last few decades [*Corell*, 2006]. Arctic Ocean regions, especially those subject to the influence of seasonal sea ice pack, are particularly sensitive to this trend. Warming waters at higher latitudes likely jeopardize fragile food webs, pushing habitability of certain ecosystems to the brink for vulnerable species, and increasing the risk of invasion by nonindigenous species (NIS) [*Gollash*, 2006; *Herborg et al.*, 2007; *Mueter and Norcross*, 2002; *Stram and Evans*, 2009]. *In situ* sea surface temperature (SST) measurements typically are made via buoys, or ocean-going vessels, but such measurements are irregular in both space and time. This is especially true in polar regions, where remoteness is compounded by sea ice and ice shelves, making exploration particularly dangerous and expensive. Satellite-based remote-sensing data have the advantage of extensive spatial coverage and high repeatability that is not possible with field observations. The moderate-resolution (4 km) Pathfinder versions 5.0 and 5.1 SST data (hereafter referred to as PFSST data) are derivative products of the data collected by the Advanced Very High Resolution Radiometer (AVHRR) instrument series flown by the National Oceanic and Atmospheric Administration (NOAA) Polar Orbiting Environmental Satellites (POES). These data provide a consistent set of SST measurements of a known quality and calibration for temperature pattern analyses of marine environments in the Arctic Ocean. A value-added Arctic SST product was created by combining processed PFSST data with The Nature Conservancy's Marine Ecoregions of the World (MEOW) biogeographic schema (fig. 3-1) and is available for download from this open-file report (http://pubs.usgs.gov/of/2011/1246/). Additionally, these data were used to analyze seasonal SST patterns at the ecoregional scale using the MEOW geographical framework.

Data Description and Processing

AVHRR SST Data

The Advanced Very High Resolution Radiometer (AVHRR) is a multi-generational, 6-channel instrument that has been flown on board a series of NOAA polar-orbiting satellites, and has been returning reliable SST data since 1981. Sea surface temperature is not measured directly; rather, it is derived from a differentiation of brightness temperatures recorded by two of the sensor's infrared (IR) channels (channels 4 and 5). Furthermore, the Pathfinder algorithm used to calculate SST accounts for the non-linear relationship between surface and brightness temperatures that arises from variable atmospheric water vapor content, and also uses matchup data from in situ buoys aggregated within 5-month weighted windows, reducing bias due to temporal trends [*Kilpatrick et al.*, 2001]. The PFSST (and later) datasets were developed jointly by the University of Miami Rosenstiel School of Marine and Atmospheric Science and the NOAA National Oceanographic Data Center (NODC) as a more accurate, downscaled (9.28–4 km) version of a previous global AVHRR dataset [*Vazquez-Cuervo et al.*, 1998]. Importantly for the study of the Arctic, the version 5 (and later) PFSST data also were improved through the implementation of an ice mask. We obtained the version 5 (PFSST monthly mean floating point data from the NASA JPL Physical Oceanography Distributed Active Archive Center (PO.DAAC) (ftp://podaac.jpl.nasa.gov/OceanTemperature/avhrr/L3/pathfinder_v5/). PFSST products (version 5.0 and 5.1) also are available through the NODC (ftp://data.nodc.noaa.gov/pub/data.nodc/pathfinder). For a detailed description of the AVHRR and Pathfinder algorithms, we direct the reader to *Vazquez-Cuervo et al*. [1998; 2010] and *Kilpatrick et al.* [2001].

AVHRR Data Quality

The PFSST data include a quality flag product in which each SST pixel is designated a value ranging from 0 (worst quality) to 7 (best quality). These quality flags convey the level of confidence attributed to the SST value calculated for each pixel location. The level of confidence is evaluated on pixel-by-pixel performance with respect to a number of tests that estimate validity and consistency of brightness temperature readings, sun angle effects, and cloudiness, which are combined to establish an overall quality rating. The version 4 Pathfinder release of the SST dataset (PFSST V41) included a standard product called "best SST," or "BSST." BSST data includes pixels with quality flags greater than 3 [*Kilpatrick et al.*, 2001]. We generated an analogous SST product from the PFSST data by disregarding SST values with corresponding quality flag values of less than 4.

Despite the rigors of the flagging algorithms, a small number of pixels with illegitimate jumps in SST gradient have been detected [*Evans et al.*, 2009]. The Arctic data presented here may potentially contain a few of these artifacts that may need to be removed by the user depending on their data requirements. Most occurrences can be eliminated by adopting a more rigorous quality standard (for example, only using data with corresponding quality flags of 7). However, this also serves to substantially reduce the amount of data available for analysis, a problem compounded by climatic conditions in the Arctic.

In addition to performing the analyses discussed here with the BSST data, we repeated the analyses using data with quality flag values of 7 only. In Table 3-1, we show the summary R-squared statistics comparing the BSST data to Q7 data using the ecoregional aggregation of monthly mean SSTs over 29 years. The only ecoregion having significantly divergent values when using the BSST product versus the Quality 7 product is the High Arctic (essentially the Arctic Ocean). This result is to be expected, however, due to the Arctic Ocean ice cover throughout much of the year. Although both BSST and Quality 7 data have ice masks to account for this, data on the periphery of the ice mask do not typically have quality flag of 7, thereby reducing the number of Quality 7 data as compared to BSST data.

Data Accuracy

Currently (2011), the only reports on accuracy of Pathfinder SST values are linked to specific studies across a variety of spatial and temporal resolutions, pathfinder versions, and quality flag thresholds. In general, the temperature values are reported to have RMS errors between 0.1 and 1.0 °C [*Kearns et al.*, 2000; *Kilpatrick et al.*, 2001; *Vazquez-Cuervo et al.*, 2010; *Xu and Ignatov*, 2010] when compared to in situ temperatures. However, it must be cautioned that in situ temperature data derived from multiple sources, such as moored buoys and shipboard observations, are prone to large random errors and rarely have excellent agreement amongst them (for example, [*Kearns et al.*, 2000]). Furthermore, in situ measurements are of bulk temperatures (typically taken between 1 and 3 m depth) rather than true sea surface temperature. Lastly, comparison to in situ data sources, such as buoys and the National Centers for Environmental Prediction (NCEP), are not independent of PFSST data because these data [*Reynolds et al.*, 2002] provide critical calibration and validation for the PFSST data product [*Kilpatrick et al.*, 2001; *Vazquez-Cuervo et al.*, 2010]. When the scaling algorithm provided with the AVHRR data is applied, the resulting SST values are rounded to the nearest 10th of degree as accuracy of the SST data is approximately 0.5 °C (Jorge Vazquez-Cuervo, written commun., February 3, 2011).

Arctic SST Product

We selected AVHRR data for their global coverage at moderate resolution (4 km), their long data record (about 30 years) relative to other satellite missions and their substantial level of processing, including extensive calibration and atmospheric correction. The data represent a time-series of monthly mean sea surface temperatures over the last 29 years. Here, we provide the monthly mean SST data in three forms: (1) georeferenced ".img" raster format, (2) georeferenced ESRI point shapefile (.shp) format, and (3) plain comma-delimited text format. There is one file of each type for each month of each year in the 1981–2009 record. They are downloadable through this OFR in zipped files of yearly bundles containing the GIS layers as well as the related metadata files.

In some places, the data appear jagged, or "moth-eaten," immediately adjacent to the coast and at very high latitude. Satellite data for some coastal regions are missing or are unusable due to low quality, most often due to climatic conditions. Furthermore, the Pathfinder data developers used a MOD12Q1 land mask, which has a 1-km resolution, to define their coastline. Missing data in the vicinity of the North Pole (as seen in fig. 3-2) is caused by several phenomena. First, the near-polar orbits of the satellites housing the AVHRR instruments never quite reach the pole. Second, sea ice plays a significant role throughout most of the year. We examined the Sea Ice Index extent product generated by the National Snow and Ice Data Center (NSIDC) [*Fetterer et al.*, 2002, updated 2009] and found that the missing data surrounding the North Pole (for example, see fig. 3-2) corresponds well with the sea ice margin delineated by the NSIDC index. Third, in some instances, pixels have been eliminated due to cloud cover and to the Pathfinder SST algorithm resulting in pixels with values less than -2.0 °C that must be eliminated due to infeasibility. For all datasets, SST values are recorded in degrees Celsius.

Data Processing

The processes and scripts used to convert the AVHRR data to SST shapefile and text data are described in *Payne et al.* [2011]. An important difference distinguishing the Arctic data from the Northern Pacific data of the previous report is that no buffer was implemented to constrain the Arctic data to the nearshore region. Furthermore, the Python scripts provided here have been modified from the original scripts used to derive the geospatial data in order to integrate the ArcGIS 10 “arcpy” module for compatibility with ArcGIS 10 and Python v. 2.6.

Arctic raster, shapefile, and text (.csv) data are available for download from the "downloads" page of this website (click "downloads" on the left-side menu). Each point in an Arctic point shapefile was created by extracting the temperature value from the centroid of a corresponding grid cell in the Arctic raster dataset. Because the data volumes are very large, the text (.csv) files are further divided into individual ecoregions, resulting in one .csv file per month per year per ecoregion for Arctic SST data. This data partition scheme was necessary to accommodate memory constraints experienced during processing (text files were generated with R [*R Development Core Team*, 2009]. These divisions were not necessary for the shapefile and raster data.

Temperature Pattern Analysis

MEOW Framework

In the effort to characterize Arctic Ocean environments at a regional scale, we analyzed the SST measurements by marine “ecoregions” as defined by The Nature Conservancy in their MEOW biogeographic schema [*Spalding et al.*, 2007]. The MEOW schema is a global hierarchical classification system of coastal zones that divides the world’s coastal areas into 12 distinct marine “realms.” The realms are further divided into 62 marine “provinces,” which are further divided into 232 “ecoregions.” The analyses presented here focus on the 19 ecoregions within the Arctic realm (fig. 3-1). Additionally, the Arctic Ocean to the north of the MEOW Arctic ecoregions is included in the analyses, resulting in the creation of one additional ecoregion named “High Arctic.”

The following protocol is used to describe the SST patterns within an individual ecoregion. All 29 years of the derived SST values of mean monthly SST grid cells within an ecoregion were pooled to calculate the monthly mean SSTs for each ecoregion, as well as a suite of other metrics derived from the monthly means as summarized in Tables 3-2 and 3-3.

Study Area

The Arctic and High Arctic ecoregions are shown in figure 3-1. We do not adhere to the strict definition of the Arctic including only the area north of the Arctic Circle (about 66.5 ºN circle of latitude). We include the entire areas of the Eastern Bering Sea and Northern Grand Banks-Southern Labrador ecoregions, which fall outside of the Arctic Circle. Much of the High Arctic is subject to perennial sea ice cover, and thus has a relatively steady annual surface temperature cycle, with little month-to-month (or within-month) variations (fig. 3-2). However, even lower latitude ecoregions (for example, the Bering Sea) are greatly affected by seasonal sea ice cover and have been the subject of recent research due to dramatic reductions in seasonal sea ice and multi-year sea ice, especially notable within the last decade. Presence of sea ice keeps benthic waters cold by preventing convection and mixing with surface water. Spatial sea ice cover and summer retreat is variable from year-to-year, and young ice can greatly influence the rate and potential for summer ice melt [*Drobot et al.*, 2008]. However, it is the thicker, multi-year ice that moderates long-term Arctic water temperatures, and multi-year ice is becoming progressively younger [*Maslanik et al.*, 2007]. The trend in sea ice reduction has been concurrent with a shift in biodiversity away from benthic shelf populations and towards pelagic species—a trend threatening to disrupt the stability of Arctic food-webs [*Grebmeier et al.*, 2006; *Mueter and Litzow*, 2008].

Arctic Annual Cycles

Table 3-2 identifies and defines the metrics used in the analysis and figure 3-3A provides a diagrammatic description of these metrics. Table 3-3 provides summary statistics for most of the metrics. Figure 3-3B shows the mean annual SST cycles experienced within Arctic ecoregions over the 29-year period with statistical metrics that are summarized in Table 3-2. The mean annual SST (29-year mean) among the Arctic ecoregions ranges from -1.2 ºC in the High Arctic Archipelago ecoregion to a maximum of 3.8 ºC in the Eastern Bering Sea. There is a significant decreasing trend of variance in SST with mean latitude. The ecoregions with the greatest variance are the White Sea, Eastern Bering Sea, and Northern Grand Banks-Southern Labrador, and those with the least variance are the High Arctic and High Arctic Archipelago ecoregions (fig. 3-3B). Undoubtedly, this is the result of sea ice extent over the Arctic Ocean. The mean annual SST cycles in the Arctic ecoregions are shown in figure 3-3B. Within an ecoregion, the range of the annual cycle is defined by the difference between the minimum 29-year monthly mean and the maximum 29-year monthly mean SST (see fig. 3-3A, Table 3-2). The minimum monthly mean SST in the Eastern Bering Sea and North and East Iceland occurs in April. The High Arctic, North and East Barents Sea, Northern Labrador, and East Greenland Shelf have minimums occurring in May, and the East Siberian Sea and Beaufort-Amundsen-Viscount Melville-Queen Maud experience SST minimums in January. The remainder of the Arctic ecoregions have minimum monthly-mean SSTs occurring in February and March. The annual cycle temperature ranges generally are greater at lower latitudes and in inland/marginal water bodies (for example, White Sea and Northern Grand Banks-Southern Labrador ranges greater than 10 ºC) as opposed to ecoregions at polar latitudes (High Arctic and High Arctic Archipelago ranges less than 2 ºC). The greatest annual cycle temperature range occurs in the White Sea ecoregion, which has a range of 11 °C, and the High Arctic ecoregion has the smallest range of about 0.8 °C.

The second type of temporal fluctuation experienced within each ecoregion is referred to as within-month SST variations, which is defined as the 5th and 95th quantiles and shown as the dotted envelopes in figure 3-3. Arctic ecoregions experience a large range of within-month temperatures. In general, this range is greatest in summer months (June–October), with some notable exceptions (for example, High Arctic). Many ecoregions have a wide span of within-month SST variability throughout the year, including North and East Barents Sea, East Greenland Shelf, North and East Iceland, West Greenland Shelf, Eastern Bering Sea, and Northern Grand Banks-Southern Labrador. These ecoregions tend to be along conduits open to the Pacific or Atlantic Ocean basins, such as the Bering Strait and Davis Strait, respectively. This flow between the Arctic Ocean and larger water bodies allows easy mixing and within-month temperature variations of as much as 10 °C.

Clustering Analysis

To compare the SST regimes of the ecoregions, we performed a Euclidean-distance measure hierarchical clustering analysis based on ecoregion SST means, minimums, maximums, ranges, and variances. In each case, the ecoregional SSTs group into two main branches (fig. 3-4), one of which contained the White Sea and Northern Grand Banks-Southern Labrador ecoregions irrespective of what SST metric was used. The High Arctic and High Arctic Archipelago ecoregions always cluster together for each SST metric, and are always grouped on the alternate branch from the White Sea and Northern Grand Banks-Southern Labrador ecoregions. Similarly, the Beaufort-Amundsen-Viscount Melville-Queen Maud and Beaufort Sea-continental coast and shelf ecoregions are nearly always grouped together by SST clustering metric and are always on the same major branch as the High Arctic and High Arctic Archipelago pair, opposing the Northern Grand Banks-Southern Labrador/White Sea at the first major clustering division. Lancaster Sound, Laptev Sea and Kara Sea are always closely related. Perhaps the most variable of the Arctic ecoregions is North Greenland, which is never found to be equivalent to any other ecoregion clustered by any of the SST metrics explored here. The Eastern Bering Sea ecoregion also shows a great deal of variation amongst the clustering metrics, but is not always uniquely discernible from all other ecoregions as is North Greenland. As seen in figure 3-4, which shows the Arctic ecoregions clustered based on all SST metrics simultaneously, five statistically significant cluster groups can be discerned. The red boxes denote clusters where $p > 0.95$.

The minimum, maximum, and mean SST Arctic ecoregion clusters correspond generally, but not perfectly, to latitudinal similarities between ecoregions. An exception is the Hudson Complex ecoregion, which despite its comparatively low-latitude experiences low SSTs and little within-month variation during winter, and relatively high SSTs with a vast within-month SST range in summer. The behavioral enigma of this ecoregion may be due to fresh water influence in the system, which controls the circulation by causing convective mixing in the winter, and rapid sea-ice breakup, melt, and water column stratification in summer (Galbraith and Larouche, 2011).

Downloads

Data Catalog

This report contains Geographic Information System (GIS) data in georeferenced vector (point) and raster formats. The vector (point) data are available as Environmental Systems Research Institute (ESRI) shapefiles and as comma-separated text (*.csv) files. Shapefiles generally include *.shp, *.shx, *.xml, and *.dbf files at a minimum. All these data files also include the *.prj files, which contain the dataset projection information. The corresponding 4-km resolution raster data are available in Imagine *.img format.

The GIS files have been bundled by year. Each year of raster data (GRID-type) has an associated compressed WinRAR zip file. The corresponding shp and csv data types have compressed WinRAR RAR files, due to the large size capacity of RAR archives. Hence, every compressed file may contain up to 12 months of data. In addition to the spatial data, we provide Federal Geographic Data Committee (FGDC) -compliant metadata in text and HTML formats. The metadata text files are bundled with their corresponding zip files, and the metadata HTML information can be viewed in your web browser by clicking the appropriate link in the table below.

To download the data, right-click on the appropriate filename link in the '**Filename**' column (that corresponds to the desired data type) in the table below. Then select '**Save Target As...**' to save a compressed WinRAR file to your local hard drive. The download zipped file size is indicated under the '**file size'** column. All downloaded files are of type ".zip". The File Type description in the table below indicates the type of files found within the downloadable zip files.

Filename	Description	File Type	File Size	Metadata
		2009		
ArcticSST2009rast.zip	Arctic Ocean monthly mean SST data for 2009 in .img raster format.	.img	6.5 MB	Available online
ArcticSST2009pt.rar	Arctic Ocean monthly mean SST data for 2009 in ESRI (point) shapefile format.	ESRI shapefile (*.shp)	35.7 MB	Available online
ArcticSST2009csv.rar	Arctic Ocean monthly mean SST data for 2009 .csv format.	Comma-separated text file (*.csv)	34.4 MB	Available online
		2008		
ArcticSST2008rast.zip	Arctic Ocean monthly mean SST data for 2008 in .img raster format.	.img	6.2 MB	Available online
ArcticSST2008pt.rar	Arctic Ocean monthly mean SST data for 2008 in ESRI (point) shapefile format.	ESRI shapefile (*.shp)	35.0 MB	Available online
ArcticSST2008csv.rar	Arctic Ocean monthly mean SST data for 2008 .csv format.	Comma-separated text file (*.csv)	34.1 MB	Available online
		2007		
ArcticSST2007rast.zip	Arctic Ocean monthly mean SST data for 2007 in .img raster format.	.img	5.2 MB	Available online
ArcticSST2007pt.rar	Arctic Ocean monthly mean SST data for 2007 in ESRI (point) shapefile format.	ESRI shapefile (*.shp)	37.7 MB	Available online
ArcticSST2007csv.rar	Arctic Ocean monthly mean SST data for 2007 .csv format.	Comma-separated text file (*.csv)	36.6 MB	Available online
		2006		

ArcticSST2006rast.zip	Arctic Ocean monthly mean SST data for 2006 in .img raster format.	.img	4.6 MB	Available online
ArcticSST2006pt.rar	Arctic Ocean monthly mean SST data for 2006 in ESRI (point) shapefile format.	ESRI shapefile (*.shp)	36.8 MB	Available online
ArcticSST2006csv.rar	Arctic Ocean monthly mean SST data for 2006 .csv format.	Comma-separated text file (*.csv)	35.6 MB	Available online
		2005		
ArcticSST2005rast.zip	Arctic Ocean monthly mean SST data for 2005 in .img raster format.	.img	4.8 MB	Available online
ArcticSST2005pt.rar	Arctic Ocean monthly mean SST data for 2005 in ESRI (point) shapefile format.	ESRI shapefile (*.shp)	34.4 MB	Available online
ArcticSST2005csv.rar	Arctic Ocean monthly mean SST data for 2005 .csv format.	Comma-separated text file (*.csv)	33.1 MB	Available online
		2004		
ArcticSST2004rast.zip	Arctic Ocean monthly mean SST data for 2004 in .img raster format.	.img	3.8 MB	Available online
ArcticSST2004pt.rar	Arctic Ocean monthly mean SST data for 2004 in ESRI (point) shapefile format.	ESRI shapefile (*.shp)	28.0 MB	Available online
ArcticSST2004csv.rar	Arctic Ocean monthly mean SST data for 2004 .csv format.	Comma-separated text file (*.csv)	26.4 MB	Available online
		2003		
ArcticSST2003rast.zip	Arctic Ocean monthly mean SST data for 2003 in .img raster format.	.img	3.3 MB	Available online

ArcticSST2003pt.rar	Arctic Ocean monthly mean SST data for 2003 in ESRI (point) shapefile format.	ESRI shapefile (*.shp)	23.4 MB	Available online
ArcticSST2003csv.rar	Arctic Ocean monthly mean SST data for 2003 .csv format.	Comma-separated text file (*.csv)	21.8 MB	Available online
		2002		
ArcticSST2002rast.zip	Arctic Ocean monthly mean SST data for 2002 in .img raster format.	.img	4.3 MB	Available online
ArcticSST2002pt.rar	Arctic Ocean monthly mean SST data for 2002 in ESRI (point) shapefile format.	ESRI shapefile (*.shp)	29.5 MB	Available online
ArcticSST2002csv.rar	Arctic Ocean monthly mean SST data for 2002 .csv format.	Comma-separated text file (*.csv)	28.2 MB	Available online
		2001		
ArcticSST2001rast.zip	Arctic Ocean monthly mean SST data for 2001 in .img raster format.	.img	3.2 MB	Available online
ArcticSST2001pt.rar	Arctic Ocean monthly mean SST data for 2001 in ESRI (point) shapefile format.	ESRI shapefile (*.shp)	22.5 MB	Available online
ArcticSST2001csv.rar	Arctic Ocean monthly mean SST data for 2001 .csv format.	Comma-separated text file (*.csv)	20.1 MB	Available online
		2000		
ArcticSST2000rast.zip	Arctic Ocean monthly mean SST data for 2000 in .img raster format.	.img	7.0 MB	Available online
ArcticSST2000pt.rar	Arctic Ocean monthly mean SST data for 2000 in ESRI (point) shapefile format.	ESRI shapefile (*.shp)	67.3 MB	Available online

ArcticSST2000csv.rar	Arctic Ocean monthly mean SST data for 2000 .csv format.	Comma-separated text file (*.csv)	67.6 MB	Available online
		1999		
ArcticSST1999rast.zip	Arctic Ocean monthly mean SST data for 1999 in .img raster format.	.img	3.9 MB	Available online
ArcticSST1999pt.rar	Arctic Ocean monthly mean SST data for 1999 in ESRI (point) shapefile format.	ESRI shapefile (*.shp)	29.2 MB	Available online
ArcticSST1999csv.rar	Arctic Ocean monthly mean SST data for 1999 .csv format.	Comma-separated text file (*.csv)	27.3 MB	Available online
		1998		
ArcticSST1998rast.zip	Arctic Ocean monthly mean SST data for 1998 in .img raster format.	.img	3.8 MB	Available online
ArcticSST1998pt.rar	Arctic Ocean monthly mean SST data for 1998 in ESRI (point) shapefile format.	ESRI shapefile (*.shp)	27.6 MB	Available online
ArcticSST1998csv.rar	Arctic Ocean monthly mean SST data for 1998.csv format.	Comma-separated text file (*.csv)	25.8 MB	Available online
		1997		
ArcticSST1997rast.zip	Arctic Ocean monthly mean SST data for 1997 in .img raster format.	.img	3.9 MB	Available online
ArcticSST1997pt.rar	Arctic Ocean monthly mean SST data for 1997 in ESRI (point) shapefile format.	ESRI shapefile (*.shp)	29.5 MB	Available online
ArcticSST1997csv.rar	Arctic Ocean monthly mean SST data for 1997 .csv format.	Comma-separated text file (*.csv)	28.1 MB	Available online

		1996		
ArcticSST1996rast.zip	Arctic Ocean monthly mean SST data for 1996 in .img raster format.	.img	3.7 MB	Available online
ArcticSST1996pt.rar	Arctic Ocean monthly mean SST data for 1996 in ESRI (point) shapefile format.	ESRI shapefile (*.shp)	27.2 MB	Available online
ArcticSST1996csv.rar	Arctic Ocean monthly mean SST data for 1996 .csv format.	Comma-separated text file (*.csv)	26.2 MB	Available online
		1995		
ArcticSST1995rast.zip	Arctic Ocean monthly mean SST data for 1995 in .img raster format.	.img	1.6 MB	Available online
ArcticSST1995pt.rar	Arctic Ocean monthly mean SST data for 1995 in ESRI (point) shapefile format.	ESRI shapefile (*.shp)	8.7 MB	Available online
ArcticSST1995csv.rar	Arctic Ocean monthly mean SST data for 1995 .csv format.	Comma-separated text file (*.csv)	6.4 MB	Available online
		1994		
ArcticSST1994rast.zip	Arctic Ocean monthly mean SST data for 1994 in .img raster format.	.img	5.3 MB	Available online
ArcticSST1994pt.rar	Arctic Ocean monthly mean SST data for 1994 in ESRI (point) shapefile format.	ESRI shapefile (*.shp)	56.4 MB	Available online
ArcticSST1994csv.rar	Arctic Ocean monthly mean SST data for 1994 .csv format.	Comma-separated text file (*.csv)	54.3 MB	Available online
		1993		
ArcticSST1993rast.zip	Arctic Ocean monthly mean SST data for 1993 in .img raster	.img	5.7 MB	Available

	format.			online
ArcticSST1993pt.rar	Arctic Ocean monthly mean SST data for 1993 in ESRI (point) shapefile format.	ESRI shapefile (*.shp)	54.8 MB	Available online
ArcticSST1993csv.rar	Arctic Ocean monthly mean SST data for 1993 .csv format.	Comma-separated text file (*.csv)	54.0 MB	Available online
		1992		
ArcticSST1992rast.zip	Arctic Ocean monthly mean SST data for 1992 in .img raster format.	.img	5.2 MB	Available online
ArcticSST1992pt.rar	Arctic Ocean monthly mean SST data for 1992 in ESRI (point) shapefile format.	ESRI shapefile (*.shp)	53.7 MB	Available online
ArcticSST1992csv.rar	Arctic Ocean monthly mean SST data for 1992 .csv format.	Comma-separated text file (*.csv)	51.3 MB	Available online
		1991		
ArcticSST1991rast.zip	Arctic Ocean monthly mean SST data for 1991 in .img raster format.	.img	6.3 MB	Available online
ArcticSST1991pt.rar	Arctic Ocean monthly mean SST data for 1991 in ESRI (point) shapefile format.	ESRI shapefile (*.shp)	63.4 MB	Available online
ArcticSST1991csv.rar	Arctic Ocean monthly mean SST data for 1991 .csv format.	Comma-separated text file (*.csv)	62.6 MB	Available online
		1990		
ArcticSST1990rast.zip	Arctic Ocean monthly mean SST data for 1990 in .img raster format.	.img	5.7 MB	Available online
ArcticSST1990pt.rar	Arctic Ocean monthly mean SST data for 1990 in ESRI (point)	ESRI shapefile	60.5	Available

	shapefile format.	(*.shp)	MB	online
ArcticSST1990csv.rar	Arctic Ocean monthly mean SST data for 1990 .csv format.	Comma-separated text file (*.csv)	60.8 MB	Available online
		1989		
ArcticSST1989rast.zip	Arctic Ocean monthly mean SST data for 1989 in .img raster format.	.img	5.4 MB	Available online
ArcticSST1989pt.rar	Arctic Ocean monthly mean SST data for 1989 in ESRI (point) shapefile format.	ESRI shapefile (*.shp)	52.4 MB	Available online
ArcticSST1989csv.rar	Arctic Ocean monthly mean SST data for 1989 .csv format.	Comma-separated text file (*.csv)	51.2 MB	Available online
		1988		
ArcticSST1988rast.zip	Arctic Ocean monthly mean SST data for 1988 in .img raster format.	.img	5.5 MB	Available online
ArcticSST1988pt.rar	Arctic Ocean monthly mean SST data for 1988 in ESRI (point) shapefile format.	ESRI shapefile (*.shp)	57.2 MB	Available online
ArcticSST1988csv.rar	Arctic Ocean monthly mean SST data for 1988 .csv format.	Comma-separated text file (*.csv)	55.4 MB	Available online
		1987		
ArcticSST1987rast.zip	Arctic Ocean monthly mean SST data for 1987 in .img raster format.	.img	5.7 MB	Available online
ArcticSST1987pt.rar	Arctic Ocean monthly mean SST data for 1987 in ESRI (point) shapefile format.	ESRI shapefile (*.shp)	56.5 MB	Available online
ArcticSST1987csv.rar	Arctic Ocean monthly mean SST	Comma-separated text	55.3	Available

	data for 1987 .csv format.	file (*.csv)	MB	online
		1986		
ArcticSST1986rast.zip	Arctic Ocean monthly mean SST data for 1986 in .img raster format.	.img	5.7 MB	Available online
ArcticSST1986pt.rar	Arctic Ocean monthly mean SST data for 1986 in ESRI (point) shapefile format.	ESRI shapefile (*.shp)	54.4 MB	Available online
ArcticSST1986csv.rar	Arctic Ocean monthly mean SST data for 1986 .csv format.	Comma-separated text file (*.csv)	53.1 MB	Available online
		1985		
ArcticSST1985rast.zip	Arctic Ocean monthly mean SST data for 1985 in .img raster format.	.img	5.8 MB	Available online
ArcticSST1985pt.rar	Arctic Ocean monthly mean SST data for 1985 in ESRI (point) shapefile format.	ESRI shapefile (*.shp)	59.1 MB	Available online
ArcticSST1985csv.rar	Arctic Ocean monthly mean SST data for 1985 .csv format.	Comma-separated text file (*.csv)	59.0 MB	Available online
		1984		
ArcticSST1984rast.zip	Arctic Ocean monthly mean SST data for 1984 in .img raster format.	.img	5.3 MB	Available online
ArcticSST1984pt.rar	Arctic Ocean monthly mean SST data for 1984 in ESRI (point) shapefile format.	ESRI shapefile (*.shp)	49.1 MB	Available online
ArcticSST1984csv.rar	Arctic Ocean monthly mean SST data for 1984 .csv format.	Comma-separated text file (*.csv)	49.2 MB	Available online
		1983		

ArcticSST1983rast.zip	Arctic Ocean monthly mean SST data for 1983 in .img raster format.	.img	4.9 MB	Available online
ArcticSST1983pt.rar	Arctic Ocean monthly mean SST data for 1983 in ESRI (point) shapefile format.	ESRI shapefile (*.shp)	52.6 MB	Available online
ArcticSST1983csv.rar	Arctic Ocean monthly mean SST data for 1983 .csv format.	Comma-separated text file (*.csv)	51.5 MB	Available online
		1982		
ArcticSST1982rast.zip	Arctic Ocean monthly mean SST data for 1982 in .img raster format.	.img	8.5 MB	Available online
ArcticSST1982pt.rar	Arctic Ocean monthly mean SST data for 1982 in ESRI (point) shapefile format.	ESRI shapefile (*.shp)	51.6 MB	Available online
ArcticSST1982csv.rar	Arctic Ocean monthly mean SST data for 1982 .csv format.	Comma-separated text file (*.csv)	51.8 MB	Available online
		1981[‡]		
ArcticSST1981rast.zip	Arctic Ocean monthly mean SST data for 1981 in .img raster format.	.img	2.7 MB	Available online
ArcticSST1981pt.rar	Arctic Ocean monthly mean SST data for 1981 in ESRI (point) shapefile format.	ESRI shapefile (*.shp)	14.9 MB	Available online
ArcticSST1981csv.rar	Arctic Ocean monthly mean SST data for 1981 .csv format.	Comma-separated text file (*.csv)	14.3 MB	Available online

[‡]These files contain only the four months of data that are available for 1981. 09/1981 – 12/1981.

Acknowledgments

This publication has been reviewed by personnel of the National Health and Environmental Effects Research Laboratory's Western Ecology Division of the U.S. Environmental Protection Agency, and the U.S. Geological Survey's Western Fisheries Research Center. The information in this document has been funded in part by the U.S. Environmental Protection Agency. However, approval does not signify that the contents reflect the views of the U.S. EPA.

References Cited

Corell, R. W. (2006), Challenges of Climate Change: An Arctic Perspective, *AMBIO: A Journal of the Human Environment*, *35*(4), 148-152.

Drobot, S., J. Stroeve, J. Maslanik, W. Emery, C. Fowler, and J. Kay (2008), Evolution of the 2007-2008 Arctic sea ice cover and prospects for a new record in 2008, *Geophys. Res. Lett.*, *35*(19), L19501.

Evans, R. H., J. Vasquez, and K. S. Casey (2009), 4 km Pathfinder Version 5 User Guide, edited, United States Department of Commerce, National Oceanographic Data Center.

Fetterer, F., K. Knowles, W. Meier, and M. Savoie (2002, updated 2009), Sea Ice Index, edited, National Snow and Ice Data Center, Boulder, CO.

Gollash, S. (2006), Assessment of the introduction potential of aquatic alien species in new environments, in *Assessment and Control of Biological Invasion Risks*, edited by F. Koike, M. N. Clout, M. Kawamichi, M. De Poorter and K. Iwatsuki, pp. 88-91, Shoukadoh Book Sellers, IUCN, Kyoto, Japan; Gland, Switzerland.

Grebmeier, J. M., J. E. Overland, S. E. Moore, E. V. Farley, E. C. Carmack, L. W. Cooper, K. E. Frey, J. H. Helle, F. A. McLaughlin, and S. L. McNutt (2006), A Major Ecosystem Shift in the Northern Bering Sea, *Science*, *311*(5766), 1461-1464.

Herborg, L.-M., C. L. Jerde, D. M. Lodge, G. M. Ruiz, and H. J. MacIsaac (2007), Predicting Invasion Risk Using Measures of Introduction Effort and Environmental Niche Models, *Ecological Applications*, *17*(3), 663-674.

IPCC (2007), Climate change 2007: impacts, adaptation and vulnerability, in *Contribution of Working Group II to the Fourth Assessment Report of the Intergovernmental Panel on Climate Change*, edited by M. L. Parry, O. F. Canziani, J. Palutikof, P. J. van der Linden and C. E. Hanson, pp. 1-976, Cambridge University Press, Cambridge.

Kearns, E. J., J. A. Hanafin, R. H. Evans, P. J. Minnett, and O. B. Brown (2000), An Independent Assessment of Pathfinder AVHRR Sea Surface Temperature Accuracy Using the Marine

Atmosphere Emitted Radiance Interferometer (MAERI), *Bulletin of the American Meteorological Society*, *81*(7), 1525-1536.

Kilpatrick, K. A., G. P. Podesta, and R. Evans (2001), Overview of the NOAA/NASA advanced very high resolution radiometer Pathfinder algorithm for sea surface temperature and associated matchup database, *J. Geophys. Res.-Oceans*, *106*(C5), 9179-9197.

Maslanik, J. A., C. Fowler, J. Stroeve, S. Drobot, J. Zwally, D. Yi, and W. Emery (2007), A younger, thinner Arctic ice cover: Increased potential for rapid, extensive sea-ice loss, *Geophys. Res. Lett.*, *34*(24), L24501.

Mueter, F. J., and B. L. Norcross (2002), Spatial and temporal patterns in the demersal fish community on the shelf and upper slope regions of the Gulf of Alaska, *Fishery Bulletin*, *100*(3), 559-581.

Mueter, F. J., and M. A. Litzow (2008), Sea ice retreat alters the biogeography of the Bering Sea continental shelf, *Ecological Applications*, *18*(2), 309-320.

Payne, M. C., D. A. Reusser, H. Lee II, and C. A. Brown (2011), Moderate-resolution sea surface temperature data for the nearshore North Pacific: U.S. Geological Survey Open-File Report 2010-1251*Rep.*, 16 pp.

R Development Core Team (2009), R: A language and environment for statistical computing., edited, R Foundation for Statistical Computing, Vienna, Austria.

Reynolds, R. W., N. A. Rayner, T. M. Smith, D. C. Stokes, and W. Wang (2002), An Improved In Situ and Satellite SST Analysis for Climate, *J. Clim.*, *15*(13), 1609-1625.

Spalding, M. D., et al. (2007), Marine ecoregions of the world: a bioregionalization of coastal and shelf areas, *BioScience*, *57*(7), 573-583.

Stram, D. L., and D. C. K. Evans (2009), Fishery management responses to climate change in the North Pacific, *ICES Journal of Marine Science*, *66*(7), 1633-1639.

Vazquez-Cuervo, J., K. Perry, and K. Kilpatrick (1998), NOAA/NASA AVHRR Oceans Pathfinder sea surface temperature data set user's reference manual version 4.0: JPL Publication D-14070*Rep.*

Vazquez-Cuervo, J., E. M. Armstrong, K. S. Casey, R. Evans, and K. Kilpatrick (2010), Comparison between the Pathfinder Versions 5.0 and 4.1 Sea Surface Temperature Datasets: A Case Study for High Resolution, *J. Clim.*, *23*(5), 1047-1059.

Xu, F., and A. Ignatov (2010), Evaluation of in situ sea surface temperatures for use in the calibration and validation of satellite retrievals, *J. Geophys. Res.-Oceans*, *115*.

Table 3-1. R-squared values from simple linear regression statistics between data with quality flag values of 4-7 (BSST) and data with quality flag value of 7 only (Q7SST) for each Arctic ecoregion.

[The only significant difference between them occurs in the High Arctic ecoregion (which is essentially the open Arctic Ocean), which is covered by sea ice for most of the year. Quality flag values on the ice margin generally are lower than 7.]

Ecoregion	BSST vs. Q7SST R-squared
Baffin Bay - Davis Strait	0.9933
Beaufort-Amundsen-Viscount Melville-Queen Maud	0.9828
Beaufort Sea - continental coast and shelf	0.9796
Chukchi Sea	0.9973
East Greenland Shelf	0.9745
East Siberian Sea	0.9867
Eastern Bering Sea	0.9997
High Arctic Archipelago	0.9735
High Arctic	0.6241
Hudson Complex	0.9964
Kara Sea	0.998
Lancaster Sound	0.9987
Laptev Sea	0.9894
North and East Barents Sea	0.9982
North and East Iceland	0.9999
North Greenland	0.9336
Northern Grand Banks - Southern Labrador	0.9999
Northern Labrador	0.9993
West Greenland Shelf	0.999
White Sea	0.9996

Table 3-2. SST metrics used in analyses presented in this study.
[Definitions explained by this table are referred to throughout the text]

SST analysis metric	Metric description	Metric dimensions
Derived SST values	SST values derived from PFSST product. Each value represents a monthly mean for each grid cell	1 value per grid cell of acceptable quality, 1 raster per month over 29 years (340 rasters)
Monthly-mean SST per ecoregion	The 29-year average of all of the derived SST values (above product) within an ecoregion for each of the 12 months.	20 ecoregions × 12 months
Mean annual cycle	12 monthly means for each ecoregion	20 annual cycles (fig. 3-3B)
Range of annual cycle	Difference between warmest (maximum) monthly mean and coolest (minimum) monthly mean per ecoregion	20 ranges
Mean annual SST (29-year mean)	Mean of the monthly mean SST per ecoregion over the 29-year period	1 value × 20 ecoregions
Variance in SST	Variance of all derived SST values within an ecoregion over the 29-year period	1 value × 20 ecoregions
Within-month SST variations (5th and 95th quantiles)	The 5th and 95th quantile values for each month of all derived SST values within each ecoregion.	2 values × 12 months × 20 ecoregions

Table 3-3**.** Statistical metrics for Arctic and High Arctic ecoregions.

Province	Ecoregion	Approx. Ecoregion Center Lat/Lon (°N,°W)	Temperature (°C)				29-year mean standard deviation (°C)
			29-year Mean	Min. monthly mean	Max. monthly mean	Range of annual cycle	
High Arctic	High Arctic	85.6, -178.8	-0.8	-1.2	-0.4	0.8	0.2
Arctic	North Greenland	81.3, -37.0	-1.0	-1.7	0.2	2.0	0.7
	High Arctic Archipelago	80.8, -90.8	-1.2	-1.9	-0.2	1.7	0.5
	North and East Barents Sea	76.7, +40.4	1.8	0.8	3.8	3.0	1.1
	Kara Sea	74.5, +81.4	-0.4	-1.6	1.7	3.3	1.2
	Laptev Sea	73.4, +123.0	-0.5	-2.0	1.3	3.3	1.2
	Lancaster Sound	72.8, -89.9	-0.6	-1.9	0.9	2.8	1.0
	East Siberian Sea	72.6, +159.3	-0.5	-1.4	0.6	2.0	0.7
	Baffin Bay-Davis Strait	71.8, -71.1	-0.3	-1.7	2.5	4.2	1.5
	Chuckchi Sea	71.2, -169.5	0.3	-1.5	3.6	5.1	1.9
	Beaufort-Amundsen-Viscount	69.9, -111.8	-0.2	-1.8	1.4	3.3	1.1

	Melville-Queen Maud						
	Beaufort Sea-continental coast and shelf	69.8, -142.0	-0.3	-1.5	1.7	3.2	1.2
	East Greenland Shelf	69.0, -30.4	3.4	1.9	4.6	2.6	0.7
	North and East Iceland	69.0, -12.6	2.7	0.5	6.4	5.9	2.1
	West Greenland Shelf	68.7, -53.8	1.9	0.5	4.9	4.3	1.6
	White Sea	65.6, +37.0	3.1	-1.1	9.9	11.0	4.1
	Northern Labrador	61.6, -63.3	1.0	-0.5	4.0	4.5	1.6
	Hudson Complex	60.0, -81.5	0.9	-1.2	5.4	6.6	2.3
	Eastern Bering Sea	60.0, -169.7	3.8	0.3	9.4	9.2	3.4
	Northern Grand Banks-Southern Labrador	52.2, -55.5	3.1	-0.7	9.9	10.6	3.9

Figure 3-1. Map of Arctic realm as defined by the Marine Ecoregions of the World (MEOW; [*Spalding et al.*, 2007]).

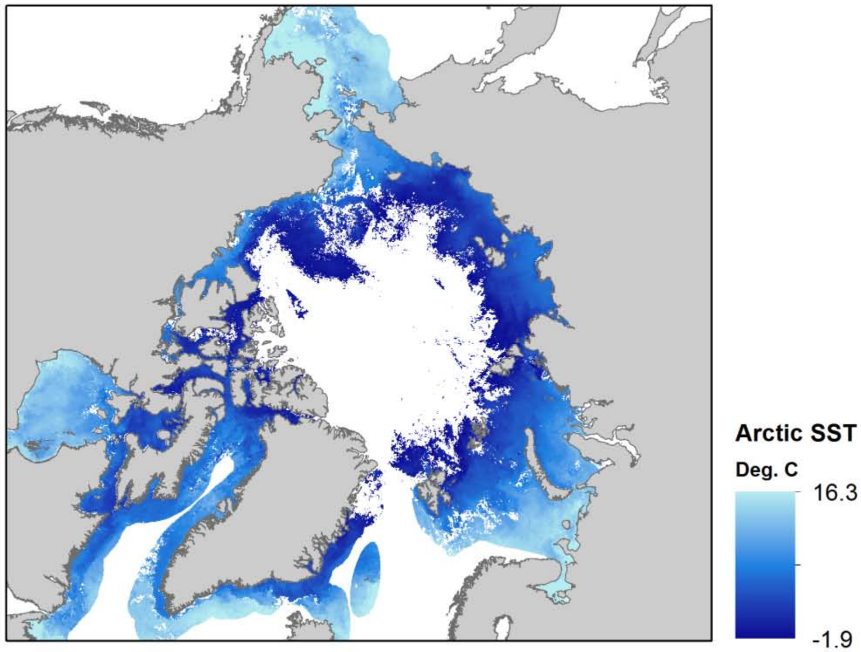

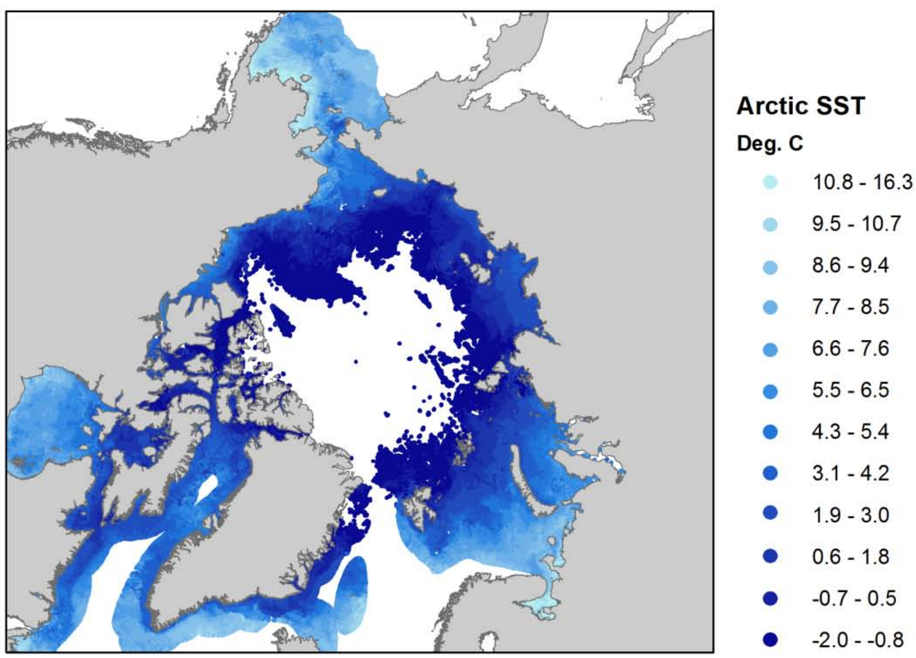

Figure 3-2. Map of monthly average SSTs in the Arctic Ocean ecoregions for September 2009. Figure 2A is raster format data, figure 2B is point shapefile format data. The absence of data at the pole approximately corresponds to the sea ice coverage for September 2009 [*Fetterer et al.*, 2002, updated 2009].

A.

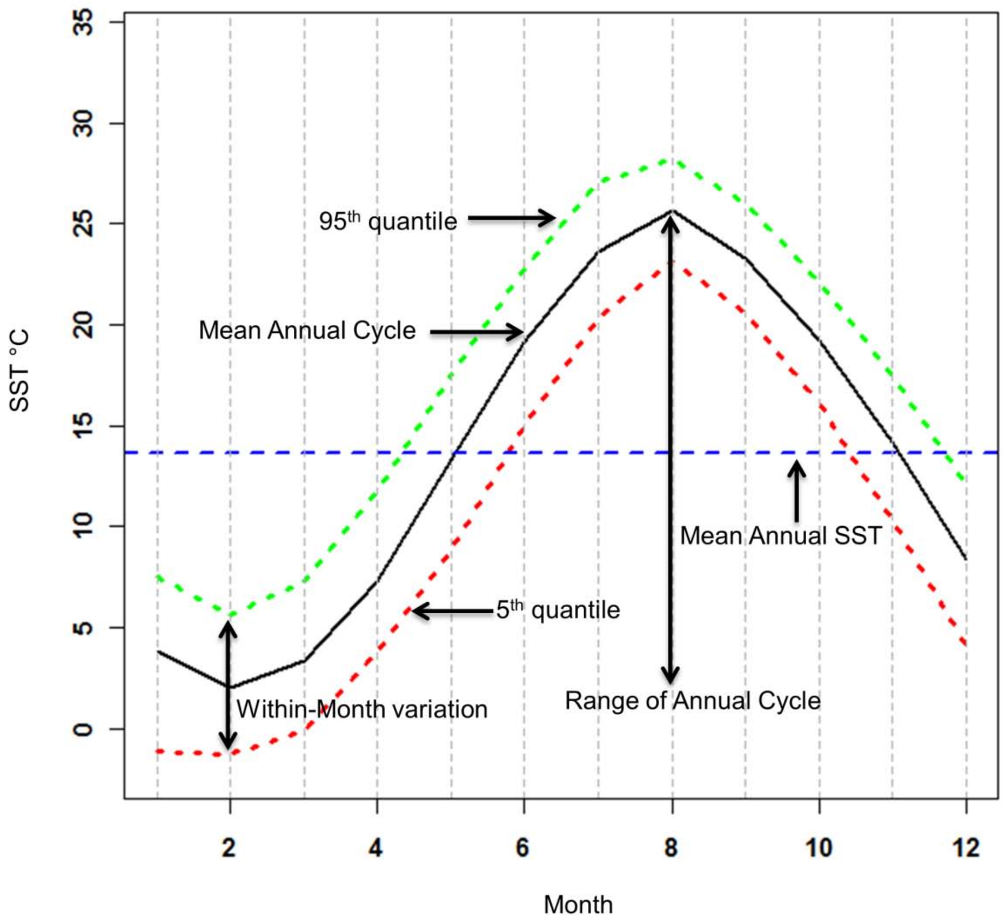

Figure 3-3. 3-3A) Legend diagram for figure 3-3B. Figure 3-3B) Arctic Ocean ecoregion plots of annual cycles of mean monthly SSTs. A high-resolution, zoomable version of this figure is available online at http://pubs.usgs.gov/of/2011/1246/.

B.

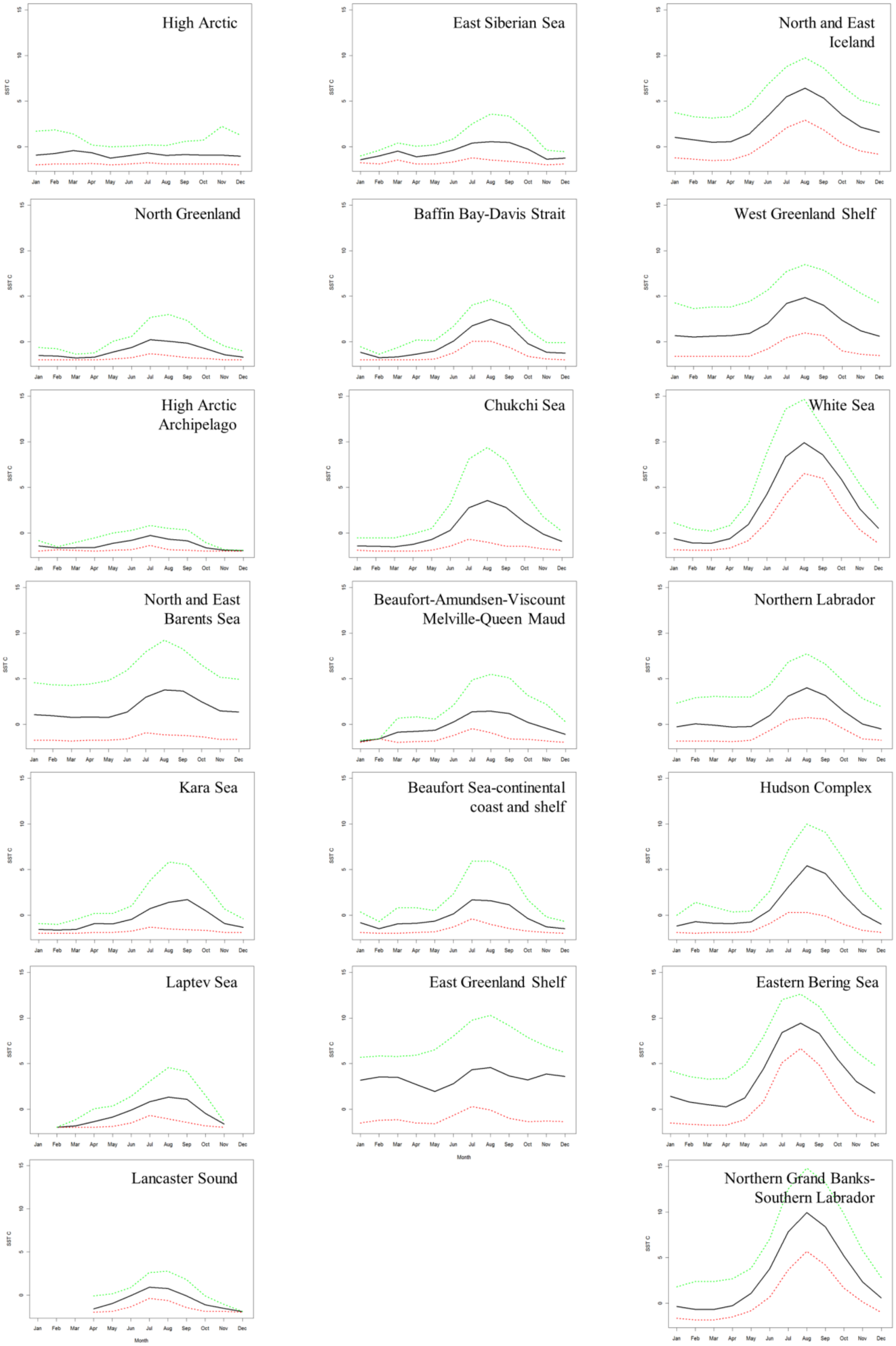
High Arctic
East Siberian Sea
North and East Iceland
North Greenland
Baffin Bay-Davis Strait
West Greenland Shelf
High Arctic Archipelago
Chukchi Sea
White Sea
North and East Barents Sea
Beaufort-Amundsen-Viscount Melville-Queen Maud
Northern Labrador
Kara Sea
Beaufort Sea-continental coast and shelf
Hudson Complex
Laptev Sea
East Greenland Shelf
Eastern Bering Sea
Lancaster Sound
Northern Grand Banks-Southern Labrador

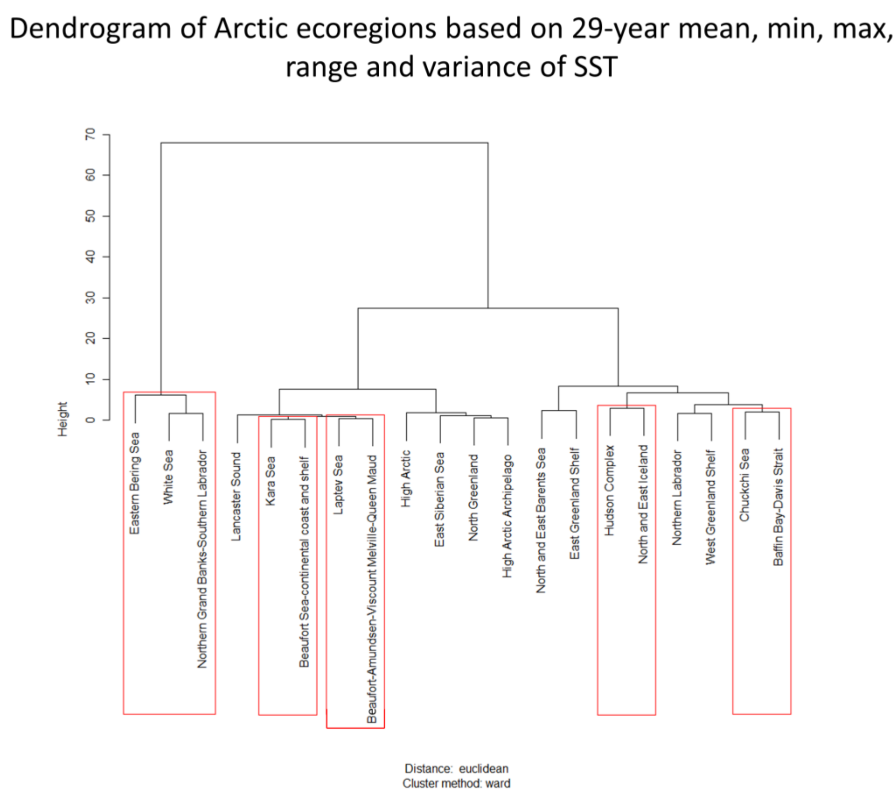

Figure 3-4. Euclidean distance cluster diagram for Arctic Ocean ecoregions based on 29-year mean, minimum, maximum, annual range and annual variance of SST. The red boxes denote clusters where p > 0.95.

Chapter 4 – General Conclusion

The manuscripts herein briefly illustrate a small sample of what types of analyses are possible with the SST dataset we generated for this project (please refer to Appendix A for a detailed description of the data generation process and limitations). The utility of satellite remote sensing data, along with geospatial statistical analyses to detect patterns and trends germane to biogeographic research and climate change science cannot be overstated. Investigations of species distribution and habitat health as related to SST patterns will provide support for such studies into the future.

Indeed, our work is already gaining some significant notice from a variety of audiences. For example, upon its publication in March 2011, the manuscript appearing as the Appendix of this thesis was singled out in an agency-wide USGS highlights newsletter. Moreover, Jorge Vasquez-Cuervo and Bob Evans (co-creators of the AVHRR Pathfinder dataset with Kenneth Casey) expressed enthusiasm for the utility of the value-added SST datasets generated through this project. Furthermore, the publication presented as chapter 2 of this thesis, was blogged about by a noted science writer upon its release in January 2012 (see http://deepbluehome.blogspot.com/2012/01/california-coast-most-susceptible-to.html). Thus our work is finding acceptance within the scientific community and beyond and we are pleased that it has garnered attention among diverse audiences.

For this project, we aggregated 4-km-resolution AVHRR Pathfinder SST data by MEOW ecoregion [*Spalding et al.*, 2007] and per month, yielding a unique 29-year, monthly-mean temperature record. Using these data, we applied marine ecological methodologies, such as Euclidean-distance hierarchical clustering and descriptive statistics (e.g. *McCune and Grace* [2002]) to identify spatio-temporal patterns of ocean temperatures within each ecoregion in our study areas (i.e. nearshore North Pacific and Arctic Oceans). Additionally, we used geospatial analysis and cartographic techniques to further our understanding of those patterns and to relate them to other biogeographic characterizations (e.g. *Hall* [1964] and *Sherman et al.* [2007]).

Analysis of the seasonal cycles revealed the following key points:

- North Pacific Ocean (nearshore region) Summary
  - The total range of mean SST in the North Pacific varied from 3.8 °C along the Kamchatka ecoregion to 24.8 °C in the Cortezian ecoregion.
  - The annual ranges of Northeast Pacific SST are smaller and less variable than Northwest Pacific SST.
  - Within the 16 ecoregions, 31-94% of the variance in SST is explained by the annual cycle, with the annual cycle explaining the least variation in the Northern California ecoregion and the most variation in the Yellow Sea ecoregion.
  - Clustering on mean monthly SSTs of each ecoregion revealed a clear break between the ecoregions corresponding to the Warm and Cold Temperate provinces of the Marine Ecoregions of the World (MEOW) schema.
  - Description of the nearshore North Pacific SST dataset along with the data themselves (presented in text, database, and GIS (shapefile and raster) formats, along with their detailed FGDC metadata) are available at http://pubs.usgs.gov/of/2010/1251.

- Arctic Ocean Summary
    - The data generated and distributed by this project for the Arctic Ocean cover the Arctic ecoregions as defined by the MEOW biogeographic schema as well as the region to the north from approximately 46 °N to about 88 °N (constrained by the season and data coverage).
    - The mean annual SST (29-year mean) among the Arctic ecoregions varies from -1.2 °C in the High Arctic Archipelago ecoregion to a maximum of 3.8 °C in the Eastern Bering Sea.
    - The annual cycle temperature ranges are generally greater at lower latitudes and in inland/marginal water bodies (e.g. White Sea and Northern Grand Banks-Southern Labrador ranges > 10 °C) as opposed to ecoregions at polar latitudes (High Arctic and High Arctic Archipelago ranges < 2 °C). The greatest annual cycle temperature range occurs in the White Sea ecoregion, which has a range of 11 °C, while the High Arctic ecoregion has the smallest range of about 0.8 °C.
    - Many ecoregions have a wide span of within-month SST variability throughout the year, including North and East Barents Sea, East Greenland Shelf, North and East Iceland, West Greenland Shelf, Eastern Bering Sea, and Northern Grand Banks-Southern Labrador. These ecoregions tend to be found along conduits open to the Pacific or Atlantic Ocean basins, such as the Bering Strait and Davis Strait, respectively.
    - The minimum, maximum, and mean SST Arctic ecoregion clusters correspond generally, but not perfectly, to latitudinal similarities between ecoregions.

- Sea ice distribution plays a major role in SST regulation in all Arctic ecoregions. An important caveat to conclusions based on the seasonal cycles derived for Arctic ecoregions is that sea ice can significantly diminish the number of viable SST values in the highest-latitude Arctic regions, particularly at the height of winter. Figure 4-1 illustrates this issue, showing the largest amounts of missing data occurring in ecoregions that experience significance sea ice cover during the coldest months, while regions that experience continual water flow (e.g. straits) have relatively more data.
- Description of the Arctic SST dataset along with the data themselves (presented in text, and GIS (shapefile and raster) formats, along with detailed FGDC metadata) are available at http://pubs.usgs.gov/of/2011/1246.

In general, the annual cycle analyses of the North Pacific and Arctic Oceans provides a decadal baseline against which future SST observations can be measured, functioning as an important piece of the climatic data puzzle useful in environmental change studies. Furthermore, results of this investigation show that some ecoregions (e.g. the California Current System ecoregions) in the North Pacific and Arctic are more vulnerable to such changes, while others will likely be more resilient and presumably already harbor hardier species accustomed to relatively large SST fluctuations in the seasonal cycle. The insight that this information provides will help guide policy makers and marine ecosystem managers.

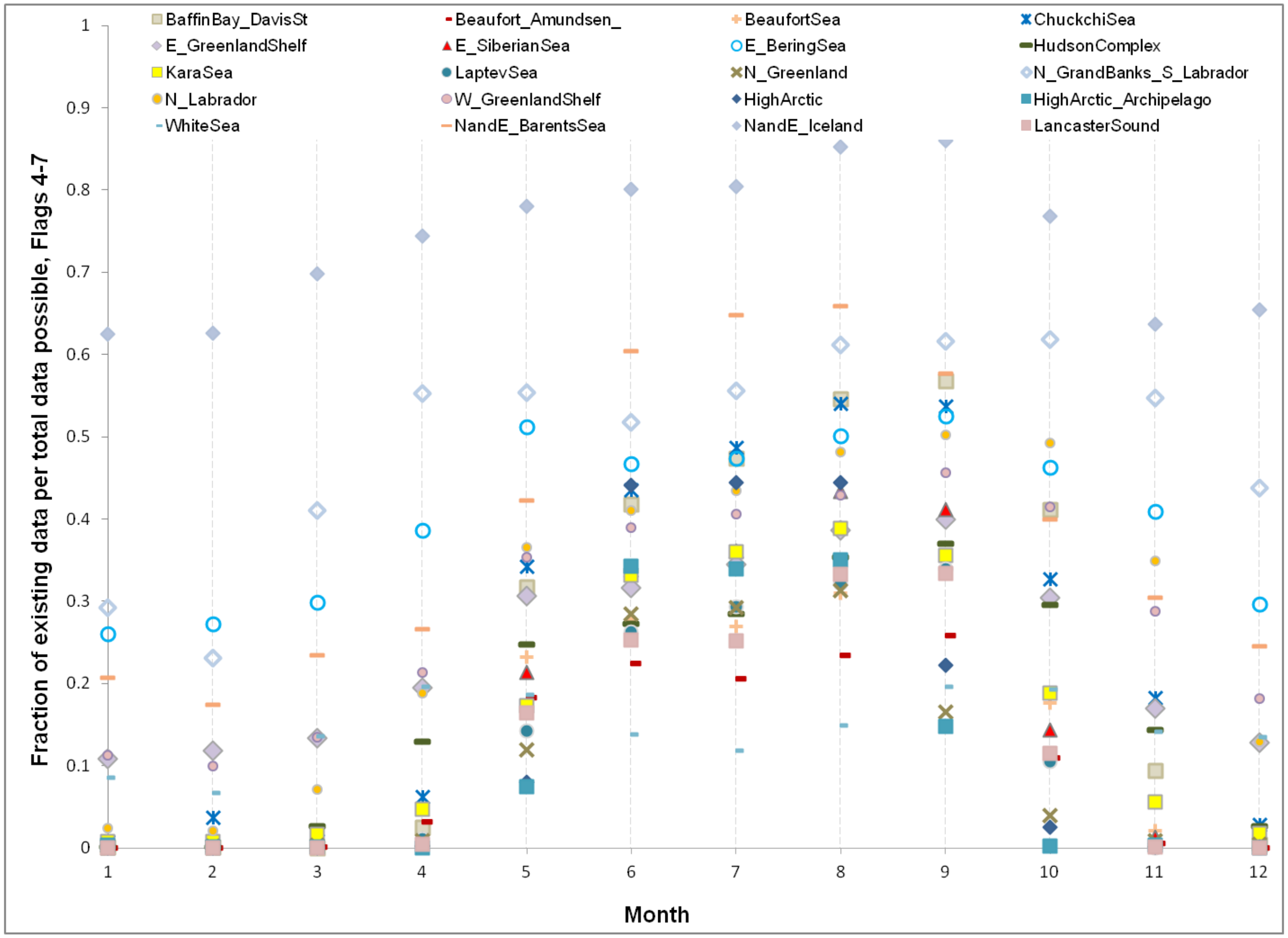

Figure 4-1. Fraction of data points for each month aggregated over the 29-year SST time series. Each individual month (e.g. all 29 Januarys) has over half-a-million possible SST point values. Although arctic ecoregions tend to have a greater percent of missing data compared to lower-latitude ecoregions, thousands of SST values meeting the quality criteria were present in the Arctic study areas for each month.

Chapter 5 – Bibliography

Adey, W. H., and R. S. Steneck (2001), Thermogeography over time creates biogeographic regions: a temperature/space/time-integrated model and an abundance-weighted test for benthic marine algae, *Journal of Phycology*, *37*(5), 677-698.

Barth, J. A., S. D. Pierce, and T. J. Cowles (2005), Mesoscale structure and its seasonal evolution in the northern California Current System, *Deep-Sea Research Part Ii-Topical Studies in Oceanography*, *52*(1-2), 5-28.

Barth, J. A., B. A. Menge, J. Lubchenco, F. Chan, J. M. Bane, A. R. Kirincich, M. A. McManus, K. J. Nielsen, S. D. Pierce, and L. Washburn (2007), Delayed upwelling alters nearshore coastal ocean ecosystems in the northern California current, *Proceedings of the National Academy of Sciences of the United States of America*, *104*(10), 3719-3724.

Blanchette, C. A., C. M. Miner, P. T. Raimondi, D. Lohse, K. E. K. Heady, and B. R. Broitman (2008), Biogeographical patterns of rocky intertidal communities along the Pacific coast of North America, *J. Biogeogr.*, *35*(9), 1593-1607.

Briggs, J. C. (1974), *Marine zoogeography [by] John C. Briggs*, x, 475 p. pp., McGraw-Hill, New York.

Briggs, J. C. (1995), *Global Biogeography*, 1 ed., 452 pp., Elsevier Science B. V., Amsterdam, The Netherlands.

Briggs, J. C. (2007), Marine longitudinal biodiversity: causes and conservation, *Diversity and Distributions*, *13*(5), 544-555.

Broitman, B. R., N. Mieszkowska, B. Helmuth, and C. A. Blanchette (2008), Climate and Recruitment of Rocky Shore Intertidal Invertebrates in the Eastern North Atlantic, *Ecology*, *89*(11), S81-S90.

Broitman, B. R., P. L. Szathmary, K. A. S. Mislan, C. A. Blanchette, and B. Helmuth (2009), Predator-prey interactions under climate change: the importance of habitat vs body temperature, *Oikos*, *118*(2), 219-224.

Casey, K. S. (2002), Daytime vs nighttime AVHRR sea surface temperature data: A report regarding Wellington et al. (2001), *Bull. Mar. Sci.*, *70*(1), 169-175.

Casey, K. S., and P. Cornillon (1999), A comparison of satellite and in situ-based sea surface temperature climatologies, *J. Clim.*, *12*(6), 1848-1863.

Casey, K. S., and D. Adamec (2002), Sea surface temperature and sea surface height variability in the North Pacific Ocean from 1993 to 1999, *J. Geophys. Res.-Oceans*, *107*(C8), 12.

Castelao, R. M., and J. A. Barth (2005), Coastal ocean response to summer upwelling favorable winds in a region of alongshore bottom topography variations off Oregon, *J. Geophys. Res.-Oceans*, *110*(C10).

Castelao, R. M., and J. A. Barth (2006), The relative importance of wind strength and along-shelf bathymetric variations on the separation of a coastal upwelling jet, *Journal of Physical Oceanography*, *36*(3), 412-425.

Checkley Jr, D. M., and J. A. Barth (2009), Patterns and processes in the California Current System, *Progress in Oceanography*, *83*(1-4), 49-64.

Chelton, D. B. (1984), Seasonal Variability of Alongshore Geostrophic Velocity Off Central California, *J. Geophys. Res.*, *89*(C3), 3473-3486.

Chelton, D. B., M. G. Schlax, R. M. Samelson, and R. A. de Szoeke (2007), Global observations of large oceanic eddies, *Geophys. Res. Lett.*, *34*(15).

Chu, P., C. Yuchun, and A. Kuninaka (2005), Seasonal variability of the Yellow Sea/East China Sea surface fluxes and thermohaline structure, *Advances in Atmospheric Sciences*, *22*(1), 1-20.

Clarke, K. R., and R. N. Gorley (2006), *PRIMER v6: User Manual/Tutorial*, 190 pp., PRIMER-E Ltd., Plymouth.

Corell, R. W. (2006), Challenges of Climate Change: An Arctic Perspective, *AMBIO: A Journal of the Human Environment*, *35*(4), 148-152.

Diaz, J. P., M. Arbelo, F. J. Exposito, G. Podesta, J. M. Prospero, and R. Evans (2001), Relationship between errors in AVHRR-derived sea surface temperature and the TOMS Aerosol Index, *Geophys. Res. Lett.*, *28*(10), 1989-1992.

Dorman, C. E., C. A. Friehe, D. Khelif, A. Scotti, J. Edson, R. C. Beardsley, R. Limeburner, and S. S. Chen (2006), Winter Atmospheric Conditions over the Japan/East Sea: The Structure and Impact of Severe Cold-Air Outbreaks, *Oceanography*, *19*(3), 96-109.

Drobot, S., J. Stroeve, J. Maslanik, W. Emery, C. Fowler, and J. Kay (2008), Evolution of the 2007-2008 Arctic sea ice cover and prospects for a new record in 2008, *Geophys. Res. Lett.*, *35*(19), L19501.

Espinosa-Carreon, T. L., P. T. Strub, E. Beier, F. Ocampo-Torres, and G. Gaxiola-Castro (2004), Seasonal and interannual variability of satellite-derived chlorophyll pigment, surface height, and temperature off Baja California, *J. Geophys. Res.-Oceans*, *109*(C3).

Evans, R. H., J. Vasquez, and K. S. Casey (2009), 4 km Pathfinder Version 5 User Guide, edited, United States Department of Commerce, National Oceanographic Data Center.

Fetterer, F., K. Knowles, W. Meier, and M. Savoie (2002, updated 2009), Sea Ice Index, edited, National Snow and Ice Data Center, Boulder, CO.

Galbraith, P. S., and P. Larouche (2011), Sea-surface temperature in Hudson Bay and Hudson Strait in relation to air temperature and ice cover breakup, 1985-2009, *Journal of Marine Systems*, *87*(1), 66-78.

Golikov, A. N., M. A. Dolgolenko, N. V. Maximovich, and O. A. Scarlato (1990), Theoretical approaches to marine biogeography, *Marine Ecology Progress Series*, *63*, 289-301.

Gollash, S. (2006), Assessment of the introduction potential of aquatic alien species in new environments, in *Assessment and Control of Biological Invasion Risks*, edited by F. Koike, M. N. Clout, M. Kawamichi, M. De Poorter and K. Iwatsuki, pp. 88-91, Shoukadoh Book Sellers, IUCN, Kyoto, Japan; Gland, Switzerland.

Grebmeier, J. M., J. E. Overland, S. E. Moore, E. V. Farley, E. C. Carmack, L. W. Cooper, K. E. Frey, J. H. Helle, F. A. McLaughlin, and S. L. McNutt (2006), A Major Ecosystem Shift in the Northern Bering Sea, *Science*, *311*(5766), 1461-1464.

Hall, C. A., Jr. (1964), Shallow-Water Marine Climates and Molluscan Provinces, *Ecology*, *45*(2), 226-234.

Herborg, L.-M., C. L. Jerde, D. M. Lodge, G. M. Ruiz, and H. J. MacIsaac (2007), Predicting Invasion Risk Using Measures of Introduction Effort and Environmental Niche Models, *Ecological Applications*, *17*(3), 663-674.

Hickey, B. M. (1979), The California current system - hypotheses and facts, *Oceanography*, *8*, 191-279.

Huey, R. B., C. A. Deutsch, J. J. Tewksbury, L. J. Vitt, P. E. Hertz, H. J. Álvarez Pérez, and T. Garland (2009), Why tropical forest lizards are vulnerable to climate warming, *Proceedings of the Royal Society B: Biological Sciences*, *276*(1664), 1939-1948.

Huyer, A. (1983), Coastal upwelling in the California current system, *Progress in Oceanography*, *12*(3), 259-284.

IPCC (2007), Climate change 2007: impacts, adaptation and vulnerability, in *Contribution of Working Group II to the Fourth Assessment Report of the Intergovernmental Panel on Climate Change*, edited by M. L. Parry, O. F. Canziani, J. Palutikof, P. J. van der Linden and C. E. Hanson, pp. 1-976, Cambridge University Press, Cambridge.

Jennings, S., and K. Brander (2010), Predicting the effects of climate change on marine communities and the consequences for fisheries, *Journal of Marine Systems*, *79*(3-4), 418-426.

Kearns, E. J., J. A. Hanafin, R. H. Evans, P. J. Minnett, and O. B. Brown (2000), An Independent Assessment of Pathfinder AVHRR Sea Surface Temperature Accuracy Using the Marine Atmosphere Emitted Radiance Interferometer (MAERI), *Bulletin of the American Meteorological Society*, *81*(7), 1525-1536.

Keister, J. E., and P. T. Strub (2008), Spatial and interannual variability in mesoscale circulation in the northern California Current System, *J. Geophys. Res.-Oceans*, *113*(C4).

Kilpatrick, K. A., G. P. Podesta, and R. Evans (2001), Overview of the NOAA/NASA advanced very high resolution radiometer Pathfinder algorithm for sea surface temperature and associated matchup database, *J. Geophys. Res.-Oceans*, *106*(C5), 9179-9197.

Longhurst, A. R. (2007), *Ecological geography of the sea --2nd ed.*, 542 pp., Elsevier Academic Press, Amsterdam ; Boston, MA

Maslanik, J. A., C. Fowler, J. Stroeve, S. Drobot, J. Zwally, D. Yi, and W. Emery (2007), A younger, thinner Arctic ice cover: Increased potential for rapid, extensive sea-ice loss, *Geophys. Res. Lett.*, *34*(24), L24501.

McCune, B., and J. B. Grace (2002), *Analysis of Ecological Communities*, 300 pp., MjM Software Design, Gleneden Beach, OR.

Mislan, K. A. S., D. S. Wethey, and H. B. (2009), When to worry about the weather: Role of tidal cycle in determining patterns of risk in intertidal ecosystems, *Global Change Biology*, *15*, 3056-3065.

Mueter, F. J., and B. L. Norcross (2002), Spatial and temporal patterns in the demersal fish community on the shelf and upper slope regions of the Gulf of Alaska, *Fishery Bulletin*, *100*(3), 559-581.

Mueter, F. J., and M. A. Litzow (2008), Sea ice retreat alters the biogeography of the Bering Sea continental shelf, *Ecological Applications*, *18*(2), 309-320.

Pauley, D., et al. (2008), Fisheries in large marine ecosystems: descriptions and diagnoses, in *The UNEP Large Marine Ecosystem Report: A perspective on changing conditions in LMEs of the world's regional seas*, edited by K. S. a. G. Hempel, pp. 23-40, UNEP, Nairobi, Kenya.

Payne, M. C., D. A. Reusser, and H. Lee II (2012), Moderate-resolution sea surface temperature data and seasonal pattern analysis for the Arctic Ocean ecoregions, *U.S. Geological Survey Open-File Report 2011-1246, available at http://pubs.usgs.gov/of/2011/1246/*.

Payne, M. C., D. A. Reusser, H. Lee, II, , and C. A. Brown (2011), Moderate-resolution sea surface temperature data for the nearshore North Pacific: U.S. Geological Survey Open-File Report 2010-1251*Rep.*, 16 pp.

Payne, M. C., D. A. Reusser, H. Lee II, and C. A. Brown (2011), Moderate-resolution sea surface temperature data for the nearshore North Pacific: U.S. Geological Survey Open-File Report 2010-1251*Rep.*, 16 pp.

Payne, M. C., C. A. Brown, D. A. Reusser, and H. Lee, II (2012), Ecoregional Analysis of Nearshore Sea-Surface Temperature in the North Pacific, *PLoS ONE*, *7*(1), e30105.

Pearce, A., F. Faskel, and G. Hyndes (2006), Nearshore sea temperature variability off Rottnest Island (Western Australia) derived from satellite data, *International Journal of Remote Sensing*, *27*(12), 2503 - 2518.

Pirhalla, D. E., V. Ransibrahmanakul, R. Clark, A. Desch, T. Wynne, and M. Edwards (2009), An Oceanographic Characterization of the Olympic Coast National Marine Sanctuary and Pacific Northwest: Interpretive Summary of Ocean Climate and Regional Processes Through Satellite Remote Sensing. *Rep. NOAA Technical Memorandum NOS NCCOS 90* 53 pp, Prepared by

NCCOS's Coastal Oceanographic Assessments, Status and Trends Division in cooperation with the National Marine Sanctuary Program, Silver Spring, MD

Qiu, B. (2001), Kuroshio and Oyashio Currents, in *Encyclopedia of Ocean Sciences*, edited by J. Steele, S. Thorpe and K. Turekian, pp. 1413-1425, Academic Press.

R Development Core Team (2009), R: A language and environment for statistical computing., edited, R Foundation for Statistical Computing, Vienna, Austria.

Reusser, D. A., and H. Lee (2011), Evolution of natural history information in the 21st century – developing an integrated framework for biological and geographical data, *J. Biogeogr.*, *38*(7), 1225-1239.

Reynolds, R. W., N. A. Rayner, T. M. Smith, D. C. Stokes, and W. Wang (2002), An Improved In Situ and Satellite SST Analysis for Climate, *J. Clim.*, *15*(13), 1609-1625.

Rivadeneira, M. M., and M. Fernandez (2005), Shifts in southern endpoints of distribution in rocky intertidal species along the south-eastern Pacific coast, *J. Biogeogr.*, *32*(2), 203-209.

Roberts, J. J., B. D. Best, D. C. Dunn, E. A. Treml, and P. N. Halpin (2010), Marine Geospatial Ecology Tools: An integrated framework for ecological geoprocessing with ArcGIS, Python, R, MATLAB, and C++, *Environmental Modelling & Software*, *25*(10), 1197-1207.

Sherman, K., M.-C. Aquarone, and S. Adams (2007), Global Applications of the Large Marine Ecosystem Concept 2007-2010, edited by U. S. D. o. Commerce, p. 71, National Marine Fisheries Service, Northeast Fisheries Science Center, Woods Hole, MA.

Sorte, C. J. B., S. L. Williams, and J. T. Carlton (2010), Marine range shifts and species introductions: comparative spread rates and community impacts, *Global Ecology and Biogeography*, *19*(3), 303-316.

Spalding, M. D., et al. (2007), Marine ecoregions of the world: a bioregionalization of coastal and shelf areas, *BioScience*, *57*(7), 573-583.

Stram, D. L., and D. C. K. Evans (2009), Fishery management responses to climate change in the North Pacific, *ICES Journal of Marine Science*, *66*(7), 1633-1639.

Tokinaga, H., and S.-P. Xie (2009), Ocean tidal cooling effect on summer sea fog over the Okhotsk Sea, *Journal of Geophysical Research*, *114*(D14102).

Trenberth, K. E., J. R. Christy, and J. W. Hurrell (1992), Monitoring Global Monthly Mean Surface Temperatures, *J. Clim.*, *5*(12), 1405-1423.

Vazquez-Cuervo, J., K. Perry, and K. Kilpatrick (1998), NOAA/NASA AVHRR Oceans Pathfinder sea surface temperature data set user's reference manual version 4.0: JPL Publication D-14070*Rep.*

Vazquez-Cuervo, J., E. M. Armstrong, and A. Harris (2004), The effect of aerosols and clouds on the retrieval of infrared sea surface temperatures, *J. Clim.*, *17*(20), 3921-3933.

Vazquez-Cuervo, J., E. M. Armstrong, K. S. Casey, R. Evans, and K. Kilpatrick (2010), Comparison between the Pathfinder Versions 5.0 and 4.1 Sea Surface Temperature Datasets: A Case Study for High Resolution, *J. Clim.*, *23*(5), 1047-1059.

Venegas, R. M., P. T. Strub, E. Beier, R. Letelier, A. C. Thomas, T. Cowles, C. James, L. Soto-Mardones, and C. Cabrera (2008), Satellite-derived variability in chlorophyll, wind stress, sea surface height, and temperature in the northern California Current System, *J. Geophys. Res.*, *113*.

Walker, N., S. Myint, A. Babin, and A. Haag (2003), Advances in satellite radiometry for the surveillance of surface temperatures, ocean eddies and upwelling processes in the Gulf of Mexico using GOES-8 measurements during summer, *Geophys. Res. Lett.*, *30*(16), 4.

Wessel, P., and W. H. F. Smith (1996), A global, self-consistent, hierarchical, high-resolution shoreline database, *J. Geophys. Res.*, *101*.

Wethey, D. S., and S. A. Woodin (2008), Ecological hindcasting of biogeographic responses to climate change in the European intertidal zone, *Hydrobiologia*, *606*, 139-151.

Wyrtki, K. (1965), The Annual and Semiannual Variation of Sea Surface Temperature in the North Pacific Ocean, *Limnology and Oceanography*, *X*(3), 307-313.

Xu, F., and A. Ignatov (2010), Evaluation of in situ sea surface temperatures for use in the calibration and validation of satellite retrievals, *J. Geophys. Res.-Oceans*, *115*.

Yashayaev, I. M., and Zveryaev, II (2001), Climate of the seasonal cycle in the North Pacific and the North Atlantic Oceans, *International Journal of Climatology*, *21*(4), 401-417.

Zhang, S.-P., S.-P. Xie, Q.-Y. Liu, Y.-Q. Yang, X.-G. Wang, and Z.-P. Ren (2009), Seasonal Variations of Yellow Sea Fog: Observations and Mechanisms*, *J. Clim.*, *22*(24), 6758-6772.

APPENDIX A

MODERATE-RESOLUTION SEA SURFACE TEMPERATURE DATA FOR THE NEARSHORE NORTH PACIFIC

Meredith C. Payne[1, 2], Deborah A. Reusser[1, 2], Henry Lee II[3], Cheryl A. Brown[3]

[1]Western Fisheries Research Center, United States Geological Survey, Newport, Oregon, United States of America, [2]Oregon State University, Corvallis, Oregon, United States of America, [3]Pacific Coastal Ecology Branch, Western Ecology Division, United States Environmental Protection Agency, Newport, Oregon, United States of America

U.S. Geological Survey, Reston, Virginia

USGS National Center
12201 Sunrise Valley Drive
Reston, VA 20192
USA

November 2011 | http://pubs.usgs.gov/of/2010/1251/

Appendix A

Abstract

Coastal sea surface temperature (SST) is an important environmental characteristic in determining the suitability of habitat for nearshore marine and estuarine organisms. This publication describes and provides access to an easy-to-use coastal SST dataset for ecologists, biogeographers, oceanographers, and other scientists conducting research on nearshore marine habitats or processes. The data cover the Temperate Northern Pacific Ocean as defined by the "Marine Ecosystems of the World" (MEOW) biogeographic schema developed by The Nature Conservancy. The spatial resolution of the SST data is 4-km grid cells within 20 km of the shore. The data span a 29-year period – from September 1981 to December 2009. These SST data were derived from Advanced Very High Resolution Radiometer (AVHRR) instrument measurements compiled into monthly means as part of the Pathfinder versions 5.0 and 5.1 (PFSST V50 and V51) Project. The processing methods used to transform the data from their native Hierarchical Data Format Scientific Data Set (HDF SDS) to georeferenced, spatial datasets capable of being read into geographic information systems (GIS) software are explained. In addition, links are provided to examples of scripts involved in the data processing steps. The scripts were written in the Python programming language, which is supported by ESRI's ArcGIS version 9 or later. The processed data files are also provided in text (.csv) and Access 2003 Database (.mdb) formats. All data except the raster files include attributes identifying realm, province, and ecoregion as defined by the MEOW classification schema.

Introduction

Recent research indicates there has been a warming trend in Pacific Ocean temperatures over the last 50 years [*IPCC*, 2007]. Nearshore regions along the North Pacific coast are particularly sensitive to this trend. In these nearshore regions, *in situ* SST measurements are typically made via buoys, but such measurements are irregular in both space and time. Satellite-based remote-sensing observations have the advantage of extensive spatial coverage and high repeatability that is not possible with field observations. The trade-off, however, is that satellite data generally have low spatial resolution compared with field measurements and therefore often cannot resolve smaller features important in coastal areas. Furthermore, high-resolution image products of large area often consist of an unmanageable amount of data, making them impractical for general use. However, a spatio-temporally continuous near-coastal SST dataset can be used to address questions about nearshore environments in ways that are not possible with offshore SST measurements. Therefore, for climate change research in coastal and estuarine environments, a moderate resolution SST product that covers the near-coastal area while keeping file size reasonable is needed.

To fill this nearshore SST data gap, a three-decade, moderate-resolution (4 km) SST dataset was generated for the nearshore areas of the North Pacific, from Baja, California to the East China Sea. This dataset is based on SST measurements from the Advanced Very High Resolution Radiometer (AVHRR) Pathfinder v. 5 data. The AVHRR data provide a consistent set of SST measurements, of a known quality, for nearshore environments in the North Pacific. The methods used to generate the data are described here. Our intent is to provide these data as a readily-available product for researchers who are addressing questions about the effects of variations in temperature on the distribution of nearshore organisms.

Data Description

AVHRR SST Data

The Advanced Very High Resolution Radiometer (AVHRR) is a multi-generational, 6-channel instrument that has been flown on board a series of NOAA polar-orbiting satellites, and has been returning reliable SST data since 1981. Sea surface temperature is not measured directly; rather, it is the result of a differentiation of brightness temperatures recorded by two of the sensor's infrared (IR) channels (channels 4 and 5). It has been shown that atmospheric aerosols and particulates (for example, volcanic ash or Saharan dust) are sources for error in IR brightness temperature measurements, and potentially introduce a cold bias [*Vazquez-Cuervo et al.*, 2004]. However, one advantage of using satellite IR retrievals to derive SST is that the long IR wavelengths are less affected by atmospheric contaminants (such as cloud or fog). Another benefit of IR wavelength measurements is that daylight is not a requirement for data collection. And while nighttime AVHRR data have been preferred for some SST analyses, it has been shown that nighttime-only AVHRR Pathfinder data do not necessarily produce superior results with respect to reproducing *in situ* temperature measurements [*Casey*, 2002]. Therefore, we chose to use the daytime series of the AVHRR Pathfinder 4 km dataset based on data availability. We found daytime data to be more abundant in our near-coastal regions of interest, especially in areas that experience frequent evening ground fog, such as the coasts of the states of Washington and Oregon.

The AVHRR Pathfinder v.5 (and later) datasets were developed jointly by the University of Miami Rosenstiel School of Marine and Atmospheric Science and the NOAA National Oceanographic Data Center (NODC) as a more accurate, downscaled (9.28 to 4 km) version of a previous global AVHRR dataset [*Vazquez-Cuervo et al.*, 1998]. We obtained the version 5 (PFSST

V50) raster data from the NASA JPL Physical Oceanography Distributed Active Archive Center (PO.DAAC) (ftp://podaac.jpl.nasa.gov/OceanTemperature/avhrr/L3/pathfinder_v5/). AVHRR products (PFSST V50 and PFSST V51) are also available through the NODC (ftp://data.nodc.noaa.gov/pub/data.nodc/pathfinder). The source data were provided in HDF-SDS (Hierarchical Data Format Scientific Data Set) format. For a detailed description of the AVHRR and Pathfinder algorithms, we direct the reader to *Vazquez-Cuervo et al.*[1998; 2010] and *Kilpatrick and et al.* [2001].

AVHRR Data Quality

The PFSST data include a quality flag product in which each SST pixel is designated a value ranging from 0 (worst quality) to 7 (best quality). These quality flags convey the level of confidence attributed to the SST value calculated for each pixel location. The level of confidence is evaluated on pixel-by-pixel performance with respect to a number of tests that estimate validity and consistency of brightness temperature readings, sun angle effects, and cloudiness, which are combined to establish an overall quality rating. The version 4 Pathfinder release of the SST dataset (PFSST V41) included a standard product called "best SST," or "BSST." BSST data includes pixels with quality flags greater than 3 [*Kilpatrick et al.*, 2001]. We generated an analogous SST product from the PFSST data by disregarding SST values with corresponding quality flag values of less than 4. Despite the rigors of the flagging algorithms, a small number of pixels with illegitimate jumps in SST gradient have been detected [*Evans et al.*, 2009]. These jumps in the SST gradient must be detected and removed by the user depending on their data requirements.

Data Accuracy

Currently the only reports on accuracy of Pathfinder SST values are linked to specific studies across a variety of spatial and temporal resolutions, pathfinder versions, and quality flag thresholds. In general, the temperature values are reported to have RMS errors between 0.1 and 1.0 °C [*Kearns et al.*, 2000; *Kilpatrick et al.*, 2001; *Vazquez-Cuervo et al.*, 2010; *Xu and Ignatov*, 2010] when compared to *in situ* temperatures. However, it must be cautioned that *in situ* temperature data derived from multiple sources, such as moored buoys and shipboard observations, are prone to large random errors and rarely have excellent agreement amongst them (e.g. [*Kearns et al.*, 2000]). Furthermore, *in situ* measurements are of bulk temperatures (typically taken between 1 – 3 meters depth) rather than true sea surface temperature. Lastly, comparison to *in situ* data sources such as buoys and the National Centers for Environmental Prediction (NCEP; [*Reynolds et al.*, 2002]) are somewhat contrived as these data [*Reynolds et al.*, 2002] provide critical calibration and validation for the PFSST data product [*Kilpatrick et al.*, 2001; *Vazquez-Cuervo et al.*, 2010]. In practice, when the scaling algorithm provided with the AVHRR data is applied, the resulting SST values imply a 1/1000 of a degree precision, a level of precision that is beyond the limitations of the original processing algorithm. Based on these considerations, the accuracy of the nearshore SST data is approximately 0.5 °C (personal communication, Jorge Vazquez-Cuervo, February 3, 2011).

Coastal SST Product

We selected AVHRR data for their global coverage at moderate resolution (4 km), their long data record (~30 years) relative to other satellite missions, and their substantial level of processing, including extensive calibration and atmospheric correction. The data represent a time-series of monthly mean sea surface temperatures over the last 29 years. The data presented here encompass the nearshore region of the entire North Pacific, from the coast to approximately 16 km from the shoreline, as defined by the Global Self-consistent, Hierarchical, High-resolution Shoreline (GSHHS) version 1.3 [*Wessel and Smith*, 1996]. In some places, the data appear jagged, or "moth-eaten," immediately adjacent to the coast. There are two reasons for this. The first is that satellite data for some regions of the coast are missing or are unusable due to low quality. The second reason for the jagged appearance of the data is that the Pathfinder developers used a MOD12Q1 land mask, which has a 1-km resolution rather than the 0.2-km resolution of the GSHHS. As detailed below, we processed the data using a number of tools to create several nearshore SST products, including georeferenced North Pacific SST shape and raster files, along with their metadata, and Access 2003 Databases.

Data Processing

The steps taken to convert AVHRR data to nearshore SST data are detailed in flow-chart form in Figure A-1. As the focus was on nearshore environments, the study area in each ecoregion is limited to within approximately 16 km of the coastline (fig. A-2). The grid cell resolution of the AVHRR PFSST data was 4 km^2 and the offshore distance was determined by counting four grid cells seaward of the coastline defined by the Global Self-consistent, Hierarchical, High-resolution Shoreline (GSHHS) dataset [*Wessel and Smith*, 1996].

The Marine Geospatial Ecology Tools v. 0.8 (MGET) were used to convert the Pathfinder PFSST V5 and V5.1 data from its native HDF-SDS format to ArcGIS GRID raster format [*Roberts et al.*, 2010]. MGET was developed by Duke University's Marine Geospatial Ecology Laboratory for exploring spatial aspects of ecological data and is integrated into the ESRI ArcGIS environment for use in conjunction with other geoprocessing tools, including Python, Matlab, R, and C++. The MGET extension is available at http://code.env.duke.edu/projects/mget. HDF to GRID conversion is a two step process. The georeferencing (header information) parameters for data conversion must be extracted first using MGET or another HDF tool. The extracted parameters are then used in the MGET conversion tool to create ArcGIS rasters (GRIDs).

A parallel processing path is followed whereby a HDF SST file, which contains the mean SSTs recorded by the AVHRR instrument over a one-month period, and its corresponding HDF Quality (hereafter qual) file are transformed (by MGET) into ArcGIS GRIDs. The SST GRIDs were then scaled using the equation provided in the AVHRR header in order to obtain SST values in degrees Celsius. Application of this scaling equation on floating point data created variable precision of the SST values (RASTERVALU) from 0 to 8 digits. The SST values were not rounded or truncated during the data processing. The qual value GRIDs were transformed into binary masks in which pixels of flag values ≥ 4 were converted into 1s and those with values 0-3 were converted to 0s (as discussed in the data description). The monthly SST data were produced by applying the qual mask to the SST GRID raster to eliminate SST values with corresponding quality flag values of less than 4. The next step was to eliminate implausible SST values (< -2.0 °C) that occasionally appear at the higher latitudes.

The ArcToolbox buffering tool (available with the ArcInfo version of the ESRI software) was used to create a buffer to isolate SST raster pixels within 16 km of the GSHHS shoreline. This buffer is essentially a polygon shapefile that functions as a clipping feature. It was used to crop the global SST rasters to the North Pacific nearshore extent. These nearshore raster data are available for download from the "downloads" page of this website (click "downloads" on the left-side menu).

For each nearshore raster data file, a point shapefile was created in which each point represents the centroid of a corresponding grid cell and was assigned the associated SST value.

The Spatial Analyst ArcGIS extension "Extract Values to Points" tool was used to collect these point values. These steps were systematically repeated to generate a point shapefile of near-coastal SST values—one for each month of each year in the 1981-2009 record. To ensure consistent results, the processes of reading in the native SST HDF files through the point extraction step was automated through a combination of using the ModelBuilder tool within ArcGIS and manual scripting in the Python 2.5 language. Each individual monthly mean file contains approximately 40,000 points. In the datasets offered here, we include the points having NoData values, designated as "-9999." As previously described, the lack of data at these points can be due to glint, sea-ice cover, atmospheric obscuration, or the coarseness of the MODIS land mask used in comparison to the GSHHS shoreline. All SST values are recorded in degrees Celsius and are found under the "RASTERVALU" heading. In addition to the nearshore raster dataset, and nearshore point shapefile dataset (also available in .csv format), a dataset is provided consisting of four Access databases created by exporting the ArcGIS .dbf files directly into Access databases (.mdb format) using the RODBC package in R. The Access 2003 databases are divided by Marine Province (Warm Temperate Northwest Pacific, Cold Temperate Northwest Pacific, Warm Temperate Northeast Pacific, Cold Temperate Northeast Pacific, see Figure A-3). This division was necessary due to the 2 GB size constraint on each Access 2003 database. The Access databases are also publically available through the download links provided on the left-hand side bar.

Downloads

GIS Data Catalog

This report contains Geographic Information System (GIS) data in georeferenced vector (point) and raster format. The vector (point) data are available in Environmental Systems

Research Institute (ESRI) shapefile format and in comma-separated text (*.csv) files. Shapefiles generally include *.shp, *.shx, *.xml, and *.dbf files at a minimum. All of these data files also include the *.prj files, which contain the dataset projection information. The corresponding 4-km resolution raster data are available in ESRI GRID format.

The GIS files have been bundled by year. Each data type (shp, GRID, csv) has a compressed WinRAR zip file—one for each year, hence every zip file may contain up to 12 months of data. In addition to the spatial data, we provide Federal Geographic Data Committee (FGDC) -compliant metadata in text and HTML formats. The metadata text files are bundled with their corresponding zip files, and the metadata HTML information can be viewed in your web browser by clicking the appropriate link in the table below.

To download the data, right-click on the appropriate filename link in the '**Filename**' column (that corresponds to the desired data type) in the table below. Then select '**Save Target As...**' to save a compressed WinRAR file to your local hard drive. The download zipped file size is indicated under the '**file size'** column. All downloaded files are of type ".zip". The File Type description in the Table below indicates the type of files found within the downloadable zip files.

Filename	Description	File Type	File Size	Metadata
		2009		
NPacSST2009rast.zip	North Pacific Nearshore monthly mean SST data for 2009 in ESRI GRID raster format.	ESRI GRID	1.7 MB	Available online
NPacSST2009pt.zip	North Pacific Nearshore monthly mean SST data for 2009 in ESRI (point) shapefile format.	ESRI shapefile (*.shp)	10 MB	Available online
NPacSST2009csv.zip	North Pacific Nearshore monthly mean SST data for 2009 .csv	Comma-separated text	3.8 MB	Available

	format.	file (*.csv)		online
		2008		
NPacSST2008rast.zip	North Pacific Nearshore monthly mean SST data for 2008 in ESRI GRID raster format.	ESRI GRID	1.7 MB	Available online
NPacSST2008pt.zip	North Pacific Nearshore monthly mean SST data for 2008 in ESRI (point) shapefile format.	ESRI shapefile (*.shp)	10 MB	Available online
NPacSST2008csv.zip	North Pacific Nearshore monthly mean SST data for 2008 .csv format.	Comma-separated text file (*.csv)	3.8 MB	Available online
		2007		
NPacSST2007rast.zip	North Pacific Nearshore monthly mean SST data for 2007 in ESRI GRID raster format.	ESRI GRID	1.8 MB	Available online
NPacSST2007pt.zip	North Pacific Nearshore monthly mean SST data for 2007 in ESRI (point) shapefile format.	ESRI shapefile (*.shp)	10 MB	Available online
NPacSST2007csv.zip	North Pacific Nearshore monthly mean SST data for 2007 .csv format.	Comma-separated text file (*.csv)	3.8 MB	Available online
		2006		
NPacSST2006rast.zip	North Pacific Nearshore monthly mean SST data for 2006 in ESRI GRID raster format.	ESRI GRID	1.7 MB	Available online
NPacSST2006pt.zip	North Pacific Nearshore monthly mean SST data for 2006 in ESRI (point) shapefile format.	ESRI shapefile (*.shp)	10 MB	Available online
NPacSST2006csv.zip	North Pacific Nearshore monthly mean SST data for 2006 .csv format.	Comma-separated text file (*.csv)	3.8 MB	Available online
		2005		

NPacSST2005rast.zip	North Pacific Nearshore monthly mean SST data for 2005 in ESRI GRID raster format.	ESRI GRID	1.7 MB	Available online
NPacSST2005pt.zip	North Pacific Nearshore monthly mean SST data for 2005 in ESRI (point) shapefile format.	ESRI shapefile (*.shp)	10 MB	Available online
NPacSST2005csv.zip	North Pacific Nearshore monthly mean SST data for 2005 .csv format.	Comma-separated text file (*.csv)	3.8 MB	Available online
		2004		
NPacSST2004rast.zip	North Pacific Nearshore monthly mean SST data for 2004 in ESRI GRID raster format.	ESRI GRID	1.7 MB	Available online
NPacSST2004pt.zip	North Pacific Nearshore monthly mean SST data for 2004 in ESRI (point) shapefile format.	ESRI shapefile (*.shp)	10 MB	Available online
NPacSST2004csv.zip	North Pacific Nearshore monthly mean SST data for 2004 .csv format.	Comma-separated text file (*.csv)	3.8 MB	Available online
		2003		
NPacSST2003rast.zip	North Pacific Nearshore monthly mean SST data for 2003 in ESRI GRID raster format.	ESRI GRID	1.5 MB	Available online
NPacSST2003pt.zip	North Pacific Nearshore monthly mean SST data for 2003 in ESRI (point) shapefile format.	ESRI shapefile (*.shp)	10 MB	Available online
NPacSST2003csv.zip	North Pacific Nearshore monthly mean SST data for 2003 .csv format.	Comma-separated text file (*.csv)	3.8 MB	Available online
		2002		
NPacSST2002rast.zip	North Pacific Nearshore monthly mean SST data for 2002 in ESRI GRID raster format.	ESRI GRID	1.6 MB	Available online

NPacSST2002pt.zip	North Pacific Nearshore monthly mean SST data for 2002 in ESRI (point) shapefile format.	ESRI shapefile (*.shp)	10 MB	Available online
NPacSST2002csv.zip	North Pacific Nearshore monthly mean SST data for 2002 .csv format.	Comma-separated text file (*.csv)	3.8 MB	Available online
		2001		
NPacSST2001rast.zip	North Pacific Nearshore monthly mean SST data for 2001 in ESRI GRID raster format.	ESRI GRID	1.5 MB	Available online
NPacSST2001pt.zip	North Pacific Nearshore monthly mean SST data for 2001 in ESRI (point) shapefile format.	ESRI shapefile (*.shp)	10 MB	Available online
NPacSST2001csv.zip	North Pacific Nearshore monthly mean SST data for 2001 .csv format.	Comma-separated text file (*.csv)	3.8 MB	Available online
		2000		
NPacSST2000rast.zip	North Pacific Nearshore monthly mean SST data for 2000 in ESRI GRID raster format.	ESRI GRID	1.8 MB	Available online
NPacSST2000pt.zip	North Pacific Nearshore monthly mean SST data for 2000 in ESRI (point) shapefile format.	ESRI shapefile (*.shp)	10 MB	Available online
NPacSST2000csv.zip	North Pacific Nearshore monthly mean SST data for 2000 .csv format.	Comma-separated text file (*.csv)	3.8 MB	Available online
		1999		
NPacSST1999rast.zip	North Pacific Nearshore monthly mean SST data for 1999 in ESRI GRID raster format.	ESRI GRID	1.7 MB	Available online
NPacSST1999pt.zip	North Pacific Nearshore monthly mean SST data for 1999 in ESRI (point) shapefile format.	ESRI shapefile (*.shp)	10 MB	Available online

NPacSST1999csv.zip	North Pacific Nearshore monthly mean SST data for 1999 .csv format.	Comma-separated text file (*.csv)	3.8 MB	Available online
		1998		
NPacSST1998rast.zip	North Pacific Nearshore monthly mean SST data for 1998 in ESRI GRID raster format.	ESRI GRID	1.7 MB	Available online
NPacSST1998pt.zip	North Pacific Nearshore monthly mean SST data for 1998 in ESRI (point) shapefile format.	ESRI shapefile (*.shp)	10 MB	Available online
NPacSST1998csv.zip	North Pacific Nearshore monthly mean SST data for 1998.csv format.	Comma-separated text file (*.csv)	3.8 MB	Available online
		1997		
NPacSST1997rast.zip	North Pacific Nearshore monthly mean SST data for 1997 in ESRI GRID raster format.	ESRI GRID	1.7 MB	Available online
NPacSST1997pt.zip	North Pacific Nearshore monthly mean SST data for 1997 in ESRI (point) shapefile format.	ESRI shapefile (*.shp)	10 MB	Available online
NPacSST1997csv.zip	North Pacific Nearshore monthly mean SST data for 1997 .csv format.	Comma-separated text file (*.csv)	3.8 MB	Available online
		1996		
NPacSST1996rast.zip	North Pacific Nearshore monthly mean SST data for 1996 in ESRI GRID raster format.	ESRI GRID	1.7 MB	Available online
NPacSST1996pt.zip	North Pacific Nearshore monthly mean SST data for 1996 in ESRI (point) shapefile format.	ESRI shapefile (*.shp)	10 MB	Available online
NPacSST1996csv.zip	North Pacific Nearshore monthly mean SST data for 1996 .csv format.	Comma-separated text file (*.csv)	3.8 MB	Available online

		1995		
NPacSST1995rast.zip	North Pacific Nearshore monthly mean SST data for 1995 in ESRI GRID raster format.	ESRI GRID	1.4 MB	Available online
NPacSST1995pt.zip	North Pacific Nearshore monthly mean SST data for 1995 in ESRI (point) shapefile format.	ESRI shapefile (*.shp)	10 MB	Available online
NPacSST1995csv.zip	North Pacific Nearshore monthly mean SST data for 1995 .csv format.	Comma-separated text file (*.csv)	3.8 MB	Available online
		1994		
NPacSST1994rast.zip	North Pacific Nearshore monthly mean SST data for 1994 in ESRI GRID raster format.	ESRI GRID	1.8 MB	Available online
NPacSST1994pt.zip	North Pacific Nearshore monthly mean SST data for 1994 in ESRI (point) shapefile format.	ESRI shapefile (*.shp)	10 MB	Available online
NPacSST1994csv.zip	North Pacific Nearshore monthly mean SST data for 1994 .csv format.	Comma-separated text file (*.csv)	3.8 MB	Available online
		1993		
NPacSST1993rast.zip	North Pacific Nearshore monthly mean SST data for 1993 in ESRI GRID raster format.	ESRI GRID	1.7 MB	Available online
NPacSST1993pt.zip	North Pacific Nearshore monthly mean SST data for 1993 in ESRI (point) shapefile format.	ESRI shapefile (*.shp)	10 MB	Available online
NPacSST1993csv.zip	North Pacific Nearshore monthly mean SST data for 1993 .csv format.	Comma-separated text file (*.csv)	3.8 MB	Available online
		1992		
NPacSST1992rast.zip	North Pacific Nearshore monthly mean SST data for 1992 in ESRI	ESRI GRID	1.7 MB	Available

	GRID raster format.			online
NPacSST1992pt.zip	North Pacific Nearshore monthly mean SST data for 1992 in ESRI (point) shapefile format.	ESRI shapefile (*.shp)	10 MB	Available online
NPacSST1992csv.zip	North Pacific Nearshore monthly mean SST data for 1992 .csv format.	Comma-separated text file (*.csv)	3.8 MB	Available online
		1991		
NPacSST1991rast.zip	North Pacific Nearshore monthly mean SST data for 1991 in ESRI GRID raster format.	ESRI GRID	1.7 MB	Available online
NPacSST1991pt.zip	North Pacific Nearshore monthly mean SST data for 1991 in ESRI (point) shapefile format.	ESRI shapefile (*.shp)	10 MB	Available online
NPacSST1991csv.zip	North Pacific Nearshore monthly mean SST data for 1991 .csv format.	Comma-separated text file (*.csv)	3.8 MB	Available online
		1990		
NPacSST1990rast.zip	North Pacific Nearshore monthly mean SST data for 1990 in ESRI GRID raster format.	ESRI GRID	1.8 MB	Available online
NPacSST1990pt.zip	North Pacific Nearshore monthly mean SST data for 1990 in ESRI (point) shapefile format.	ESRI shapefile (*.shp)	10 MB	Available online
NPacSST1990csv.zip	North Pacific Nearshore monthly mean SST data for 1990 .csv format.	Comma-separated text file (*.csv)	3.8 MB	Available online
		1989		
NPacSST1989rast.zip	North Pacific Nearshore monthly mean SST data for 1989 in ESRI GRID raster format.	ESRI GRID	1.7 MB	Available online
NPacSST1989pt.zip	North Pacific Nearshore monthly mean SST data for 1989 in ESRI	ESRI shapefile	10 MB	Available

	(point) shapefile format.	(*.shp)		online
NPacSST1989csv.zip	North Pacific Nearshore monthly mean SST data for 1989 .csv format.	Comma-separated text file (*.csv)	3.8 MB	Available online
		1988		
NPacSST1988rast.zip	North Pacific Nearshore monthly mean SST data for 1988 in ESRI GRID raster format.	ESRI GRID	1.7 MB	Available online
NPacSST1988pt.zip	North Pacific Nearshore monthly mean SST data for 1988 in ESRI (point) shapefile format.	ESRI shapefile (*.shp)	10 MB	Available online
NPacSST1988csv.zip	North Pacific Nearshore monthly mean SST data for 1988 .csv format.	Comma-separated text file (*.csv)	3.8 MB	Available online
		1987		
NPacSST1987rast.zip	North Pacific Nearshore monthly mean SST data for 1987 in ESRI GRID raster format.	ESRI GRID	1.8 MB	Available online
NPacSST1987pt.zip	North Pacific Nearshore monthly mean SST data for 1987 in ESRI (point) shapefile format.	ESRI shapefile (*.shp)	10 MB	Available online
NPacSST1987csv.zip	North Pacific Nearshore monthly mean SST data for 1987 .csv format.	Comma-separated text file (*.csv)	3.8 MB	Available online
		1986		
NPacSST1986rast.zip	North Pacific Nearshore monthly mean SST data for 1986 in ESRI GRID raster format.	ESRI GRID	1.9 MB	Available online
NPacSST1986pt.zip	North Pacific Nearshore monthly mean SST data for 1986 in ESRI (point) shapefile format.	ESRI shapefile (*.shp)	10 MB	Available online
NPacSST1986csv.zip	North Pacific Nearshore monthly mean SST data for 1986 .csv	Comma-separated text	3.8 MB	Available

	format.	file (*.csv)		online
		1985		
NPacSST1985rast.zip	North Pacific Nearshore monthly mean SST data for 1985 in ESRI GRID raster format.	ESRI GRID	1.8 MB	Available online
NPacSST1985pt.zip	North Pacific Nearshore monthly mean SST data for 1985 in ESRI (point) shapefile format.	ESRI shapefile (*.shp)	10 MB	Available online
NPacSST1985csv.zip	North Pacific Nearshore monthly mean SST data for 1985 .csv format.	Comma-separated text file (*.csv)	3.8 MB	Available online
		1984		
NPacSST1984rast.zip	North Pacific Nearshore monthly mean SST data for 1984 in ESRI GRID raster format.	ESRI GRID	1.7 MB	Available online
NPacSST1984pt.zip	North Pacific Nearshore monthly mean SST data for 1984 in ESRI (point) shapefile format.	ESRI shapefile (*.shp)	10 MB	Available online
NPacSST1984csv.zip	North Pacific Nearshore monthly mean SST data for 1984 .csv format.	Comma-separated text file (*.csv)	3.8 MB	Available online
		1983		
NPacSST1983rast.zip	North Pacific Nearshore monthly mean SST data for 1983 in ESRI GRID raster format.	ESRI GRID	1.7 MB	Available online
NPacSST1983pt.zip	North Pacific Nearshore monthly mean SST data for 1983 in ESRI (point) shapefile format.	ESRI shapefile (*.shp)	10 MB	Available online
NPacSST1983csv.zip	North Pacific Nearshore monthly mean SST data for 1983 .csv format.	Comma-separated text file (*.csv)	3.8 MB	Available online
		1982		

NPacSST1982rast.zip	North Pacific Nearshore monthly mean SST data for 1982 in ESRI GRID raster format.	ESRI GRID	1.7 MB	Available online
NPacSST1982pt.zip	North Pacific Nearshore monthly mean SST data for 1982 in ESRI (point) shapefile format.	ESRI shapefile (*.shp)	10 MB	Available online
NPacSST1982csv.zip	North Pacific Nearshore monthly mean SST data for 1982 .csv format.	Comma-separated text file (*.csv)	3.8 MB	Available online
		1981*		
NPacSST1981rast.zip	North Pacific Nearshore monthly mean SST data for 1981 in ESRI GRID raster format.	ESRI GRID	641 KB	Available online
NPacSST1981pt.zip	North Pacific Nearshore monthly mean SST data for 1981 in ESRI (point) shapefile format.	ESRI shapefile (*.shp)	3.4 MB	Available online
NPacSST1981csv.zip	North Pacific Nearshore monthly mean SST data for 1981 .csv format.	Comma-separated text file (*.csv)	1.3 MB	Available online

*These files contain only the four months of data that are available for 1981. 09/1981 – 12/1981.

Access Databases

The nearshore North Pacific SST data are available for download as MS Access databases (in 2003 .mdb format). Unlike the GIS data, these data are not ordered by year. Rather, they are arranged by geographical province (fig.A- 3). Each province database includes all of the individual monthly tables over all available years (September 1981 — December 2009) for points located within the specified province. To download the databases, click on the appropriate province name in the table below.

Province	Description	File Type	File Size	Metadata
Cold Temperate Northeast Pacific	Access 2003 database containing Nearshore SSTs of the Cold Temperate Northeast Pacific Ocean Province over the period 9/1981 - 12/2009.	.mdb	590 MB	Available online
Cold Temperate Northwest Pacific	Access 2003 database containing Nearshore SSTs of the Cold Temperate Northwest Pacific Ocean Province over the period 9/1981 - 12/2009.	.mdb	1.8 GB	Available online
Warm Temperate Northeast Pacific	Access 2003 database containing Nearshore SSTs of the Warm Temperate Northeast Pacific Ocean Province over the period 9/1981 - 12/2009.	.mdb	1.1 GB	Available online
Warm Temperate Northwest Pacific	Access 2003 database containing Nearshore SSTs of the Warm Temperate Northwest Pacific Ocean Province over the period 9/1981 - 12/2009.	.mdb	454 MB	Available online

Scripts

Here a number of scripts are provided that were developed to process the SST data. The scripts are written in the Python Language. Python is a freely-available, open-source scripting language that is object oriented and is supported by ArcGIS as a framework for creating and executing Geoprocessor tasks. Python also runs as a stand-alone programming language. The scripts were built using Python release 2.5.1, which is included with ESRI's ArcGIS 9.3.1. ArcGIS 9.3.x also supports Python version 2.5.4, but does not support later Python versions. Python is downloadable from http://www.python.org/download/releases/2.5.4/.

The PythonWin development environment provides a Graphic User Interface (GUI) for the python scripting editor. PythonWin is located in the "Python for Windows extensions" bundle available at http://sourceforge.net/projects/pywin32/. To use the scripts provided, the user will need access to ArcGIS 9.x software and install the Marine Geospatial Ecology Tools (MGET). MGET is available at http://code.env.duke.edu/projects/mget. The first step involved in preparing HDF SDS files for conversion to ArcGIS GRID files (preceding use of the processing scripts) is a manual renaming of the files to conform to ArcGIS specifications; specifically, the rasters may have filenames no longer than 13 characters and must begin with a letter (they may not begin with a number or symbol). The original HDF filenames violate both of these rules. As file naming conventions are a personal preference, a name-converting script is not provided here. However, for clarity of the processing scripts provided, note that our file-naming convention is "sstallyyyymm.hdf" for SST rasters, and "qualyyyymm.hdf" for quality rasters (where y = year and m = month).

These scripts can be modified to the users' needs or run in sequence (as presented below) to obtain a similar dataset to those made available in this report. The point and polygon shapefile included in the data processing steps of the scripts are available for download in zipped form from the table below.

Python Scripts

Script	**Description**	**File Type**
SST_HDF2ArcRaster.py	This script imports AVHRR Pathfinder SST data in HDF SDS format and converts them into georeferenced, scaled, SST rasters in ArcGIS GRID format with the help of the Marine Geospatial Ecology Tools (MGET).	.py
Qual_HDF2ArcRaster.py	This script imports AVHRR Pathfinder quality flag data in HDF SDS format and converts them into georeferenced, scaled, SST rasters in ArcGIS GRID format with the help of the Marine Geospatial Ecology Tools (MGET).	.py

CreateBSST.py	This script uses the SST and Qual ArcGIS grids constructed with the "SST_HDF2ArcRaster.py" and "Qual_HDF2ArcRaster.py" scripts to apply a quality constraint to the SST data.	.py
NPac_ns_SST.py	The purpose of this script is to clip the global SST grids to a nearshore region (20 km offshore) of the North Pacific Ocean. A clipping polygon shapefile, "lowres_TNP_coast_Buffer.shp" is provided below.	.py
NPac_ns_SST_pts.py	This script uses the nearshore grids created with the "NPac_ns_SST.py" script. It employs the ArcGIS Spatial Analyst extension, "Extract Values to Points" tool to extract SSTs from a nearshore SST raster underlying the 'TNP_pts.shp' point shapefile provided below that traces the perimeter of the Temperate Northern Pacific.	.py

Shapefiles

Filename	Description	File Type	File Size	Metadata
lowres_TNP_coast_Buffer.zip	Polygon shapefile used in the 'NPac_ns_SST.py' script to clip georeferenced global SST rasters to a nearshore (< 20 km from shoreline) North Pacific SST raster.	ESRI shapefile (*.shp)	2.3 MB	Available online
TNP_pts.zip	Point shapefile used in the 'NPac_ns_SST_pts.py' script to extract nearshore SST point values from nearshore raster grid cells. The attribute table for NPac_pts.shp also includes relational information to MEOW*	ESRI shapefile (*.shp)	14.4 MB	Available online

*Marine Ecosystems of the World (Spalding and others, 2007)

Acknowledgments

This publication has been reviewed by personnel of the National Health and Environmental Effects Research Laboratory's Western Ecology Division of the EPA, and the USGS Western Fisheries Research Center. The information in this document has been funded in part by the U.S. Environmental Protection Agency. However, approval does not signify that the contents reflect the views of the U.S. EPA.

Figure A-1. Flowchart detailing the data processing steps taken to convert AVHRR Pathfinder 4 km HDF data into North Pacific nearshore SST data in the form of ESRI GRIDs, ESRI shapefiles, text .csv files, and Access 2003 Databases. The flowchart color scheme emphasizes the relation of a particular input to its processes and outputs by using the same shades. New inputs or inputs derived through the combination of previous outputs have unique colors. Yellow rectangular boxes denote pre-existing (canned) MGET or ArcGIS tools used in processing. The final products marked with star symbols represent the datasets available through this report. A high-resolution, large version of this flowchart is available at http://pubs.usgs.gov/of/2010/1251/.

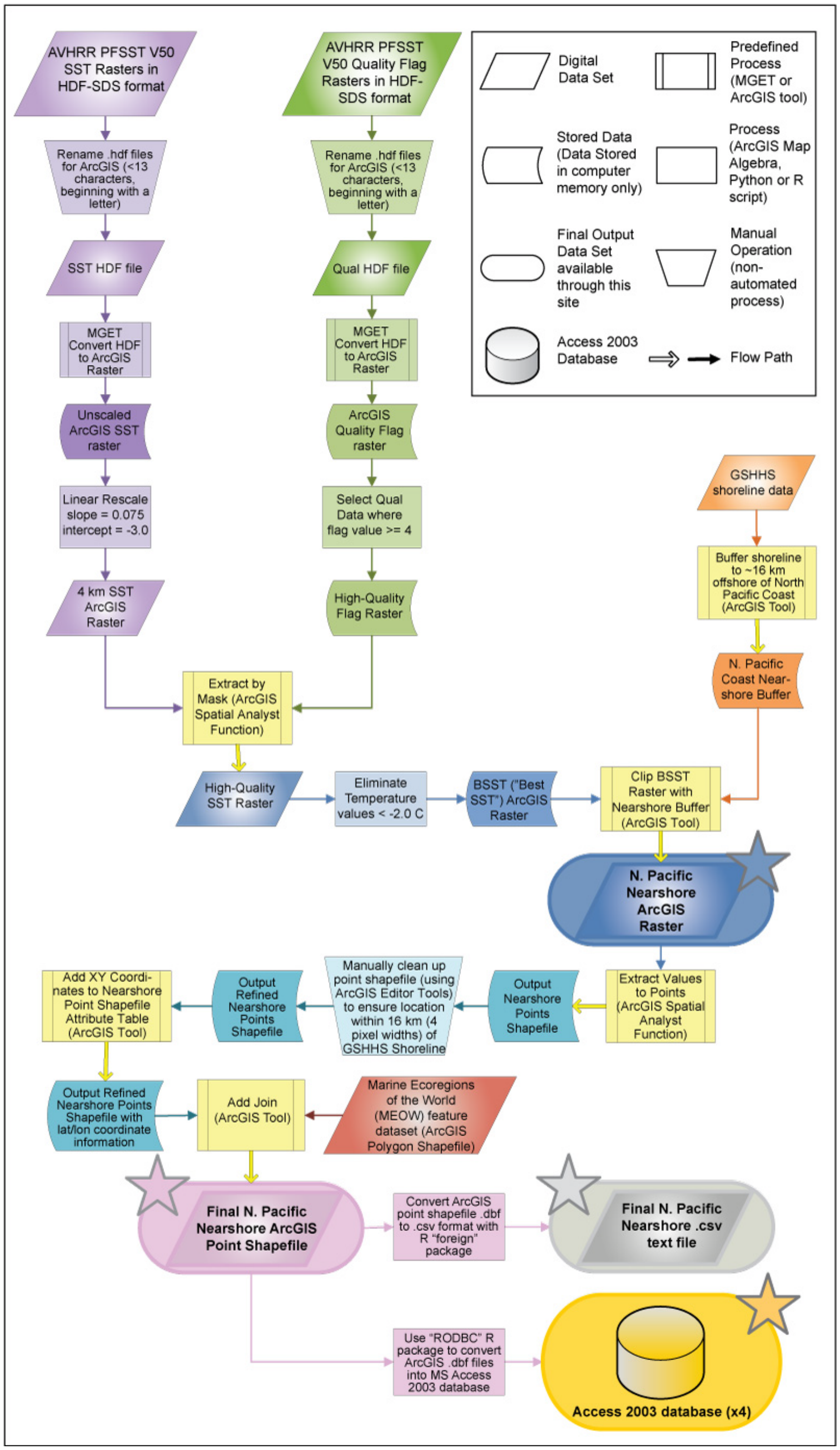

AVHRR PFSST V50 SST Rasters in HDF-SDS format
AVHRR PFSST V50 Quality Flag Rasters in HDF-SDS format
Digital Data Set
Predefined Process (MGET or ArcGIS tool)
Stored Data (Data Stored in computer memory only)
Process (ArcGIS Map Algebra, Python or R script)
Final Output Data Set available through this site
Manual Operation (non-automated process)
Access 2003 Database
Flow Path
Rename .hdf files for ArcGIS (<13 characters, beginning with a letter)
Rename .hdf files for ArcGIS (<13 characters, beginning with a letter)
SST HDF file
Qual HDF file
MGET Convert HDF to ArcGIS Raster
MGET Convert HDF to ArcGIS Raster
Unscaled ArcGIS SST raster
ArcGIS Quality Flag raster
Linear Rescale slope = 0.075 intercept = -3.0
Select Qual Data where flag value >= 4
4 km SST ArcGIS Raster
High-Quality Flag Raster
GSHHS shoreline data
Buffer shoreline to ~16 km offshore of North Pacific Coast (ArcGIS Tool)
N. Pacific Coast Near-shore Buffer
Extract by Mask (ArcGIS Spatial Analyst Function)
High-Quality SST Raster
Eliminate Temperature values < -2.0 C
BSST ("Best SST") ArcGIS Raster
Clip BSST Raster with Nearshore Buffer (ArcGIS Tool)
N. Pacific Nearshore ArcGIS Raster
Add XY Coordi-nates to Nearshore Point Shapefile Attribute Table (ArcGIS Tool)
Output Refined Nearshore Points Shapefile
Manually clean up point shapefile (using ArcGIS Editor Tools) to ensure location within 16 km (4 pixel widths) of GSHHS Shoreline
Output Nearshore Points Shapefile
Extract Values to Points (ArcGIS Spatial Analyst Function)
Output Refined Nearshore Points Shapefile with lat/lon coordinate information
Add Join (ArcGIS Tool)
Marine Ecoregions of the World (MEOW) feature dataset (ArcGIS Polygon Shapefile)
Final N. Pacific Nearshore ArcGIS Point Shapefile
Convert ArcGIS point shapefile .dbf to .csv format with R "foreign" package
Final N. Pacific Nearshore .csv text file
Use "RODBC" R package to convert ArcGIS .dbf files into MS Access 2003 database
Access 2003 database (x4)

Figure A-1.

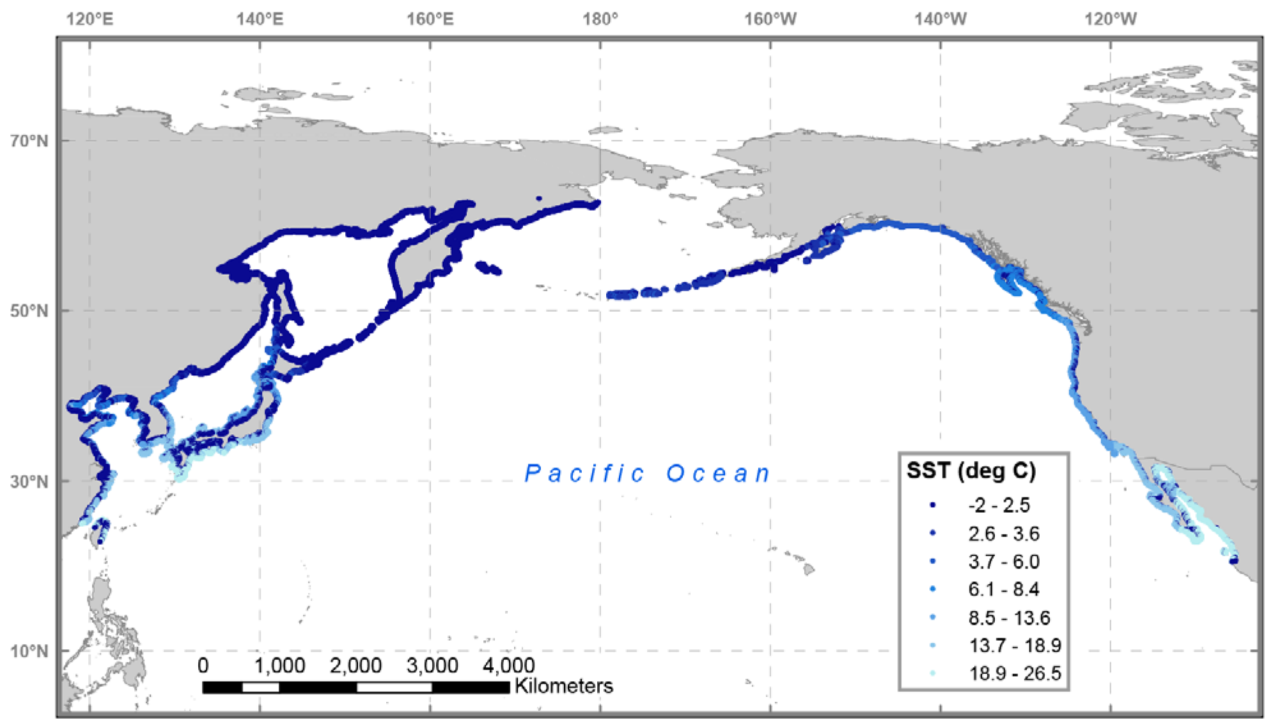

Figure A-2. Example of a monthly mean SST map (April 2009) of the North Pacific Ocean nearshore region. Resolution is 4 km. The color gradient along the nearshore corresponds to the SSTs at those locations.

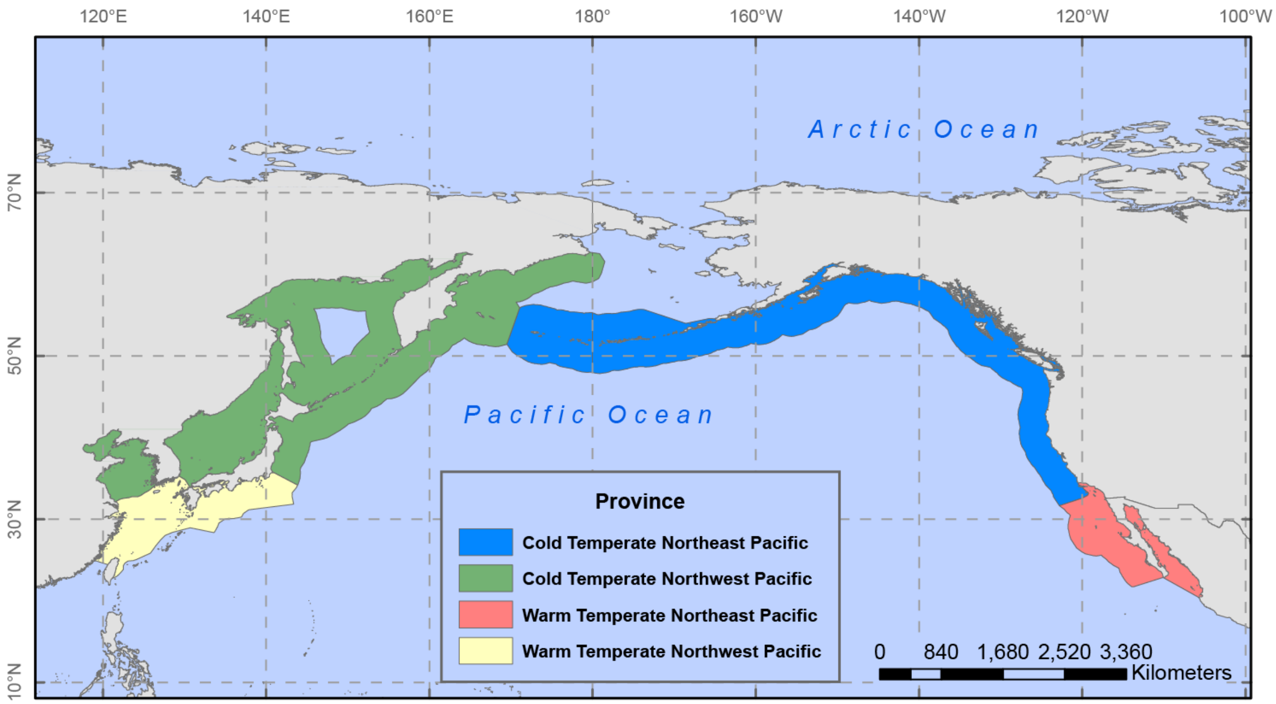

Figure A-3. Map of the four Marine Ecosystem of the World (MEOW) Provinces that comprise the Temperate Northern Pacific and Arctic Realms [*Spalding et al.*, 2007]. The Cold Temperate Northeast Pacific includes the Aleutian Islands and the Pacific coast of North America, from Alaska to Southern California. The Warm Temperate Northeast Pacific contains the Baja Region. The Cold Temperate Northwest Pacific includes the Kamchatka coast of the Bering Sea and the Kuril Islands as well as the inland seas of Okhotsk, Japan, and the Yellow Sea, and much of the Japanese coast. Lastly, the Warm Temperate Northwest Pacific encompasses the East China Sea, the south coast of Korea and the Pacific coasts of Kyushu, Shikoku, and part of the Honshu Islands of Japan.

References Cited

Casey, K. S. (2002), Daytime vs nighttime AVHRR sea surface temperature data: A report regarding Wellington et al. (2001), *Bull. Mar. Sci.*, *70*(1), 169-175.

Evans, R. H., J. Vasquez, and K. S. Casey (2009), 4 km Pathfinder Version 5 User Guide, edited, United States Department of Commerce, National Oceanographic Data Center.

IPCC (2007), Climate change 2007: impacts, adaptation and vulnerability, in *Contribution of Working Group II to the Fourth Assessment Report of the Intergovernmental Panel on Climate Change*, edited by M. L. Parry, O. F. Canziani, J. Palutikof, P. J. van der Linden and C. E. Hanson, pp. 1-976, Cambridge University Press, Cambridge.

Kearns, E. J., J. A. Hanafin, R. H. Evans, P. J. Minnett, and O. B. Brown (2000), An Independent Assessment of Pathfinder AVHRR Sea Surface Temperature Accuracy Using the Marine Atmosphere Emitted Radiance Interferometer (MAERI), *Bulletin of the American Meteorological Society*, *81*(7), 1525-1536.

Kilpatrick, K. A., G. P. Podesta, and R. Evans (2001), Overview of the NOAA/NASA advanced very high resolution radiometer Pathfinder algorithm for sea surface temperature and associated matchup database, *J. Geophys. Res.-Oceans*, *106*(C5), 9179-9197.

Reynolds, R. W., N. A. Rayner, T. M. Smith, D. C. Stokes, and W. Wang (2002), An Improved In Situ and Satellite SST Analysis for Climate, *J. Clim.*, *15*(13), 1609-1625.

Roberts, J. J., B. D. Best, D. C. Dunn, E. A. Treml, and P. N. Halpin (2010), Marine Geospatial Ecology Tools: An integrated framework for ecological geoprocessing with ArcGIS, Python, R, MATLAB, and C++, *Environmental Modelling & Software*, *25*(10), 1197-1207.

Spalding, M. D., et al. (2007), Marine ecoregions of the world: a bioregionalization of coastal and shelf areas, *BioScience*, *57*(7), 573-583.

Vazquez-Cuervo, J., K. Perry, and K. Kilpatrick (1998), NOAA/NASA AVHRR Oceans Pathfinder sea surface temperature data set user's reference manual version 4.0: JPL Publication D-14070*Rep.*

Vazquez-Cuervo, J., E. M. Armstrong, and A. Harris (2004), The effect of aerosols and clouds on the retrieval of infrared sea surface temperatures, *J. Clim.*, *17*(20), 3921-3933.

Vazquez-Cuervo, J., E. M. Armstrong, K. S. Casey, R. Evans, and K. Kilpatrick (2010), Comparison between the Pathfinder Versions 5.0 and 4.1 Sea Surface Temperature Datasets: A Case Study for High Resolution, *J. Clim.*, *23*(5), 1047-1059.

Wessel, P., and W. H. F. Smith (1996), A global, self-consistent, hierarchical, high-resolution shoreline database, *J. Geophys. Res.*, *101*.

Xu, F., and A. Ignatov (2010), Evaluation of in situ sea surface temperatures for use in the calibration and validation of satellite retrievals, *J. Geophys. Res.-Oceans*, *115*.